MORPHOLOGICAL CORRELATES OF SPATIAL NAVIGATION, ORIENTATION AND MEMORY IN FRUIT BATS

Dissertation

zur

Erlangung der naturwissenschaftlichen Doctorwürde

(Dr. sc. nat.)

vorgelegt der

Mathematisch-naturwissenschaftlichen Fakulität

der

Universität Zürich

Von

Catherine Wairimu Gatome

aus Kenya

Promotionskomitee

Prof. Hans-Peter Lipp

Prof. Thomas Lutz

Prof. David Wolfer

Zürich 2010

Contents

Table

Figures

ZUSAMMENFASSUNG

Das Fliegen hat den Fledermäusen ermöglicht den Raum dreidimensional zu nutzen, verschiedene Nischen zu besetzen, sowie die Echoortung zu entwickeln. Damit wurden auch Gehirnstrukturen geprägt welche mit Navigation, Orientierung und räumlichem Gedächtnis assoziiert sind. Bei den nichtecho-orientierten aber auf Geruchsinformationen angewiesenen Fruchtfledermäusen findet sich denn auch eine markante Entwicklung von Schizocortex, Paleocortex, Hippocampus, aber auch des Bulbus ofactorius. Diese Studie konzentriert sich daher auf diese Strukturen.

Mittels immunhistochemischen und stereologischen Methoden untersuchten wir bei *Epomophorus wahlbergi* und *Eidolon helvum* die Zytoarchitektur der Area entorhinalis (entorhinaler Cortex, EC), insbesondere in der Cortexschicht II, die Neurogenese im piriformen (olfaktorischen) Cortex und Gyrus dentatus des Hippocampus, sowie die Moosfaserverteilung in der CA3-Region des Hippocampus. Diese Befunde wurden mit der Zytoarchitektur der Maus und Ratte verglichen.

Der entorhinale Kortex der Fruchtfledermäuse ist vergleichbar mit dem anderer Säugerarten. Er gliedert sich in eine mediale (MEA) und laterale (LEA) Area entorhinalis. Von besonderem Interesse war die Schicht II der Area entorhinalis, weil diese Sternzellen (stellate cells) enthält die aufgrund neurophysiologischer Untersuchungen als „grid cells" funktionieren, welche die Position des Individuums in Bezug auf externe Landmarken kodieren. Wir fanden bei *Epomophorus wahlbergi* eine gut-differenzierte Schicht II in der MEA, aber nicht in der LEA, und bei *Eidolon helvum* eine gut-differenzierte Schicht II nur in der LEA. Dies lässt vermuten, dass art-spezifische Veränderungen im EC mit unterschiedlichen sensorischen Verarbeitungsprozessen verbunden sind.

Eine Detailanalyse der Schicht II des EC zeigte, dass *Eidolon helvum* in der MEA einen deutlich kleineren Anteil an polygonalen Sternzellen aufweist. Darüber hinaus fanden sich artspezifische Unterschiede im zellulären Aufbau der MEA bei der Ratte und der Maus, besonders beim Anteil der Sternzellen. Dies deutet auf mögliche Artunterschiede in der neuronalen Aktivität zur Erfassung der räumlichen Position.

Die quantitative und qualitative Analyse des Gyrus dentatus zeigt bei Fruchtfledermäusen, im Vergleich zu Nagern, eine geringere Anzahl von Körnerzellen, sowie eine reduzierte Moosfaserprojektion auf die basalen Dendriten der Pyramidenzellen in der CA3

Hippocampusregion. Der Gyrus dentatus der Fruchtfledermäuse hat die Fähigkeit behalten, neue Neurone zu bilden, aber die Proliferationsrate ist niedrig. Dies widerspiegelt vermutlich die Langlebigkeit dieser Arten.

Der pirifome (olfaktorische) Cortex ist ein atypischer Cortex, der aufgrund einer beachtlichen Neurogeneseaktivität bei den untersuchten adulten Fruchtfledermäusen, vermutlich auch strukturelle Plastizität aufweist. Neugebildete Neurone wandern in einem "migratory stream" aus der subventrikulären Proliferationszone im Unterhorn des Seitenventrikels zum olfaktorischen Cortex. Aehnliches wurde bei Nagern und Primaten beschrieben. Das macht die Fruchtfledermäuse zu einem vielversprechenden Modell für olfaktorische Experimente im Zusammenhang mit der räumlichen Orientierung.

Im Vergleich zu Primaten teilen die Fruchtfledermäuse, in den untersuchten Regionen, den Aufbau der Schicht V der Area entorhinalis, sowie eine niedrige Rate der hippocampalen Neurogenese; mit anderen Arten die frühe altersbedingte Abnahme der adulten Neurogenese im Hippocampus und der Area piriformis. Das reflektiert aber wahrscheinlich eher evolutionäre Konvergenz bei der Verarbeitung von räumlich-sensorischen Informationen als eine Verwandtschaft mit Primaten wie sie gelegentlich postuliert wurde.

Summary

Flight has allowed the bats to use their space in three-dimensions, occupy diverse niches and develop a unique sensory modality, echolocation. This study investigates the morphological characteristics associated with spatial navigation, orientation and memory in non-echolocating African fruit bats. These characteristics have led to diversifications in brain structures that are associated with spatial performance. In fruit bats, the high encephalisation corresponds to structures associated with spatial demands related to foraging behaviour, including the schizocortex, paleocortex, olfactory bulbs, hippocampus, and olfactory bulbs.

Using immunohistochemical and stereological techniques, we studied the cytoarchitecture of the entorhinal cortex (EC), the cellular composition of the medial entorhinal area (MEA) layer II, neurogenesis in piriform cortex and dentate gyrus of the hippocampus, and the mossy fibre distribution in Wahlberg's epauletted fruit bat (*Epomophorus wahlbergi*) and the straw-coloured fruit bat (*Eidolon helvum*). These findings were compared to the cytoarchitecture of mouse and rat.

Our findings indicate that the entorhinal cortex of the fruit bats shares similarity in organisation with several species and can be differentiated into a MEA and lateral entorhinal area (LEA) component, and five fields, two in MEA and three in LEA. We noted that Wahlberg's epauletted fruit bat had a well-differentiated layer II in the MEA but not so in the LEA, and the straw-coloured fruit bat had a well-differentiated layer II only in the LEA. We concluded that species-specific changes in the EC are related to specific sensory processing requirements.

A special focus was laid on stellate cells in the layer II of the entorhinal cortex as they represent most likely a correlate of "grid cells" involved in spatial localization of the individual. This analysis showed that the layer II of the MEA particularly of the straw-coloured fruit bat presents with a low proportion of polygonal stellate cells. We also noted species-specific differences in the cellular composition of the MEA in the rat and mouse, particularly in the proportion of stellate cells. This implies differences in neural activity in line with species-specific stimulus processing in the EC.

Qualitative and quantitative analysis of the dentate gyrus revealed a low number of granule cells. The intra- and infrapyramidal mossy fibres in fruit bats have a scattered distribution and appear smaller in size in comparison to rodents. The dentate gyrus has retained the ability to generate new neurons, but the proliferation rate was low as predicted in long-lived late-maturing species.

The piriform cortex is an atypical cortex which has also retained structural plasticity as indicated by considerable adult neurogenic activity. Newly generated neurons tangentially followed a migratory stream, from the subventricular zone bordering the temporal lateral ventricle to the piriform cortex, as also described in primates and rodents. This makes the fruit bat a good model for experiments related to olfactory use in spatial navigation.

From a comparative point of view, fruit bats share certain brain characteristics with primates, such as in the organisation of layer V of the entorhinal cortex and the low rate of hippocampal neurogenesis; with other species age-related decline in hippocampal and piriform neurogenesis. This is possibly related to convergences in evolution in the processing of sensory information and regulation of brain function.

ABBREVIATIONS

EC	Entorhinal cortex
MEA	Medial entorhinal cortex
LEA	Lateral entorhinal cortex
DG	Dentate gyrus
SP-MF	Suprapyramidal mossy fibre
IIP-MF	Intra-and Infrapyramidal mossy fibre

AIMS OF THE THESIS

Using a comparative morphological approach, we investigated structures that are known to be involved in spatial navigation, orientation and memory as can be inferred from other species, the ecology and behaviour of bats and previously described brain characteristics. We undertook to do the following:

- Describe the chemo- and cytoarchitecture of the entorhinal cortex, making a comparison between two closely related fruit bat species, rodents and primates.

- Compare the cellular composition of layer II of the medial entorhinal cortex between two closely related fruit bats, rat and mouse, identifying the various cellular components and providing estimates of size, neuronal proportions and densities.

- Investigate hippocampal neurogenesis, making comparisons with the microbats, rodents and primates with the aim to determine its characteristics in fruit bats, species which use sensory mechanisms that approximate those of the rodents and primates.

- Investigate piriform neurogenesis, expected to be prominent in fruit bats because of their reliance on olfaction, for locating ripe fruit and orientation as inferred from the foraging behaviour.

- Consider evolutionary relationships in the investigated structures in bats by making comparisons with rodents and primates providing information on brain, behaviour and evolutionary relationships.

INTRODUCTION

THE FRUIT BATS

Order: Chiroptera (Bats)

Suborder: Megachiroptera (Fruit bats)

Family: Pteropodidae

Subfamily: Pteropodinae

Study species and collection

The bats (Chiroptera) are the second largest taxonomic group after rodents, and are composed of two families, the Microchiroptera (microbats) and Megachiroptera (fruit bats). These suborders share an evolutionary history [Teeling et al. 2000; Shen et al. 2010] but are diverse in sensory use. Echolocation is developed in the microbats for use in homing, foraging and social interactions while the fruit bats rely on olfactory and visual senses [Barton et al. 1995; Hutcheon et al. 2002]. Only one fruit bat family, *Rousettus*, uses echolocation. Frugivory is a shared dietary preference between the fruit bats and the fruit-eating microbats although it appears to have developed independently in the two groups [Hutcheon et al. 2002].

Study species: The two study species, Wahlberg's epauletted fruit bat (*Epomophorus wahlbergi)* (Fig. 1a) and the straw-coloured fruit bat (*Eidolon helvum)* (Fig. 1b) are endemic to Africa.

Wahlberg's epauletted fruit bat: Wahlberg's epauletted fruit bats were trapped within the National Museums of Kenya grounds in Nairobi, Kenya. The roosts were located under the eaves of buildings, in groups of about 10 individuals. Adult females carried their young on foraging flights. Young and adult animals were trapped. Criteria for age determination in bats include tooth wear, closure of the femoral epiphyseal plate, forearm measurements and body weight. Adults weighed between 60 – 80 grams, and young between 40 – 50 grams. These species was roosting silently with little interaction between group members. Wahlberg's epauletted fruit bat set off for foraging at about 1900 hours and can fly about 4 km to foraging sites [Acharya 1992]. The young are sexually mature at 15 months [Acharya 1992] and the lifespan for this species in captivity is over 10 years. This species shows sexual dimorphism, and males can be

differentiated from females from the white epaulettes on their shoulders [Kingdon 1984a; Nowak 1994].

Straw-coloured fruit bat: The trapping of this species was done in Uganda, where large colonies are found roosting within the capital city, Kampala. Colonies number hundreds to thousands of individuals roosting on palm trees at heights of 20 – 30 meters. The bats were highly alert and disturbances, such as advancing a net towards them set them off. Loud vocalisations were heard from the roost. The bats left the roost between 1845 and 1900 hours and returned between 0500 and 0600 hours. Adults carried juveniles weighing between 90 – 110 grams on foraging flights. The adult weighed between 250 – 280 grams. Sexual dimorphism is less distinct [Funmilayo 1979; Kingdon 1984a; DeFrees and Don 1988; Nowak 1994]. Foraging distances of over 30 km can be covered in a single night [Kingdon 1984b], and this species has been known to migrate annually covering several thousand kilometres [Richter and Cumming 2008]. Their lifespan is approximately 21 years in captivity [DeFrees and Don 1988].

Figure 1: Fruit bats at roost

Wahlberg's epauletted fruit bat

Straw-coloured fruit bat

Ecological demands

Flight has led to the Chiroptera invading many different habitat niches, and therefore they exhibit extreme diversity in morphological and functional brain features [Baron et al. 1996b]. In the fruit bats, the brain development has been subject to ecological demands related to their large home range, complex habitats, dietary specialisation, social organisation, and flight behaviour. Predatory challenges are low but roosting in open places leaves them vulnerable to occasional attacks, and their brain development is also related to behavioural flexibility and high alertness.

The two fruit bats are closely matched in their ecological adaptations and behaviour, making them good candidates for a comparative study. Similarities include diet, roost location within large cities, and sizeable home ranges. Differences include the larger home range, high flying and migratory behaviour in the straw-coloured fruit bat, as well as its highly gregarious nature.

Examining individual neural systems provides information on the evolutionary diversification of the mammalian brain in response to specific ecological demands. Generally, fruit bats are highly neocorticalised compared to similar-sized rodents and microbats, related to their ecological and behavioural demands [Baron et al. 1996b]. Dietary preference has been shown to influence the size of the brains in bats [Hutcheon et al. 2002], insectivores and primates [Barton et al. 1995] either through the selective adaptation to stimuli that need to be processed for feeding or in the associated information storage and retrieval systems [Harvey and Krebs 1990]. The sensory requirements for foraging have led during evolution to the selective enlargement of specific brain regions involved in this kind of processing [Harvey and Krebs 1990]. These include the olfactory bulbs, lateral geniculate nuclei, septohippocampal limbic structures (septum, hippocampus, schizocortex, diencephalon) and paleocortex (amygdala, piriform cortex and other structures) [Barton et al. 1995; de Winter and Oxnard 2001]. A more detailed understanding of selection pressures and specialisations requires data on functionally specific subsystems which have interrelated functions [Barton et al. 1995], such as those involved in spatial navigation, orientation and memory.

Although the selected fruit bats are phylogenetically close, there is extensive diversification in their brain structures. The straw-coloured fruit bat is considered a more primitive member of the subfamily based on skull characteristics, separating it into a distinct niche [Baron et al. 1996a]. The striatum, amygdala, paleocortex (retrobulbar region, anterior olfactory nucleus, olfactory tubercle and piriform cortex) and septum are the best developed telencephalic structures. In Wahlberg's epauletted fruit bat, the most progressive telencephalic structures are the olfactory bulbs, amygdala, striatum, and neocortex [Baron et al. 1996d]. The schizocortex (entorhinal (EC) and perirhinal cortex, presubiculum and parasubiculum) and hippocampus are the least progressive structures in both species [Baron et al. 1996c]. It would therefore seem that they have a greater need for the processing of olfactory and emotive input and that related to behavioural flexibility and cognitive ability.

Several brain structures play a role in spatial navigation, orientation and memory, including the hippocampus, entorhinal and piriform cortices and olfactory bulbs, and these structures are markedly larger in fruit bats compared to microbats. In primates, insectivores [Barton and Harvey 2000] and bats [Baron et al. 1996d] there is a size correlation between the hippocampus

and entorhinal cortex, reflecting close anatomical and functional links between these structures [O'Keefe and Conway 1978]. This could be attributed to their increased need to form spatio-temporal representations of specific locations [Baron et al. 1996c; de Winter and Oxnard 2001]. The piriform cortex and olfactory bulbs have strong interconnections with the entorhinal cortex and disynaptic access to the hippocampal formation [Haberly and Price 1978]. There is data to suggest that there is an association between hippocampal functions and odour memory encoding and storage in the piriform cortex [Chaillan et al. 1996]. Olfaction may be important for spatial orientation and navigation, as shown in locating a food resource (fruit) that is spatially and temporally unpredictable in its occurrence [Hodgkison et al. 2007; Raghuram et al. 2009].

THE ENTORHINAL CORTEX

The entorhinal cortex (EC) is part of the parahippocampal region that plays a critical role in memory, learning and navigation. Investigations in various species have shown great diversity in the EC, ranging from the three-layered EC in the tenrec (a primitive insectivore) that is uniform in its appearance [Künzle and Radtke-Schuller 2000] to the well-developed primate EC which shows increased cellularity and better organised layers and fields [Amaral et al. 1987]. There is no reason therefore to assume that the EC of the bat would resemble that of any other species. We briefly review, below, the morphological and functional differentiation of the EC based on other species.

Cytoarchitecturally, the EC is a transitional region between the allocortex and neocortex, characterised by a cell-sparse layer IV (lamina dissecans) instead of a granular layer, present in all investigated mammalian species [Amaral et al. 1987]. A medial (MEA) and lateral (LEA) EC division is recognised in most mammalian species, including bats [Brodmann 1909; Rose 1912]. These divisions show differences in cytoarchitecture, inputs and outputs [Kerr et al. 2007]. Further investigations of the MEA and LEA have led to the identification of additional fields [Amaral et al. 1987] which vary in cytoarchitectural organisation and cortical location between species. The classifications of these fields have led to a number of schemes in different species [Amaral et al. 1987; Insausti et al. 1997; Uva et al. 2004; Wóznicka et al. 2006]. Of all the fields defined based on cytoarchitectural patterns, functional specialisation can only be attributed to the primate E_O LEA field, which is the sole recipient of direct input from the olfactory bulb

[Amaral et al. 1987] and field CE in the rat which may preferentially deal with visuo-spatial information [Insausti et al. 1997; Brun et al. 2008].

From investigations in the rat, the EC inputs and outputs have been shown to be diverse and have made the structure increasingly complex to understand. Cortical input into the EC shows a preference, targeting distinct parts and partitioning it into (i) MEA and LEA divisions; (ii) caudal and lateral EC parts and; (iii) medial and rostral EC parts [Insausti 1993]. The MEA receives its main input from the postrhinal cortex, while the LEA receives its input mostly from the perirhinal cortex [Burwell and Amaral 1998]. The caudal and lateral EC parts receive primarily visual and visuospatial input while medial and rostral EC parts receive olfactory and emotive input [Burwell and Amaral 1998]. The caudal and lateral EC parts are better developed and organised than medial and rostral parts [Insausti 1993], which may be tested in the bats.

Functional studies have also differentiated the EC based on spatial tuning, with the MEA being strongly spatially tuned (more robust grid cells and better spatial selectivity) compared to the LEA [Hargreaves et al. 2005]. A gradient in the spatial tuning has been observed, with the ventromedial MEA showing less specific spatial tuning (an increase in grid spacing and field size) in comparison to dorsocaudal MEA [Hafting et al. 2005].

Typically, the EC has been defined as that cortical part that projects to the hippocampus and EC efferents can be differentiated based on hippocampal termination levels and patterns. The caudal and lateral EC parts project to septal levels of the hippocampus, while medial and rostral EC parts project to temporal levels. Input from the MEA targets the middle molecular layer of the dentate gyrus (DG) and stratum lacunosum-moleculare of CA3, while the LEA projections terminate onto the outer molecular layer and stratum lacunosum-moleculare of the DG and CA3 hippocampal regions, respectively [Witter et al. 2000]. The termination of the MEA projections in the molecular layer can be identified using cholecystokinin reactivity as can those from the medial perforant pathway using encephalin [Fredens et al. 1984] . Likewise, the terminal fields are recognised by Timm's stain.

Previous investigations on the connection pattern between the EC and hippocampus in fruit bats were limited by the lack of a description of the cytoarchitectural organisation of the EC

[Buhl and Dann 1991]. Our study aims to provide detailed information on the architecture of the EC in the bats which have unique spatial demands by virtue of flight and are navigating in three-dimensions. The fruit bats have a high encephalisation index [Baron et al. 1996d], and therefore the neocortical-hippocampal connections are expected to be prominent, and the EC would therefore be anticipated to be well-developed. Our description would be useful to a comparative understanding of the entorhinal-hippocampal system and functional future studies of the EC in bats.

LAYER II OF THE MEDIAL ENTORHINAL CORTEX

The MEA in the rat, largely processes information from visual, visuospatial and olfactory cortical regions [Burwell and Amaral 1998], that is useful to spatial navigation and orientation. Cortical efferents to the EC primarily target layers II and III, and these layers also form the main input into the hippocampus [Witter 2007]. Layer II stains prominently in Nissl staining and characteristically presents with clustering of the cells. Layer II is fairly heterogenous in cyto- and chemoarchitecture, and function, reviewed below.

Layer II contains a special type of modified pyramidal cell, referred to as the stellate cell. It is the most abundant cell type in MEA layer II. Other cell types include pyramidal, horizontal bipolar and tripolar cells, and various interneurons. Stellate cells have large polygonal or ovoid soma, elongated perpendicular to the pial surface. Four or more thick primary dendrites emerge from the soma in a radial or bi-tufted pattern [Klink and Alonso 1997]. Stellate cells are a diverse class, showing differences in somal shape and size [Schwartz and Coleman 1981], expanse and calibre of the dendritic [Klink and Alonso 1997] and axonal arbours [Lorente de Nó 1933]; up to eight classes have been identified using intracellular staining [Klink and Alonso 1997]. Pyramidal cells are medium-sized to large cells with conical or triangular soma. They have a large apical process oriented perpendicularly or obliquely to the pial surface, which may bifurcate at the border between layers I and II. Horizontal bipolar and tripolar cells have round or elongated somata are usually located at the border between layers I and II [Schwartz and Coleman 1981; Klink and Alonso 1997]. The stellate, pyramidal and horizontal cells (principal cells) are known to project to the hippocampus [Schwartz and Coleman 1981]. Other cell types such as the small round cells [Jones et al. 1993] and those of fusiform appearance [Wouterlood et al. 2000], are likely to be interneurons. There are also other interneurons such as basket and

chandelier cells that share somal characteristics with the projecting neurons, making it challenging to differentiate them in Nissl stain.

Layer II cells can also be differentiated chemoarchitecturally. GABAergic interneurons can be differentiated using calcium binding proteins, such as caliretinin, calbindin and parvalbumin, which recognise subsets of interneurons [Rogers and Resibois 1992; Tuñón et al. 1992; Wouterlood et al. 1995; Wouterlood et al. 2000]. Interneurons comprise about 10% of the entorhinal cell population [Kumar and Buckmaster 2006]. Neurofilament markers also preferentially stain types of principal cells within layer II suggesting sub-populations [Beall and Lewis 1992]. There is no marker currently available to differentiate the glutaminergic neurons or principal cells in MEA layer II.

In studies in the rat, physiological characterisation has distinguished between stellate cells and non-stellate cells in the MEA layer II. Stellate cells exhibit sub-threshold theta oscillations and spike clustering, which are not observed in pyramidal neurons [Alonso and Klink 1993; Hasselmo and Brandon 2008]. These physiological properties of the stellate cells make them the most likely correlate for the grid cell, a functional cell type that is concerned with the spatial representation of location in an animal's environment [Hafting et al. 2005]. Pyramidal neurons in MEA layer II show persistent spiking activity, which is associated with the activity of the grid cells in coding spatial location [Hasselmo and Brandon 2008]. Physiological properties of the grid cells suggest that they comprise the path-integration-based system [McNaughton et al. 2006; Hasselmo and Brandon 2008]. There is no information on the function of other MEA layer II cells.

Unbiased estimates of neuronal cell numbers and size in the MEA layer II exist in the rat [Merrill et al. 2001; Rapp et al. 2002], but overall estimates conceal the cellular heterogeneity of this layer. In the mouse, estimates of EC neuronal numbers from a transgenic mouse model are the only existing data [Irizarry et al. 1997]. Differentiating the cellular composition would be useful to functional investigations. It would also be useful in determining species differences and changes along the mediolateral and dorsoventral axis, which may have functional implications. Species differences in the composition of layer II cells are very likely based on sensory information processing requirements, for example in the computing location vectors for three-dimensional flight in bats [Ulanovsky and Moss 2007]. Functional cell types in the MEA layer II

have been reported to vary in rat and mouse [Fyhn et al. 2008]. Additionally, observed changes in grid properties, that is, increase in field size from dorsal to ventral, are suggested to be attributed to changes in cellular densities [Brun et al. 2008] or possibly distributions of specific phenotypes. We therefore expect differences in the composition of the MEA layer II associated with flight behaviour and sensory stimuli, within the bats and between bats and rodents.

This data would be used in modelling studies useful to the understanding of the EC. For example as an indicator for disease-associated cellular changes in mouse transgenic models of Alzheimer's disease [McGowan et al. 2006], where the pathology is mainly observed in layer II and is associated with changes in the neuronal numbers, densities and sizes [Beall and Lewis 1992].

HIPPOCAMPAL PLASTICITY

Research in the hippocampus has confirmed that it has an important role in emotion, memory and learning, and spatial performance [O'Keefe and Nadel 1978]. Hippocampal-dependent spatial abilities, such as home range navigation and foraging are critically important to fruit bats for survival. Spatial performance has a large influence on the size of the hippocampus in bats; hippocampal size in birds has also been correlated with the need to process spatial information [Krebs et al. 1989]. Those bats that are fast-flyers and forage in open spaces away from vegetation and other obstacles have low hippocampal size indices [Baron et al. 1996c]. In addition to habitat type, comparative analysis of the size of the hippocampus of numerous bat species has shown that foraging demands are another main factor determining the size of the hippocampus [Safi and Dechmann 2005]. Fruit-eating bats may have greater foraging demands than insectivorous microbats and rodents, needing to remember the spatial-temporal distribution of their food. In fruit-eating microbats, over 40% of their brain volume is thought to be concerned with audition [Suthers I970], and they have therefore not developed their hippocampi to the same extent as fruit bats [Hutcheon et al. 2002]. Not surprising, the fruit bats have the largest hippocampus among the bats [Hutcheon et al. 2002]. Migratory behaviour does not correlate with the relative size of the hippocampus among fruit bats, and it is likely that they rely on celestial [Baron et al. 1996c] and or magnetic cues [Holland et al. 2006].

It is notable that even while schizocortex and hippocampus are larger in fruit bats than microbats and have higher size indices compared to similar-sized rodents, these structures are not the most progressive in the telencephalon of the two species [Baron et al. 1996a]. Buhl and Dann [1991] made the observation of a 3 – 6 cell layer thick DG in *Pteropus* fruit bat species, compared to a 10 – 12 granule cell-layer thickness in rodents. We therefore expect low granule cell counts in fruit bats.

The fruit bats are long-lived [Wilkinson and South 2002] and they maintain a roost over long periods of time allowing them to build a spatial map of their environment within an early period in life, and thereafter may navigate using well-learned routes. Navigation by well-learned routes which does not require the flexible application of past experiences does not recruit the hippocampus [McNamara and Shelton 2003], suggesting lower reliance on this structure. Rodents on the other hand are short-lived and under severe predatory pressure and require an accurate knowledge of their space, suggesting a higher reliance on the hippocampus. Some rodents also have sizeable home ranges. A high granule cell number has been correlated to large home territories in wild rodents [Amrein et al. 2004a], and it is therefore of interest to conduct granule cell counts in the straw-coloured fruit bat.

Projecting neurons of EC layer II terminate onto the molecular layer of the DG. This input is likely to modulate the function of the DG in a species-specific way. The DG is a phylogenically old structure that has retained the ability to generate new neurons. Input from the perforant pathway has been shown to be important for the survival and integration of newly generated neurons into the DG [van Praag et al. 2002]. The new neurons are continuously produced in the adult vertebrate brain [Altman and Das 1965] from progenitor cells located in the sub-granular zone (SGZ) of the DG. From here they migrate into the granule cell layer [Cameron et al. 1993] and make synapses with CA3 cells [Markakis and Gage 1999]. Previous reports of low to absent hippocampal neurogenesis in microbats [Amrein et al. 2007] suggest a need for a comparison with fruit bats. It may be that this process is attenuated in bats in general, or is modulated by echolocation.

In rodents, the role of new hippocampal neurons in spatial memory and learning is not clear [Leuner et al. 2006] and studying natural populations is one approach towards determining its functional relevance [Amrein et al. 2008]. Likely roles include replacing old neurons to keep

circuits functionally young [Nottebohm 2002], supporting complex forms of spatial memory [Dupret et al. 2008] and improving spatial information processing through enhancing memory encoding in CA3 [Treves et al. 2008]. Although the hippocampus is functionally differentiated along its longitudinal axis [Moser and Moser 1998; Fanselow and Dong 2010] and a sub-regional analysis of the DG would be preferred in deducing a spatial or non-spatial role for the new neurons [Snyder et al. 2009], there is currently no agreement on how to differentiate septal and temporal hippocampus.

Large home ranges in rodents are correlated with high rates of cell proliferation and neurogenesis [Amrein et al. 2004b]. Thus, if large home ranges are associated with high levels of proliferation one would expect high rates in fruit bats also. On the other hand, lifespan also influences the extent of neurogenesis, with long-lived late-maturing species such as primates, having a lower rate of hippocampal cell proliferation and neurogenesis [Kornack and Rakic 1999]. This would, conversely, predict a low rate in fruit bat, which live long (~20 years) and mature late (sexual maturity at 15 months in Wahlberg's epauletted fruit bat).

The temporal development of the hippocampus in rodents is likely to maintain a high degree of plasticity in adulthood than the early developing one in primates [Kornack and Rakic 1999]. Thus, if the temporal development and lifespan are the key factors in predicting dentate neurogenesis in fruit bats, one would also expect to find a high number of early formed granule cells as compared to the number observed in fully grown adults. This prediction has been tested in this thesis by comparing granule cell count in young and adult age groups in Wahlberg's epauletted fruit bats. Concurrently, we have also investigated other forms of morphological plasticity such as the size of the infra- and intrapyramidal mossy fibres of the hippocampus, a feature that has been correlated to hippocampal development, spatial abilities, lifestyle and habitat type in rodents [Schwegler and Crusio 1995; Pleskacheva et al. 2000].

THE OLFACTORY SYSTEM

The olfactory system is the most variable sensory system in Chiroptera, and the development of the main olfactory bulb and olfactory cortex vary in relation to the use of olfaction, in foraging behaviour, communication between group members and mother-young relationships. In fruit bats, olfactory stimuli have been considered dominant in searching, detection and selection of

fruit [Nowak 1994; Baron et al. 1996c; Hutcheon et al. 2002; Raghuram et al. 2009] and may be particularly important in nocturnal foraging, when the use of vision is restricted [Barton et al. 1995]. The main olfactory structures, olfactory bulbs and paleocortex, take up a large part of the telencephalon of fruit bats [Baron et al. 1996c]. The piriform cortex (a phylogenetically old, three-layered cortex) forms the largest component of the paleocortex [Haberly and Bower 1989].

The entorhinal cortex is closely associated with the piriform cortex – in fact in insectivores it is difficult to differentiate the two regions [Künzle and Radtke-Schuller 2000] and in rodents there are extensive reciprocal connections between the piriform and entorhinal cortex [Haberly and Price 1978]. This may suggest that both regions are involved in the processing of both olfactory and spatial information. The hippocampus receives and processes polysensory information, including olfactory input from the piriform cortex through the lateral entorhinal cortex [Schwerdtfeger et al. 1990]. Physiological studies have shown that stimulation of the lateral olfactory tract and piriform cortex evokes potentials in the DG [Wilson and Steward 1978; Habets et al. 1980]. Odour-driven hippocampal place cells that fire in response to a specific odour at a particular place [Wood et al. 1999] suggest the combining of odour (object) and spatial information [Eichenbaum 1999] in hippocampal representations. Fruit bats can detect the smell of ripe bananas from an experimental distance setup of 1.5 metres [Luft et al. 2003] and when flying at speed of 15 km/h [Baron et al. 1996c]. Therefore, the olfactory-entorhinal-hippocampal circuits may be important for the establishment or recall of olfactory memories associated with events [Shipley et al. 2004], such as spatial ones. These olfactory memories may be important for spatial orientation and navigation, guiding the foraging behaviour of fruit bat [Hodgkison et al. 2007; Raghuram et al. 2009].

The piriform cortex, like the DG shows cellular plasticity. It functions as an association cortex, detecting and learning correlations between olfactory representations and past experiences [Haberly 2001]. The olfactory bulb [Lois et al. 1996] and piriform cortex [Shapiro et al. 2007] receive a continuous supply of newly generated neurons which originate from the subventricular zone of the lateral ventricle. This process has been observed in several mammalian species, including fruit bats, suggesting that it has been conserved throughout evolution and reflects a shared importance of olfaction. The olfactory system of fruit-eating bats is adapted to a large variety of fruit odours [Luft et al. 2003], and odour discrimination and memory in the piriform cortex may be dependent on the survival of new neurons, as in the

olfactory bulbs where they are necessary for readapting to ongoing environmental changes [Petreanu and Alvarez-Buylla 2002; Rochefort et al. 2002; Barnes et al. 2008]. We therefore expect a fairly prominent cellular plasticity in the piriform of fruit-eating microbats and fruit bats.

The following chapters will document our findings and answers to the questions raised in detail, in form of publications that have already appeared or are under review.

PUBLICATIONS

THE ENTORHINAL CORTEX OF THE MEGACHIROPTERA: A COMPARATIVE STUDY OF WAHLBERG'S EPAULETTED FRUIT BAT AND THE STRAW-COLOURED FRUIT BAT.

Brain structure and function 214: 375 - 393

Brain Struct Funct (2010) 214:375–393
DOI 10.1007/s00429-010-0239-z

ORIGINAL ARTICLE

The entorhinal cortex of the Megachiroptera: a comparative study of Wahlberg's epauletted fruit bat and the straw-coloured fruit bat

Catherine W. Gatome · Lutz Slomianka · Dieter K. Mwangi · Hans-Peter Lipp · Irmgard Amrein

Received: 16 October 2009 / Accepted: 9 January 2010 / Published online: 4 February 2010

Abstract This study describes the organisation of the entorhinal cortex of the Megachiroptera, straw-coloured fruit bat and Wahlberg's epauletted fruit bat. Using Nissl and Timm stains, parvalbumin and SMI-32 immunohistochemistry, we identified five fields within the medial (MEA) and lateral (LEA) entorhinal areas. MEA fields E_{CL} and E_C are characterised by a poor differentiation between layers II and III, a distinct layer IV and broad, stratified layers V and VI. LEA fields E_I, E_R and E_L are distinguished by cell clusters in layer II, a clear differentiation between layers II and III, a wide columnar layer III and a broad sublayer Va. Clustering in LEA layer II was more typical of the straw-coloured fruit bat. Timm-staining was most intense in layers Ib and II across all fields and layer III of field E_R. Parvalbumin-like staining varied along a medio-lateral gradient with highest immunoreactivity in layers II and III of MEA and more lateral fields of LEA. Sparse SMI-32-like immunoreactivity was seen only in Wahlberg's epauletted fruit bat. Of the neurons in MEA layer II, ovoid stellate cells account for ~38%, polygonal stellate cells for ~8%, pyramidal cells for ~18%, oblique pyramidal cells for ~6% and other neurons of variable morphology for ~29%. Differences between bats and other species in cellular make-up and cytoarchitecture of layer II may relate to their three-dimensional habitat. Cytoarchitecture of layer V in conjunction with high encephalisation and structural changes in the hippocampus suggest similarities in efferent hippocampal → entorhinal → cortical interactions between fruit bats and primates.

Keywords *Epomophorus wahlbergi* · *Eidolon helvum* · Parvalbumin · SMI-32 · Timm-staining · Stereology

Abbreviations

EC	Entorhinal cortex
MEA	Medial entorhinal cortex
LEA	Lateral entorhinal cortex
PrS	Presubiculum
PaS	Parasubiculum
PRh	Perirhinal cortex
POR	Postrhinal cortex
PPC	Prepiriform cortex
E_{CL}	Caudal-limiting entorhinal field
E_C	Caudal entorhinal field
E_I	Intermediate entorhinal field
E_L	Lateral entorhinal field
E_R	Rostral entorhinal field

Introduction

Although detailed descriptions of the entorhinal cortex (EC) are available for most of the common species used in neuroscience research, they comprise only a small segment of the mammalian radiation. To our knowledge, no contemporary descriptions are available for one of the most species-rich mammalian orders, the Chiroptera. The few available studies date back to the beginning of the twentieth century. Rose (1912) described this region as bearing a strong semblance to the EC of other mammals. Brodmann

C. W. Gatome · L. Slomianka · H.-P. Lipp · I. Amrein (✉)
Institute of Anatomy, University of Zurich,
Winterthurerstrasse 190, 8057 Zurich, Switzerland
e-mail: i.amrein@anatom.uzh.ch

D. K. Mwangi
Department of Veterinary Anatomy and Physiology,
University of Nairobi, PO Box 30197, Nairobi 00100, Kenya

(1925) identified a medial and lateral subdivision in a megachiropteran species, *Pteropus edwardsi*. Later, Rose (1926) in his study of a microchiropteran species, *Vesperugo pipistrellus*, identified an additional subdivision, which he named area entorhinalis intermedia. In recognising only the medial and lateral entorhinal areas, early works generally do not conform to the parcellation of the EC developed more recently in other species. Buhl and Dann (1991) traced entorhinal afferents to the hippocampus in two megachiropteran species, but lacked information on the entorhinal fields, and therefore could not draw conclusions on topographical organisation of the entorhinal–hippocampal connections. Here, we provide a description of the EC in Megachiroptera (fruit bats), which is comparable with the parcellation that has been derived from recent cytoarchitectural and connectional studies in other species. The inclusion of two closely related species, Wahlberg's epauletted fruit bat (*Epomophorus wahlbergi*) and the straw-coloured fruit bat (*Eidolon helvum*), was prompted by perceptible differences between the species in the EC.

While the debate on the phylogenetics of the Chiroptera lingers on, the argument for a common ancestor of the Megachiroptera and primates (Maseko and Manger 2007; Pettigrew et al. 1989, 2008), and hence a diphyletic origin of the Mega- and Microchiroptera, has been weakened by mounting evidence from recent molecular phylogenetic analyses (Jones and Teeling 2006; Teeling et al. 2000). These favour a monophyletic origin of the two chiropteran suborders (Simmons et al. 2008). That notwithstanding, the Megachiroptera do share a number of brain characteristics with primates (Johnson et al. 1994; Lapointe et al. 1999). Of the analysed characters, most are related to the visual system. The Megachiroptera have a distinctly primate-like retinotectal pathway; retinal input into the midbrain is decussated so that only the contralateral hemifield is represented. The location of the lateral geniculate nucleus magnocellular layers adjacent to the optic tract and the presence of a middle temporal visual area are characteristics only described in the primates, Megachiroptera and Dermoptera (Pettigrew et al. 1989). More recently, features of the cholinergic, catecholaminergic and serotonergic systems were found to exhibit many similarities to those in primates (Maseko et al. 2007). A general evolutionary trend of the megachiropteran brain has been the enlargement of the telencephalon, most notably the neocortex—a trend which is also seen in primates (Baron et al. 1996b). Several cytoarchitectural characteristics of the hippocampus also resemble that of primates (Buhl and Dann 1991; Rosene and Van Hoesen 1987). Considering the similarities in brain structure, the Megachiroptera may present a small mammal model for investigating primate-like neural phenomena.

In the rat and mouse, grid cells have been described in layers II and III of the dorsocaudal region of the medial EC (Fyhn et al. 2008; Fyhn et al. 2004). Metric information is integrated in the entorhinal cortex by the grid and head-direction cells and fed to the hippocampal place cells (Jeffery 2007; Moser et al. 2008; O'Keefe and Burgess 2005). Place cells have recently been described in moving echolocating bats (Ulanovsky and Moss 2007), and it is probable that they are also modulated by grid cells. Bats may offer the possibility to study the spatial firing properties of the grid cells in three-dimensions. The specific neuronal phenotype of grid cells has not been identified. Physiological characterisation of the possible phenotypes has focused on the classical stellate and pyramidal cell (Alonso and Klink 1993). Based on morphology, our study estimates the relative contribution of neuronal phenotypes to the cell population of layer II.

Materials and methods

Animals

Wahlberg's epauletted fruit bats were captured in Nairobi, Kenya, and straw-coloured fruit bats were captured in Kampala, Uganda. Permits and licences were granted by the National Museums of Kenya and the Uganda National Council of Science and Technology (No. 024/07/1). The animals were aged as adults based on the following criteria: closure of the femoral and humeral epiphyseal plate, body weight above 60 g (Wahlberg's epauletted fruit bat) or 200 g (straw-coloured fruit bat), forearm length over 70 mm (Wahlberg's epauletted fruit bat) or 110 mm (straw-coloured fruit bat) and sexual maturity (evidence of lactation or pregnancy). The actual ages of the animals are not known, although individuals of this family have lived in captivity for over 20 years (Kingdon 1984).

Four adult female animals of each species were used in this study (straw-coloured fruit bat: mean body weight 267 g, mean brain weight 4.0 g; Wahlberg's epauletted fruit bat: mean body weight 82 g, mean brain weight 1.9 g).

Histology

Tissue preparation

Animals were deeply anaesthetized with sodium pentobarbital (Nembutal®, 60 mg/ml; 50 mg/kg) and transcardially perfused first with heparinised 0.9% saline, followed by 0.6% sodium sulphide solution and then cold 4% paraformaldehyde in 0.1 M phosphate buffer with 15% picric acid. Brains were removed and postfixed overnight at 4°C in fixative and then transferred to 30% sucrose for 24 h. The right hemisphere was processed for immunohistochemistry,

(MicroBrightField Inc., Colchester, Vermont, USA). Adjustments were made to the brightness and colour of the images to restore their appearance in the microscope. No local changes were made unless noted in the figure legends. For three-dimensional modelling, EC fields were traced in Nissl-stained horizontal sections and assigned colours. Images were aligned using AutoAligner 6.0.0 (Bitplane AG, Zurich, Switzerland), and a three-dimensional representation was produced using Imaris 6.2.0 (Bitplane AG, Zurich, Switzerland).

Terminology

For the delineation of the EC, we initially consulted a Megachiroptera brain atlas (Baron et al. 1996a). Our description of the laminar structure follows Amaral et al. (1987), who used a composite of the descriptions provided by Ramón y Cajal (1988) and Lorente de Nó (1933). We have adopted Brodmann's cytoarchitectonic division of the EC into lateral entorhinal area (LEA; area 28a) and medial entorhinal area (MEA; area 28b) based on a distinction between layer II and layer III, which is clear in LEA but not in MEA (Brodmann 1909). The apparent size and position of the entorhinal fields, as they appeared in the three-dimensional reconstructions, matched best with the two-dimensional map provided by Amaral et al. (1987), and their nomenclature was adopted. We could, however, not consistently distinguish the E_{Lc} and E_{Lr} fields and treat them here collectively as E_L. In the bats, the E_L field lies in between fields E_I and E_R. Also, the E_O field, which appears as a small area rostral to E_R in primates, could not be consistently distinguished from the E_R field. MEA is comprised of caudal-limiting (E_{CL}) and caudal (E_C) entorhinal fields. LEA is constituted by two lateral fields, rostral (E_R), lateral (E_L), and a transitional area, the intermediate (E_I) entorhinal field.

One possible alternative to the primate nomenclature would have been that developed in rats (Insausti et al. 1997) and mice (van Groen 2001). However, most subfields identified based on histoarchitectural criteria in bats are very difficult to align topographically with those identified in rats and mice, which cast doubts on a possible homology of these fields. For example, the ME field is prominently ventral in location, in contrast to the E_C field in the bats which extends proportionally from dorsal to ventral. The lateral fields, DIE and DLE, extend rostrocaudally but in bats, as in primates, the corresponding fields, E_L and E_R, extend mediolaterally, obliquely to the rhinal sulcus. Although functional specialisations of the EC necessarily will result in differences in the detailed structure of subfields between species or larger phylogenetic groups, which have justified species-specific nomenclatures (e.g., guinea-pig: Uva et al. 2004; dog: Woźnicka et al. 2006), we do not believe that this is a productive approach in the long term for a cortical region that most likely shares basal functional aspects in all mammals.

Cellular morphological phenotypes were distinguished based on the earlier descriptions of Ramón y Cajal (1988), Germroth et al. (1991), Klink and Alonso (1997a) and Schwartz and Coleman (1981).

Results

Location and delineation of the entorhinal cortex

The location of the entorhinal cortex in the species investigated here corresponds to Brodmann's (1925) description of the area 28 in *Pteropus*, a related fruit bat species (Fig. 1a, b). Three-dimensional representations of the EC in Wahlberg's epauletted fruit bat and the straw-coloured fruit bat show the location and relationships of the fields (Fig. 1e–h). This corresponds to a caudo-ventral and lateral location of the EC in the piriform lobe (Fig. 1c, d). The rostral and lateral boundary of the EC is formed by the perirhinal and prepiriform cortex. Caudally and medially, it borders the para- and presubiculum. The ventro-medial boundary is delimited by part of the hippocampo-amygdaloid transition.

Medial entorhinal area (MEA)

Laminar structure Generally, layer I varies little. Layer II is not well delineated from layer III. A cell-sparse layer IV (lamina dissecans) is visible throughout the MEA, and layers V and VI are wide and densely populated (Fig. 2a, b).

Caudal-limiting entorhinal field (E_{CL})

This is the most caudal field of MEA, bordering the para- and presubiculum caudally and medially (Fig. 2a, b). It extends medio-laterally and briefly apposes the postrhinal cortex laterally (Fig. 1g, h).

Cytoarchitecture In both species, layer I is broad and has small light-staining neurons that are sparsely distributed. Layer II is well delineated from layer I and is densely populated in both species (Fig. 2c, d). Layer III is patchily populated by neurons of similar size. It is separated from layer V by a distinct, cell-sparse layer IV. Layer V is wide and has three sublayers. Sublayer Va is well developed and loosely populated by large intensely staining pyramidal neurons, and appears stratified in the straw-coloured fruit bat (Fig. 2a, c). Sublayer Vb has a dense population of small moderately staining cells (Fig. 2c, d). Sublayer Vc is

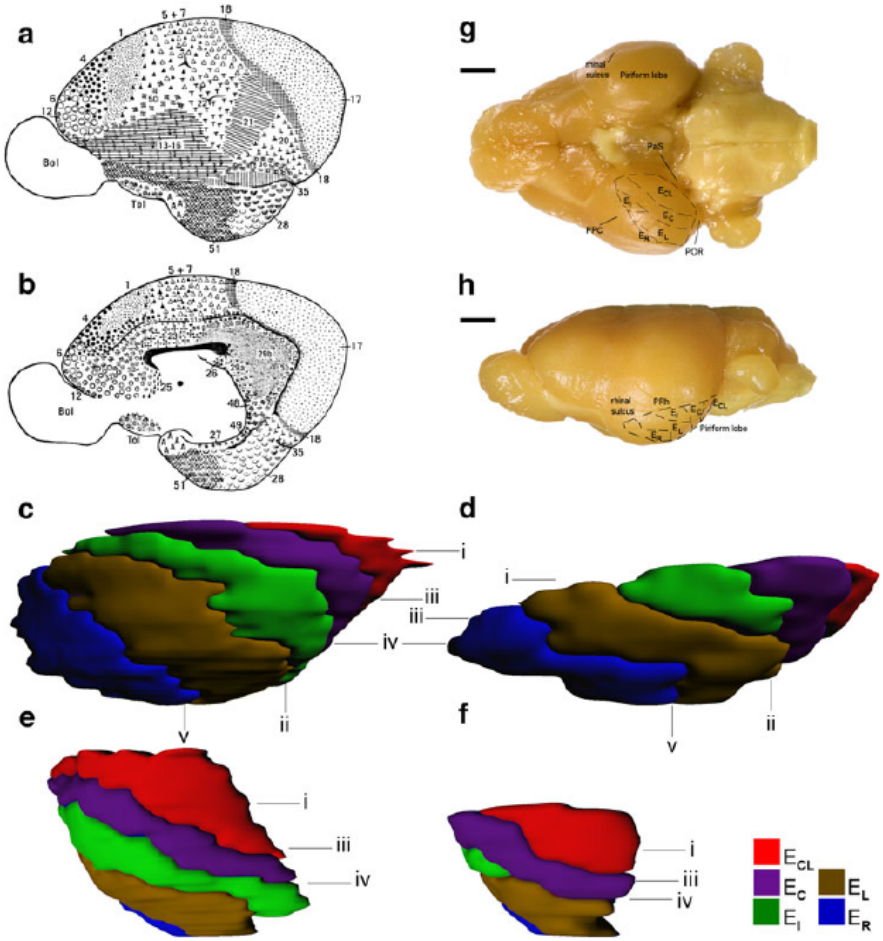

Fig. 1 Schematic drawing of the brain of Pteropus reproduced from Brodmann (1909). Lateral (**a**) and medial (**b**) views showing the location of Brodmann area 28. Three-dimensional representation of the entorhinal fields in the straw-coloured fruit bat (**c**, **e**) and Wahlberg's epauletted fruit bat (**d**, **f**) showing the approximate level of Figs. 2 and 3(*i*), 4(*ii*), 6(*iii*), 7, 8(*iv*) and 9(*v*). **c**, **d** Lateral view. **e**, **f** Caudal view showing the approximate level of Figs. 4(*iv*) and 9(*v*). Brain of Wahlberg's epauletted fruit bat showing a schematic drawing of the EC fields in the piriform lobe, and in relation to the perirhinal cortex (PRh), parasubiculum (PaS), postrhinal cortex (POR), prepiriform cortex (PPC) and rhinal sulcus. **g** Ventral view. **h** Lateral view. *Scale bars* 200 μm (**g**, **h**)

inconsistently visible as a narrow, cell-sparse zone separating layer V from layer VI. The three sublayers are more obvious in the straw-coloured fruit bat (Fig. 2a, c). Layer VI is wide and densely populated by small intensely staining neurons. Both layers V and VI are organised in radial columns. In both species, layer VI is not well demarcated from the white matter.

Chemoarchitecture Timm-staining of layer I of E_{CL} is pale superficially and dark innermost, dividing layer I into two parts, Ia and Ib (Fig. 3a, b). This pattern is recurrent in all medial and lateral entorhinal fields. Staining decreases from a dark layer II adjacent to layer I to a moderately stained deep layer III. This decrease is gradual in the straw-coloured fruit bat, whereas it appears more sudden, about half-way in layer III, in Wahlberg's epauletted fruit bat. Layer III is separated from layer V by a narrow light staining band corresponding to layer IV. Sublayer Va stains moderately in contrast to the lightly stained layers Vb and VI. There are no further apparent differences between the two species.

A sharp decrease in parvalbumin-like immunoreactivity marks the border of the caudal-limiting field towards the parasubiculum (Fig. 4c, d). Layer I has several processes oriented perpendicular to the cortical surface, which appear smooth or beaded (Fig. 5a). Layer II has few polygonal cell bodies with radial processes directed into layers I and III (Fig. 5a, b). The majority of cell bodies are located either proximally or distally in layer II. An intensely staining, dense fibre plexus extends in layers II and III (Fig. 5a). Layer III contains several cell bodies that are variable in size and shape (Fig. 5a, c–e). These include medium-sized to large polygonal cell bodies with vertically directed processes into layers II and IV, and spherical cell bodies with horizontal and ascending processes (Fig. 5c–e). Medium-sized to large polygonal cell bodies with radial processes that can be traced within the layer and into layer II are also observed (Fig. 5e). Most of these cell bodies are located in the lower half of layer III. More medial and caudal, immunoreactive cell bodies in layer III send processes into the parasubiculum (Fig. 5f). Staining

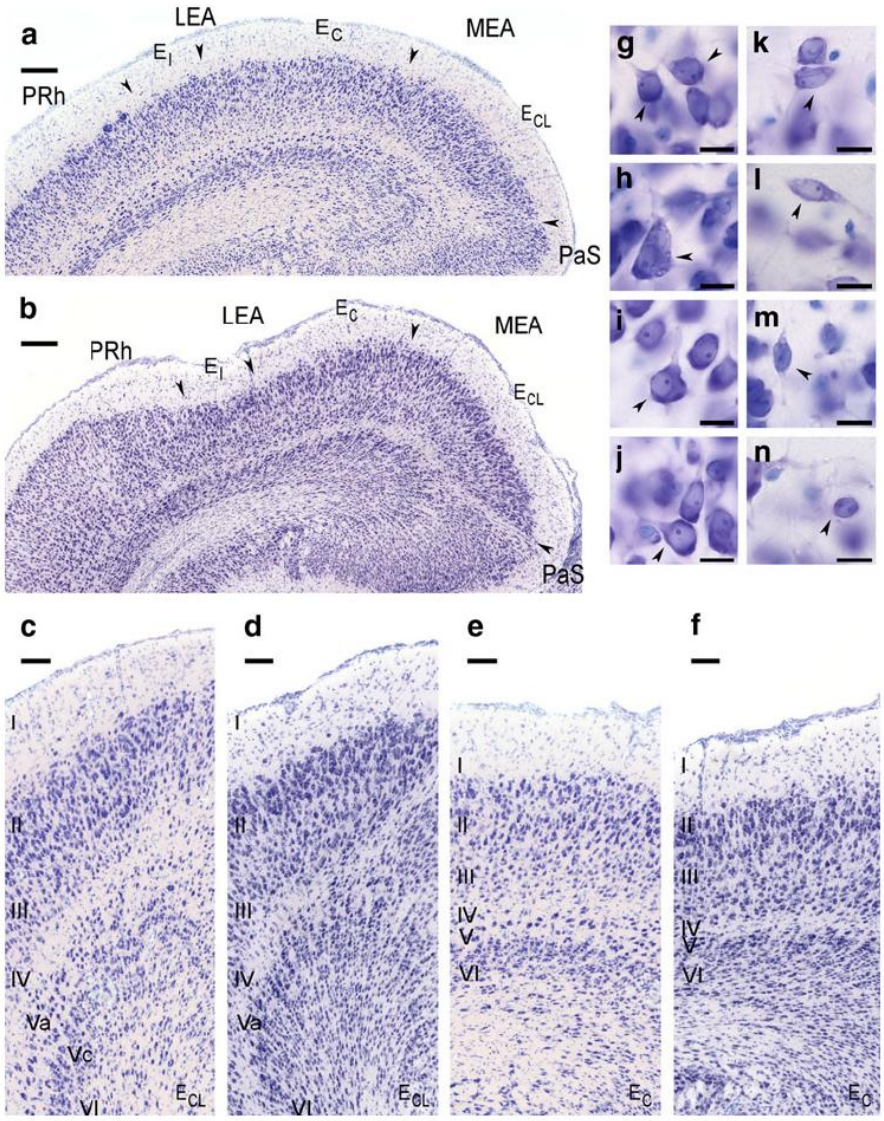

Fig. 2 Horizontal sections at a dorsal level showing rostrocaudal extent of fields E_{CL}, E_C, and E_I, indicated by *arrows* in the straw-coloured fruit bat (**a**, **c**, **e**, **g**) and Wahlberg's epauletted fruit bat (**b**, **d**, **f**, **h**). **c**, **d** E_{CL} layer II is well delineated from layer I; layer IV is prominent, and layers V and VI are radial and columnar. **e**, **f** E_C has an indistinct layer II and stratified Va in **e** and distinct layer II in **f**. Nissl-stained sections showing different neuronal phenotypes (indicated by *arrows*) in MEA layer II in Wahlberg's epauletted fruit bat (**g**, **i**–**m**) and the straw-coloured fruit bat (**h**, **m**). Pial surface is in the *top*. **g** Ovoid stellate cell, **h** polygonal stellate cell, **i** pyramidal cell, **j** oblique pyramidal cell, **k** horizontal tripolar cell, **l** bipolar cell, **m** fusiform cell, **n** small round cell. *Scale bar* **a**, **b** 300 μm; **c**–**f** 250 μm; **g**–**n** 50 μm

sharply drops at the border with layer IV (Fig. 5c). Layer IV has few small cell bodies with radiating processes and spindle-shaped cell bodies with short ascending and descending processes (Fig. 5g). Processes from cell bodies in the layers III and V cross through layer IV (Fig. 5c, h). Layer V has little reactivity. Large and medium-sized polygonal and conical cell bodies with processes directed into layers III, VI and white matter are observed (Fig. 5i, j). A sparse fibre plexus is observed in layers V and VI (Fig. 5h, j, k). Cells are rare in layer VI (Fig. 5k). There are no apparent species differences.

In Wahlberg's epauletted fruit bat, a SMI-32-like immunoreactive fibre plexus and few cell bodies are present in layers II and III (Fig. 4f). SMI-32-like immunoreactivity is not observed in the EC of the straw-coloured fruit bat (Fig. 4e), while characteristic SMI 32-like staining of neocortical neurons is present in this species (Fig. 5n).

Caudal entorhinal field (E_C)

This is the central field of the MEA, located lateral to field E_{CL} and adjacent to the LEA (Fig. 2a, b). Dorso-laterally it apposes the perirhinal cortex and parasubiculum ventro-medially (Fig. 1g, h).

Cytoarchitecture Layer I is broad and well delineated from the layer II. Layer II is wide, moderately cell-dense, and

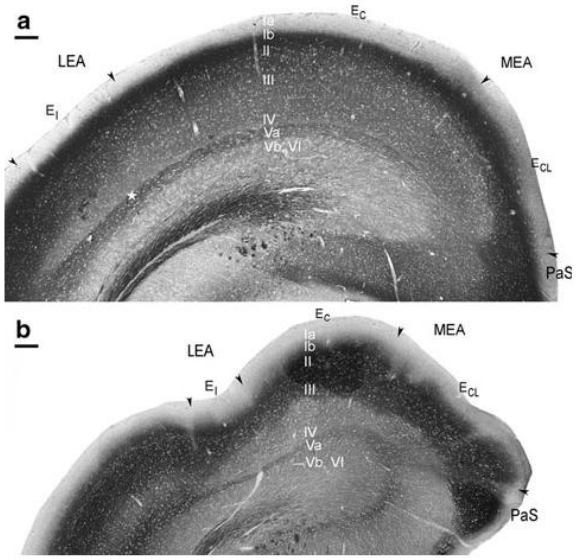

Fig. 3 Timm-stained horizontal sections showing the rostrocaudal extent of E_{CL} and E_C. Deep layer I and II stain darkly, layer III is moderately staining and is separated from a dark sublayer Va by a narrow pale layer IV. Deeper layers are pale staining. **a** Straw-coloured fruit bat. A staining artefact was removed (indicated by *star*). **b** Wahlberg's epauletted fruit bat. *Scale bar* 300 μm

some layer II cells scatter into the deep part of layer I. It is less cell-dense compared to layer II in E_{CL}. Similar to E_{CL}, cells are homogeneously distributed within the layer (Fig. 2a, b, e, f). In the straw-coloured fruit bat (Fig. 2e), and Wahlberg's epauletted fruit bat (Fig. 2f), layer II is populated by varied neuronal phenotypes. Cell-sparse zones between layers II and III are infrequent. Layer III pyramidal neurons are homogenously sized and organised in columns. Layer IV is prominent although narrower in comparison to E_{CL}. Layer V is wide and sublayers Va and Vb are visible; Va is loosely populated and has the stratified appearance observed in field E_{CL} in the straw-coloured fruit bat (Fig. 2e), and Vb is closely apposed to layer VI. Layers V and VI of E_C are not only narrow in comparison to E_{CL} but are also organised in a radial columnar pattern. In both species, layer VI is not sharply demarcated from the white matter.

Chemoarchitecture The Timm-staining of E_C shows similarity in pattern and intensity to field E_{CL} (Fig. 3a, b). Parvalbumin-like immunoreactivity decreases in comparison to E_{CL}, but the staining pattern is the same (Fig. 4c, d). Layer I has immunoreactive processes, and the fibre plexus in layers II and III stains intensely. Cell bodies are observed in layers II to VI.

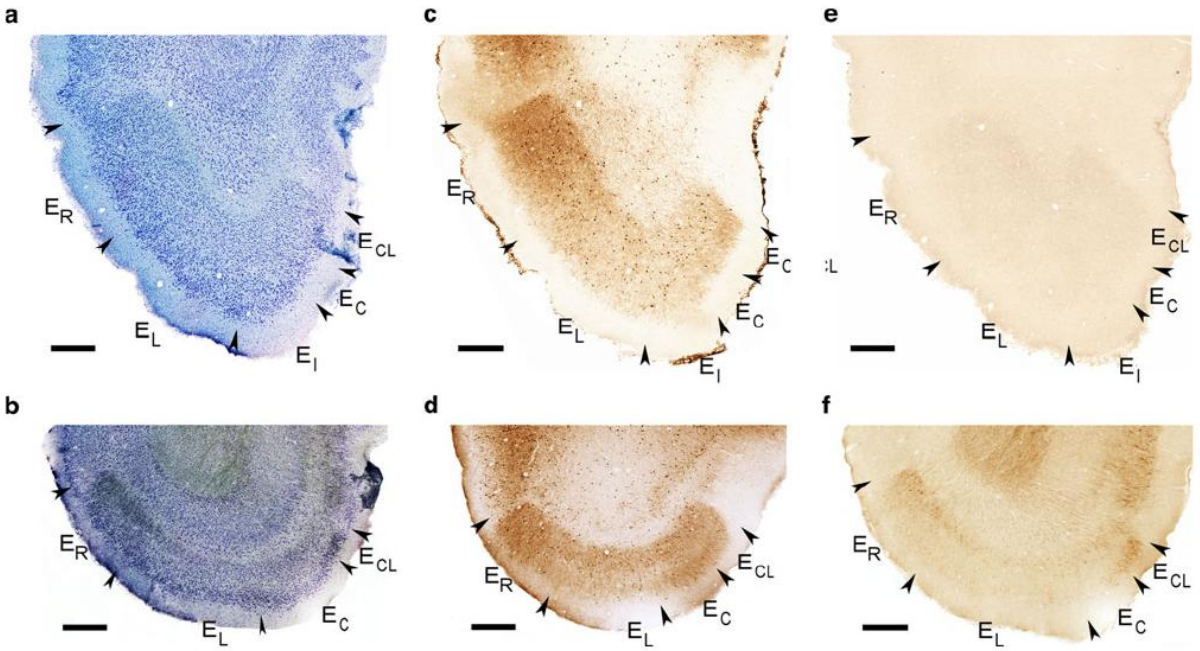

Fig. 4 Coronal sections at a caudal level showing the mediolateral extent of the fields, indicated by *arrows*, in the straw-coloured fruit bat (**a**, **c**, **e**) and Wahlberg's epauletted fruit bat (**b**, **d**, **f**). **a**, **b** Nissl-stained. **c**, **d** Parvalbumin-like reactivity of neurons and fibre plexus involving layers II and III. Most reactivity is observed in E_{CL}, E_L and E_R. **e** Lack of SMI 32-like staining in the straw-coloured fruit bat. **f** SMI 32-like staining in layers II and III of E_{CL}, E_L and E_R of Wahlberg's epauletted fruit bat. *Scale bar* 300 μm

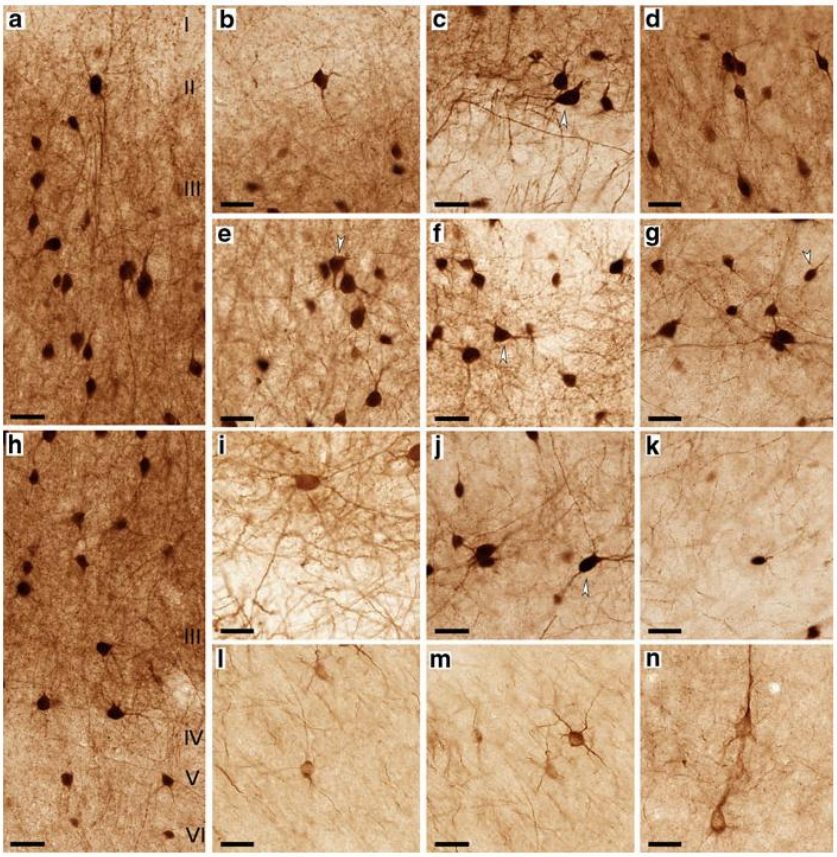

Fig. 5 Parvalbumin-like stained sections in Wahlberg's epauletted fruit bat (**a**–**h**, **j**, **k**) and the straw-coloured fruit bat (**i**). **a** Fibre plexus and several neurons and processes in layers I–III. **b** Multipolar neuron in layer II with processes that extend into layer I. **c** Layer III is well delineated from the weakly stained layer IV. Large spherical multipolar neuron with an ascending thick and descending thin processes, next to a horizontally oriented neuron (*arrow*). **d** Medium-sized conical neurons with thick ascending processes in mid layer III. **e** Large inverted multipolar neuron (*arrow*) with a thick descending process next to a spherical multipolar neuron in layer III. **f** Large multipolar neuron (*arrow*) in layer III sends a process into the weakly stained border between E_{CL} and parasubiculum. **g** Unipolar neuron (*arrow*) in layer IV and few spherical neurons in layers V. **h** Survey of layers II–VI. **i** Multipolar neuron in layer V with radial processes. **j** Large conical neuron (*arrow*) with long smooth ascending and descending processes in layer V. **k** Small unipolar cell in layer VI. SMI 32-like staining in Wahlberg's epauletted fruit bat (**l**, **m**). **l** Pyramidal neuron in layer III. **m** Multipolar neuron in layer III. **n** SMI 32-like stained pyramidal neurons in the somatosensory cortex in the straw-coloured fruit bat. *Scale bar* 100 μm

SMI-32-like staining is weak in Wahlberg's epauletted fruit bat (Fig. 4f), and absent in the straw-coloured fruit bat (Fig. 4e).

Lateral entorhinal area (LEA)

The LEA approximates the perirhinal cortex rostrally and dorsally, the prepiriform cortex ventrolaterally, and the hippocampo-amygdaloid transition area ventromedially.

Laminar structure Within the three fields of the LEA, variations in cellular density and arrangement across the layers are observed (Figs. 6a, b, 7a, b). Neurons in layer II group together in patches and clusters. A narrow cell-free zone is visible between layers II and III, especially in more lateral and rostral fields. Layer IV is generally narrow and visible mainly in field E_I, adjacent to the MEA. Layers V and VI are narrower and organised in rows. Sublayer Va is wide in most of this subdivision. Layers Vb and VI in the LEA are narrow and closely apposed in comparison to those in the MEA.

Intermediate entorhinal field (E_I)

This field is the most caudal and medially located of the LEA (Fig. 6a, b). It is dorso-medial to rhinal sulcus, and it first apposes the perirhinal cortex dorso-medially and subsequently field E_L (Fig. 1g, h). Characteristics of both the MEA and LEA are observed in the laminar organisation of E_I; the superficial layers share characteristics with the LEA,

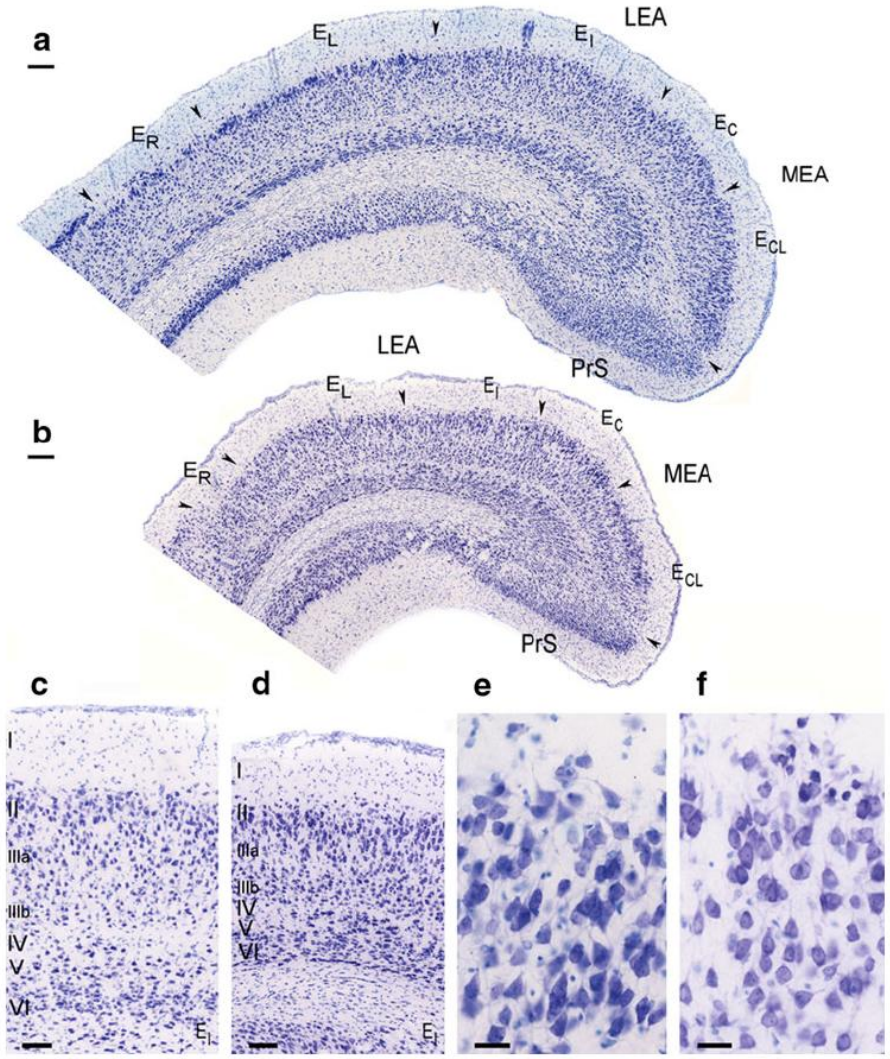

Fig. 6 Horizontal sections at mid dorsoventral level showing the extent of fields E_I, E_L and E_R, indicated by *arrows*, in the straw-coloured fruit bat (**a**, **c**, **e**) and Wahlberg's epauletted fruit bat (**b**, **d**, **f**). **c**, **d** E_I field has a layer II with dispersed neurons, and deep layers have a radial columnar organisation. Layer VI is not well delineated from the white matter in **c**. **e** Small dark staining neurons in layer II. **f** Multiple neuronal phenotypes in layer II. *Scale bar* **a**, **b** 300 μm; **c**, **d** 250 μm; **e**, **f** 100 μm

while the deep layers show characteristics more consistent with MEA. This field could therefore be termed a transition area. It extends to the ventral pole of the EC in the straw-coloured fruit bat (Fig. 1c, e), apposing the parasubiculum ventro-medially and the hippocampal-amygdaloid transition area ventro-rostrally. It is only found in the dorsal one-half of the EC in Wahlberg's epauletted fruit bat (Fig. 1d, f).

Cytoarchitecture Layer I is broad and has lightly stained sparsely distributed small neurons. Layer II is wide (Fig. 6a, b). Neurons disperse from layer II into layer I and some of them appear as ectopic neurons in layer I (Fig. 6c–f). Small dark staining cells are noted in Wahlberg's epauletted fruit bat (Fig. 6f). Occasionally narrow cell-sparse zones are found within layer II and between layers II and III. Neurons in layer III are more evenly distributed than in field E_C, and superficially (sublayer IIIa) neurons are larger than those deeper in the layer (Fig. 6c, d). Layer IV is prominent in both species. Sublayer Va in E_I is comparable in width to E_C. The large pyramids are stratified within the layer in the straw-coloured fruit bat (Fig. 6a, c), but appear closely associated with sublayer Vb in Wahlberg's epauletted fruit bat (Fig. 6b, d). Deeper, layer V is confluent with layer VI, and these layers are narrower compared to those in E_C, but retain the radial columnar organisation (Fig. 6c, d). Layer VI gradually merges with the white matter in the straw-coloured fruit bat (Fig. 6a, c).

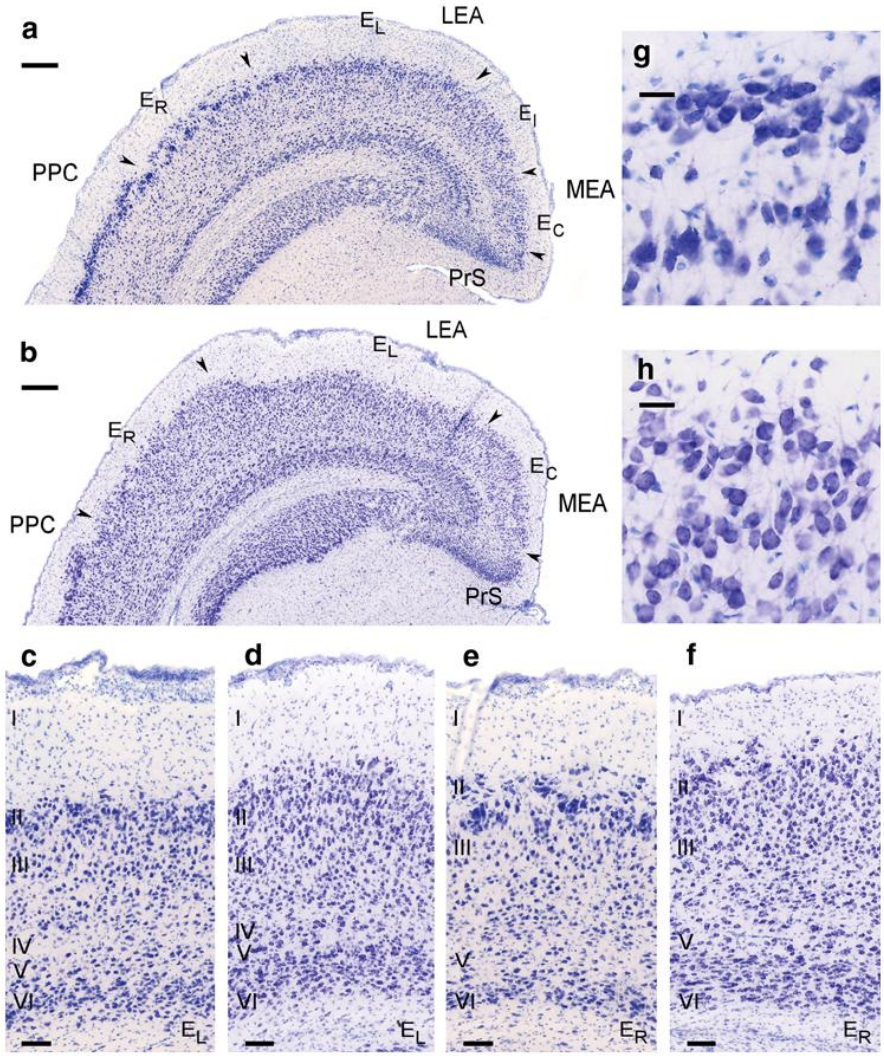

Fig. 7 Horizontal sections at a ventral level showing extent of the lateral fields, E_I, E_L and E_R, indicated by *arrows*, in the straw-coloured fruit bat (**a**, **c**, **e**, **g**) and Wahlberg's epauletted fruit bat (**b**, **d**, **f**, **h**). **c**, **d** E_L has a layer II with clustered neurons better visible in **c**, patchy layer III and wide Va. **e**, **f** E_R has clustered layer II neurons, more distinct in **e**. **g**, **h** Layer II clusters. *Scale bar* **a**, **b** 300 μm; **c**–**f** 250 μm; **g**, **h** 100 μm

Chemoarchitecture In both species, Timm-staining pattern and intensity in E_I are similar to that of the E_{CL} and E_C fields (Figs. 3a, b, 8a, b). A pale layer IV is occasionally observed (Fig. 8b). A moderately stained layer V is present (Fig. 8a, b). Parvalbumin-like staining is faint, comprising a loose fibre plexus, few cell bodies and processes in layers II–V (Fig. 9c, d). SMI-32-like staining is weak in Wahlberg's epauletted fruit bat (Fig. 9f) and absent in the straw-coloured fruit bat (Fig. 9e).

Lateral entorhinal field (E_L)

This field is rostral to E_I. It apposes the perirhinal cortex dorso-laterally, and is caudal to E_R ventrally (Fig. 7a, b). Ventro-medially it apposes the presubiculum and subsequently the hippocampal-amygdaloid transition area.

Cytoarchitecture Layer I is broad, and ectopic layer II neurons are common (Fig. 7c, d). Layer II in the straw-coloured fruit bat has dense cell clusters that are separated by areas of low cell density (Figs. 6a, 7a). Although there are cell dense areas within layer II of Wahlberg's epauletted fruit bat, variations in cell density are much less pronounced than in the straw-coloured fruit bat (Figs. 6b, 7b). A narrow cell-sparse zone is infrequently visible between layers II and III. In both species, layer III is wide and moderately populated. In the straw-coloured fruit bat, neurons are more dispersed than in field E_I (Fig. 7a). In both species, superficially (sublayer IIIa), neurons are densely distributed and appear larger compared to those deeper in the layer (Fig. 7c, d). Layer IV is sometimes present. Layer Va is wider and more populated than in E_I in both species (Figs. 6a, b, 7a, b). Sublayer Vb and layer VI

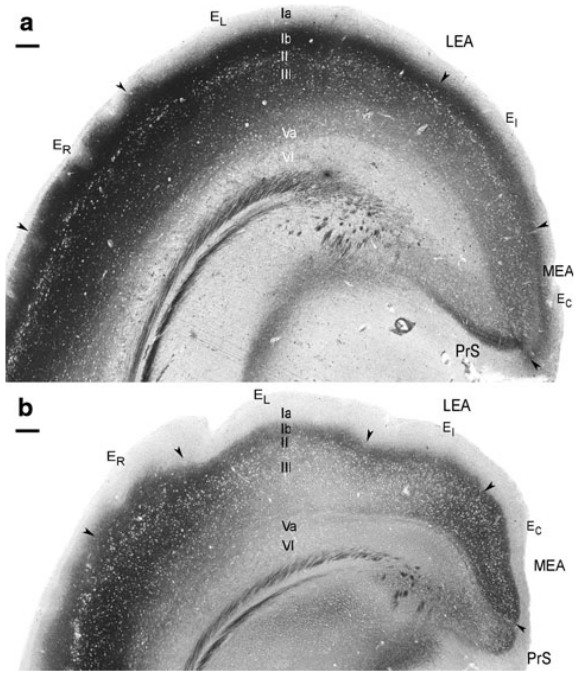

Fig. 8 Timm-stained horizontal sections at a ventral level showing the rostrocaudal extent of fields E_I, E_L and E_R, indicated by *arrows*. Deep layers I, II and III stain darkly, Va stains moderately and Vb and layer VI are pale staining. **a** Straw-coloured fruit bat. **b** Wahlberg's epauletted fruit bat. *Scale bar* 300 μm

are closely apposed, but, in contrast to E_I, they do not appear laminated (Fig. 7c, d). Layers Vb and VI are narrower in comparison to those in E_I, which is more marked in the straw-coloured fruit bat (Fig. 7a).

Chemoarchitecture A strong Timm reaction is noted in the E_L field in the straw-coloured fruit bat (Fig. 8a) and less so in Wahlberg's epauletted fruit bat (Fig. 8b). A pale sublayer Ia contrasts with a darkly stained sublayer Ib. Layers II and III stain moderately in Wahlberg's epauletted fruit bat and darkly in the straw-coloured fruit bat. A moderately stained layer Va is observed. Layers Vb and VI are lightly stained. In both species, parvalbumin-like immunoreactive processes and cell bodies stain with moderate intensity (Figs. 4c, d, 9c, d). In Wahlberg's epauletted fruit bat, SMI 32-like weakly stained cell bodies and processes in layer III are noted (Fig. 4f). No staining is observed in the straw-coloured fruit bat (Figs. 4e, 9e).

Rostral entorhinal field (E_R)

Rostrally, this lateral field is located close to a very shallow rhinal sulcus, dorso-laterally adjoining the perirhinal (Figs. 1h, 6a, b) and prepiriform cortex ventrolaterally (Figs. 1g, 7a, b).

Cytoarchitecture In both species, layer I narrows and layer II is characterised by a decrease in cell density in comparison to other fields (Figs. 6a, b, 7a, b). Layer II has two sublayers separated by cell-sparse zones. This is more distinct in the straw-coloured fruit bat (Figs. 6a, 7a), where superficially sublayer IIa neurons forms narrow and discontinuous bands (Fig. 7e, g). Sublayer IIb is wider than IIa. Cell clusters and areas of lower cell density alternate in a manner similar to layer II in E_L (Fig. 7a, e). Frequent narrow cell-sparse zones extend through layer II into layer III (Fig. 7e). In Wahlberg's epauletted fruit bat, IIa neurons are few, scattered and tend to be located close to IIb (Figs. 6b, 7b). Sublayer IIb is more cell-dense (Fig. 7f, h) than in the straw-coloured fruit bat, and cell clusters are not observed (Fig. 7b, f). Layer II narrows and appears to merge with layer III at the junction of the EC with the perirhinal (Fig. 6a, b) and prepiriform cortex (Fig. 7a, b). Elsewhere, layer II is separated from layer III by cell-sparse zones. Layer III is wide and patchily organised superficially, less noticeably in Wahlberg's epauletted fruit bat (Fig. 7e, f). Deeper, layer III has a population of smaller pyramidal neurons. Layer IV is infrequently observed in Wahlberg's epauletted fruit bat and cannot be distinguished in the straw-coloured fruit bat. Sublayer Va is wider and more populated in comparison to field E_L (Fig. 7a, b). The large pyramidal neurons are stratified within the layer in the straw-coloured fruit bat (Fig. 7a, e), but this organisation is less obvious in Wahlberg's epauletted fruit bat (Fig. 7b, f). Layers Vb and VI have the same width as those in E_L in Wahlberg's epauletted fruit bat (Fig. 7b), but these layers thin along the rostral–lateral extent in the straw-coloured fruit bat (Fig. 7a). A columnar organisation of layers Vb and VI is observed in the straw-coloured fruit bat (Fig. 7a, e).

Chemoarchitecture Field E_R shows a pale layer Ia, dark Ib, II and III, moderately staining Va and pale Vb and VI (Fig. 8a, b). The Timm-staining pattern and intensity is similar to that of field E_L in the straw-coloured fruit bat (Fig. 8a). Darkly stained protuberances are observed in sublayer Ia, giving a wavy appearance (Fig. 8a, b). Parvalbumin-like immunoreactivity in E_R is strong (Fig. 9c, d) with a pattern that is similar to that of E_{CL} (Fig. 4c, d). The fibre plexus is intensely stained, as are the cell bodies and processes in layers II to V. Layer VI is weakly reactive. Parvalbumin-like reactivity decreases at the border between E_R and perirhinal (Fig. 9c, d) and prepiriform cortex (Fig. 4c, d). In Wahlberg's epauletted fruit bat, SMI 32-like staining is observed between layers II and VI (Figs. 4f, 9f). Fine and sometimes thick, vertically oriented processes run between the layers and cross the white matter. Layer II has few cell bodies. A band of conical and polygonal cell bodies is seen in the

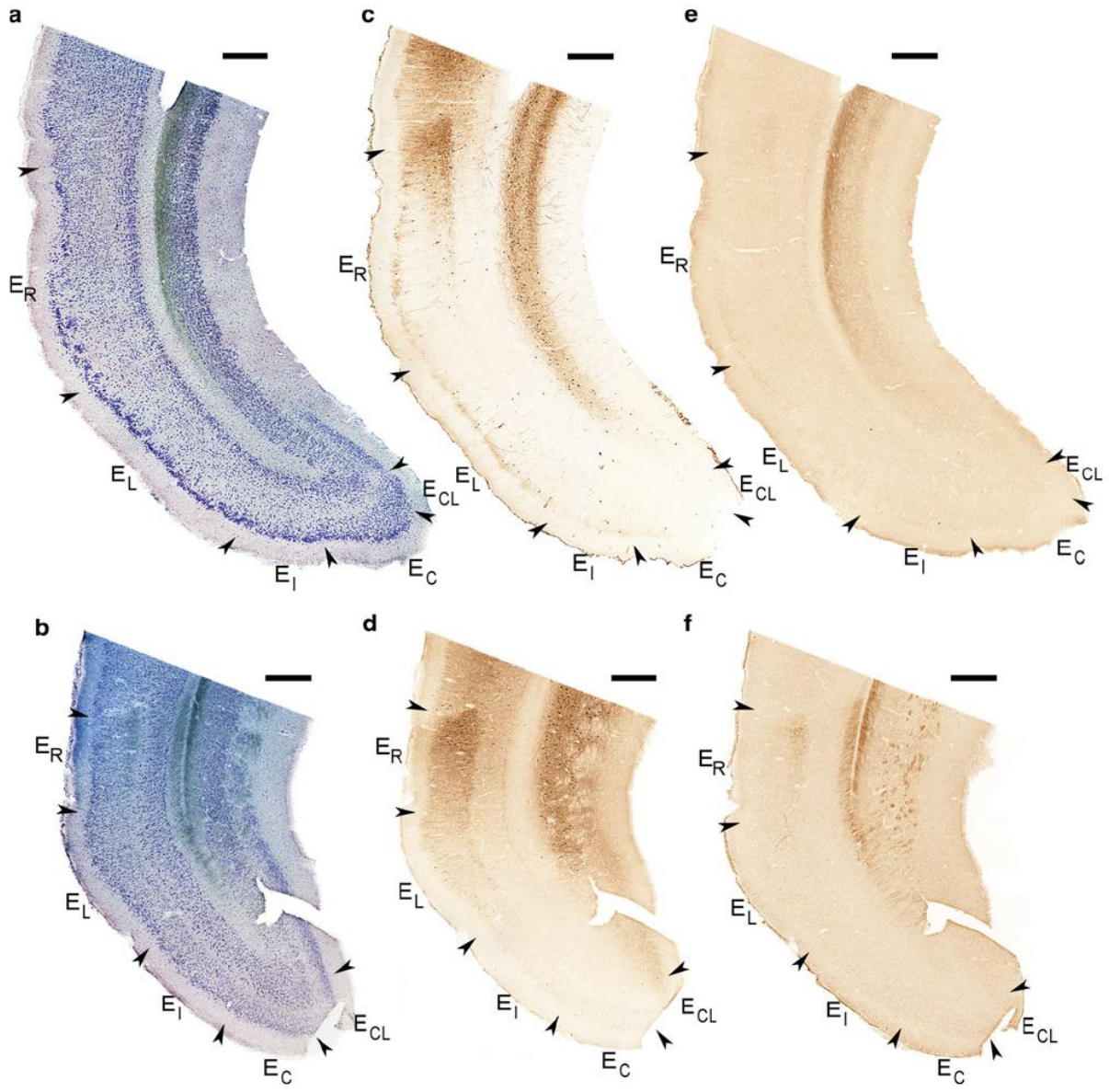

Fig. 9 Coronal sections at a rostral level showing the mediolateral extent of the fields, indicated by *arrows*, in the straw-coloured fruit bat (**a**, **c**, **e**) and Wahlberg's epauletted fruit bat (**b**, **d**, **f**). **a**, **b** Nissl-stained. **c**, **d** Parvalbumin-like reactivity of neurons and fibre plexus in field E_R. **e** Lack of SMI 32-like staining. **f** SMI 32-like staining in layer III in field E_R. *Scale bar* 300 μm

deep part of layer III (Figs. 4f, 5l, m). Some of these cell bodies are small, stain lightly and have apical and basal processes that can be traced for a short distance within the layer. Other cell bodies are larger, stain intensely, and their radiating processes can be traced in adjacent layers (Fig. 5l, m). Layer V has rare large cell bodies. The intensity of staining increases rostrally in this field.

Cell numbers and phenotypes in MEA layer II

Morphological phenotypes Ovoid stellate cells are spherical and oriented vertically (Fig. 2g). Large, trapezoid stellate cells that are either transversely or vertically oriented are referred to as polygonal stellate (Fig. 2h). Pyramidal cells are medium-sized to large, conical bodies with a large apical process oriented perpendicular to the pial

Table 1 MEA layer II neuronal phenotypes, profile areas and proportions

Cell type	Species	*N*	Mean area (μm^2)	SD (μm^2)	Proportion (%)
Ovoid stellate	*E. helvum*	352	162	44	35.8
	E. wahlbergi	193	164	46	40.8
Polygonal stellate	*E. helvum*	48	193	51	4.9
	E. wahlbergi	61	212	60	12.9
Pyramidal	*E. helvum*	181	196	51	18.4
	E. wahlbergi	83	232	61	17.5
Oblique pyramidal	*E. helvum*	62	192	43	6.3
	E. wahlbergi	23	212	66	4.9
Other	*E. helvum*	339	115	39	34.5
	E. wahlbergi	113	98	26	23.9
All cells measured	*E. helvum*	982	156	54	100
	E. wahlbergi	473	168	67	100

Table 2 Total number of neurons in MEA layer II

Species	Animal	Estimated total cell number	CE
E. helvum	1	56,067	0.06
	2	61,632	0.08
	3	56,265	0.09
	4	74,123	0.08
E. wahlbergi	1	31,712	0.09
	2	27,344	0.1
	3	33,147	0.08
	4	30,497	0.1

surface (Fig. 2i). Oblique pyramidal cells resemble the pyramidal cells, but have an apical process that is directed obliquely to the pial surface (Fig. 2j). 'Other' cells include generally small cells of tripolar (Fig. 2k), round (Fig. 2l), bipolar (Fig. 2m), or fusiform (Fig. 2n) appearance and medium-sized multipolar neurons. Cells of this class are located mostly superficially in layer II.

Sectional areas of neuronal phenotypes and the contribution of these phenotypes to the layer II cell population are listed in Table 1. Significant main effects were found for species, cell type and species × cell type interactions ($P < 0.001$ for all comparisons), with Wahlberg's epauletted fruit bat having a larger mean cell area for the polygonal stellate and pyramidal cell types, while 'other cells' are smaller in this species. In the comparison of cell sizes, stringent Bonferroni and lenient LSD posthoc testing produced identical outcomes in terms of significant differences between phenotypes. Ovoid stellate cells are different in size from all other cell types ($p_{LSD} < 0.001$ for all comparisons); polygonal stellate, oblique pyramidal and pyramidal cells are similar in size (polygonal stellate vs. pyramidal: $p_{LSD} = 0.46$, polygonal stellate vs. oblique pyramidal: $p_{LSD} = 0.37$, pyramidal vs. oblique pyramidal: $p_{LSD} = 0.09$) but different from other cell types ($p_{LSD} < 0.001$ for all other comparisons).

Layer II in the straw-coloured fruit bat has an estimated mean total cell count (Table 2) of 62,022 (SD 8,469, CE = 0.08), and in Wahlberg's epauletted fruit bat 30,675 (SD 2,470, CE = 0.09).

Discussion

We have provided a detailed description of the laminar and areal organisation of the megachiropteran entorhinal cortex using markers that have helped to define these regions in other species as well. In the following, the differences between the two bat species, rodents and primates, summarised in Table 3, are discussed from an anatomical and functional perspective.

Cytoarchitectonic comparison

Medial entorhinal area (MEA) Layer II of the most caudal and medial field is broad, continuous and well delineated from layer I above in the bats, primates and rodents. The islands described in the adjacent field, E_C (primates) (Amaral et al. 1987), are not well developed in the bats and rodents (Insausti et al. 1997). Layer III is similarly organised in the bats, primates and rodents, starting off patchy caudally, but progressively adopting a columnar arrangement in E_C and in the less caudal MEA field (ME) in rodents. Differences in cellular density in IIIa and IIIb are described in ME, but this is neither observed in the bats nor described in the primates. Layer IV is well developed in the bats and rodents but poorly visible or absent in the primates. Layer V in the bats, primates and rodents is well developed, with sublayers Va and Vb. The

Table 3 Summary of cytoarchitectural comparison between bats, primates and rodents

Region	Comparison
E_{CL}/CE	Layers II and III mostly similar
	Poorly developed layer IV in primates
	Layer Va moderately developed in rodents, well developed in bats and best developed in primates
E_C/ME	Layer II well differentiated in rodents and Wahlberg's epauletted fruit bat but islands only in primates
	Layer III bilaminar only in rodents
	Deep layers as in the E_{CL}/CE
E_I/VIE	Layer II moderately differentiated in bats and rodents, distinct islands only in primates
	Well developed layers III and IV in rodents, primates and bats
	Well-defined Va only in primates and bats
E_L/DLE	Layer II well differentiated in the straw-coloured fruit bat and rodents but distinct islands only in primates, poorly differentiated layer II in Wahlberg's epauletted fruit bat
	Wide layer III in bats and primates, narrow in rodents
	Layer IV absent in primates
	Layer Va well developed in primates and bats, indistinct Va in rodents
E_R/DIE	Indistinct islands in layer II of the straw-coloured fruit bat and rodents, wide cell islands in primates
	Bilaminar wide layer III in bats, rodents and primates
	Layer IV well developed in mouse, poorly developed in Wahlberg's epauletted fruit bat and rat, absent in straw-coloured fruit bat and primates
	Layer Va poorly developed in rodents, well developed in bats, all sublayers best developed in primates
	Well-developed layer VI in mouse, primates, and Wahlberg's epauletted fruit bat

CE, ME, VIE, DIE, DLE refer to regions in rodents

pyramidal cells of Va appear as 1–2 bands in Wahlberg's epauletted fruit bat, and appear closely apposed to Vb, which is also observed in rodents. Sublayer Va in the straw-coloured fruit bat is as well developed as in primates, showing 3–4 bands of pyramids. Sublayer Vc, which is prominent in the medial fields in primates, is infrequently visible in the bats and not described in rodents (Amaral et al. 1987; Blaizot et al. 2004; Insausti et al. 1997; van Groen 2001).

Lateral entorhinal area (*LEA*) Of the lateral fields, E_I shows similarity between the two bat species. The intermediate field is referred to as VIE in the rodents (Insausti et al. 1997). Similar characteristics found in rodents, primates and bats include layer II clusters and a patchy layer III. Layer II islands are a feature in the primates that is absent in both bats and rodents. The bilaminar layer III, presence of layer IV and a well-defined Va are characteristics shared by the bats and primates in E_I but not rodents (Amaral et al. 1987; Insausti et al. 1997; van Groen 2001).

Clustering in layer II is observed in E_L field in the straw-coloured fruit bat, primates and the corresponding DLE in rodents (Amaral et al. 1987; Insausti et al. 1997; van Groen 2001). If clustering is a distinctive feature of this subdivision, then Wahlberg's epauletted fruit bat has a poorly differentiated layer II. Cell-sparse zones infrequently separate layers II and III in the rodents and bats but only in a caudal part of the LEA in primates. Layer III has a bilaminar character, observed in rodents and bats, but not in primates. While layer III is narrow in the rodents, it is wide in the bats and primates. Layer IV is infrequently visible in the bats and rodents and absent in the primates. Layer Va is prominent in the bats and primates (Amaral et al. 1987). Layer V in rodents is narrow and comprised mostly of sublayer Vb, and few pyramids in Va (Insausti et al. 1997; van Groen et al. 2003). Layer VI has a less-stratified appearance in bats, primates and rodents.

The layer II clusters in E_R field are separated by cell-sparse zones into indistinct islands in the straw-coloured fruit bat, but they do not develop into the wide cell islands distinctive of primate LEA layer II (Amaral et al. 1987; Blaizot et al. 2004). The corresponding field in rodents, DIE (Insausti et al. 1997; van Groen 2001) appears similar to the straw-coloured fruit bat. Cell-sparse zones separating layers II and III in the E_R field described in the primates

and rodents are observed in the bats, less frequently in Wahlberg's epauletted fruit bat. The wide and bilaminar character of layer III in the bats is consistent with descriptions made in related fields in primates and rodents. In the straw-coloured fruit bat and primates, layer IV is not visible in the E_R field (Amaral et al. 1987). Similar observations have been made in a corresponding field, Pr2 in the rhesus monkey (van Hoesen and Pandya 1975). Layer IV is present in the mouse (van Groen 2001) and infrequently observed in Wahlberg's epauletted fruit bat and the rat (Insausti et al. 1997). Layer Va is wide and has 3–4 rows of pyramids, more so in the straw-coloured fruit bat, resonating with descriptions made in primates (Amaral et al. 1987; Blaizot et al. 2004). The pyramids associated with this layer appear incidentally in rodents (Insausti et al. 1997; Mulders et al. 1997). All three sublayers of layer V are only consistently observed in primates. Layers Vb and VI narrow rostrally in the straw-coloured fruit bat. In the rat, only layer VI narrows (Insausti et al. 1997). In Wahlberg's epauletted fruit bat, mouse (van Groen et al. 2003) and primates (Amaral et al. 1987), layer VI is well developed.

Chemoarchitectonic comparison

Timm-staining reveals the laminar organisation of the EC, which assisted in delineating the EC from adjacent structures, and distinguished between medial and lateral subdivisions and their layers. In the two species, dark staining is observed in layers Ib and II in all fields and part of layer III in the E_R field. Layer Va stains moderately, and layers IV, Vb and VI are pale. The staining pattern corresponds to the presence of zinc in the boutons of the terminals of telencephalic afferents to the EC (Perez-Clausell and Danscher 1985; Slomianka 1992), where zinc may serve as a neuromodulator of excitatory transmission (Frederickson et al. 2005; Paoletti et al. 2009). The distribution of zinc-containing boutons in bats is comparable to observations made in the guinea pig, dog and pig (Geneser-Jensen et al. 1974; Holm and Geneser 1989; Woźnicka et al. 2006). In the rat and mouse, the staining is moderate in layers Ib and II of MEA and increases gradually across layer III to become very intense at the layer III/IV boundary (Slomianka 1992; Slomianka and Geneser 1991).

Parvalbumin-like immunostaining varies along a mediolateral gradient, and is comparable in the two fruit bats. Staining mainly occurs in the E_R, E_L and medial fields, and an intermediate reactivity in the E_I field. Parvalbumin is present in GABAergic interneurons of the EC in layers II, III, V and VI and predominantly expressed by chandelier and basket cells (DeFelipe et al. 1989; Fonseca et al. 1993; Hendry et al. 1989). Observations in the fruit bats are consistent with reported distributions of parvalbumin in rat (Wouterlood et al. 1995), guinea pig (Uva et al. 2004), macaque (Pitkänen and Amaral 1993) and human EC (Beall and Lewis 1992; Tuñón et al. 1992). Thus, there does not seem to be much difference in the role of this calcium-binding protein and the part of the inhibitory circuitry identified by it in the EC across species (Hof and Sherwood 2005).

SMI-32 recognises a high molecular weight (200kD) non-phosphorylated neurofilament protein H (Sternberger and Sternberger 1983) in neuronal soma, dendrites and some large calibre axons of specific subpopulations of neurons resulting in a distinct cellular and laminar staining pattern. This protein also occurs in a subset of cortical neurons selectively lost in Alzheimer's disease (Hof et al. 1990; Morrison et al. 1987). In Wahlberg's epauletted fruit bat, immunoreactivity in particular defines layer III of the EC. Most of the staining is observed in the E_R and medial fields. Rostrally, the staining in layers II, III and V concurs with observations made in the E_L field of the macaque and human, where a rostral–caudal gradient was noted (Beall and Lewis 1992; Saleem et al. 2007). The prevalent staining of layer III is in contrast to the macaque, where it mainly involves layers II and V of LEA (Saleem et al. 2007). A comparative analysis in the visual cortex shows similarities in regional staining patterns between closely related species; these patterns are shown to be predictive of evolutionary relationships (Hof et al. 2000). This may imply that the two bat species may not be as phylogenetically close as we presume. It could also be that the EC is a less adept model for this hypothesis, and a lack of immunoreactivity in the EC of the straw-coloured fruit bat may indicate that the function subserved by SMI-32 immunoreactive cytoskeletal components may either not be required or is assumed by another protein (Campbell and Morrison 1989; Goldstein et al. 1983). There are similar reports of a lack of SMI-32 immunoreactivity in the EC that include an Australian echidna (*Tachyglossus aculeatus*) and the Tamar wallaby (*Macropus eugenii*) (Ashwell et al. 2005; Hassiotis et al. 2004, 2005).

Cytoarchitectural synopsis

Overall, the organisation of the EC cannot be categorised as either primate- or rodent-like; rather the EC shows a mosaic of characters. The two bat species share, e.g., a well-developed layer Va throughout the EC with primates, while they share with rodents the absence of distinct layer II islands in most EC fields. Species-specific characteristics are largely restricted to layer II, which is better differentiated in the MEA of Wahlberg's epauletted fruit bat, while it, in comparison to the straw-coloured fruit bat, is poorly differentiated in the LEA. Buhl and Dann (1991) already noted a primate-like dispersion of hippocampal pyramidal

Table 4 Indices for encephalisation (EI), neocorticalization (NEO) and the sizes of the hippocampus (HIP) and schizocortex (SCH) for the bats investigated in this study, rat and the major primate groups

Species	EI	NEO	HIP	SCH
E. helvum[a]	311	1,088	283	373
E. wahlbergi[a]	302			
E. labiatus[a]	292	999	281	328
Rattus norwegicus[b]	155	475	132	122
Prosimian primates[c]	415	2,100	~290	~360
Simian primates[c]	801	5,100	~280	~320
Human[c]	3,012	20,000	~500	~680

For *E. wahlbergi* only the encephalisation index is available. *Epomophorus labiatus*, which is equal in body weight to *E. wahlbergi*, was included to present values for NEO, HIP and SCH

[a] Data from Baron et al. (1996b)

[b] Calculated from Baron et al. (1996b) and Kruska (1975)

[c] Calculated from Stephan et al. (1986)

cells, which we also observed in the species investigated here, and which in other species provide hippocampal afferents to the EC layer Va (Swanson and Cowan 1977). The EC layer Va, in turn, provides afferents to neocortical areas (Swanson and Köhler 1986).

Fruit bats share with primates high indices for encephalization and neocorticalization as well as high indices for the size of the schizocortex (Table 4). The schizocortex contains, in addition to the entorhinal cortex, the pre- and parasubiculum as well as the perirhinal cortex. While an interference from these additional structures with the outcomes of quantitative comparisons cannot be excluded, the entorhinal cortex is the major constituent of the schizocortex. Also, the relation between indices for the hippocampus and schizocortex is very similar between bats and primates but differs from that of the rat. It is therefore not surprising that structural similarities exist in layer V of bats and primates. The cortical and sub-cortical inputs into layer V and intrinsic associational connections suggest that it may play a more significant role in memory operations (Burwell and Amaral 1998; Hamam et al. 2000, 2002; Kerr et al. 2007; Suzuki and Amaral 1994). At least for CA → entorhinal → cortical interactions bats may serve as a primate-like model.

If the morphology of layer II, which appears more rodent-like in structure, can be used as a guideline, this is not true for cortical → entorhinal → dentate interactions. However, EC layer II also differs between the two bats, and both bats apparently differ in the cellular composition and relative sizes of MEA layer II from primates and rodents (see below). We previously suggested that changes in the structure and connectivity of the phylogenetically rather pliable dentate gyrus may subserve species-specific demands on hippocampal function (Slomianka and Geneser 1991; Slomianka and West 1989). Species- and/or group-specific changes in the cortical region providing input to the dentate gyrus, as observed in the EC layer II of bats, should therefore be expected.

MEA layer II neuronal phenotypes and proportions

Cytoarchitectonic descriptions of the MEA in the rat (Insausti et al. 1997), mouse (Slomianka and Geneser 1991), dog (Woźnicka et al. 2006), macaque (Amaral et al. 1987), baboon (Blaizot et al. 2004) and human (Insausti et al. 1995) indicate that the stellate cell is the dominant neuronal phenotype. Quantitative studies estimated that stellate cells constitute 67–81% of the neuronal population and pyramidal cells between 16 and 32% in the rat and human MEA layer II (Mikkonen et al. 2000; Schwartz and Coleman 1981). We found that this layer contains an unusually large proportion of small cells (24 and 35%) that are neither stellate nor pyramidal. The stellate cell in the bats, as the single dominant phenotype at 36 and 41%, is well below reported values of over 60%. However, estimates of the pyramidal cell at ~18% are rather close to those of other species. Intracellular neuronal staining (Mikkonen et al. 2000) may have been biased by the selection of large cells in restricted EC areas, while Schwartz and Coleman (Schwartz and Coleman 1981) estimated proportions within only hippocampally projecting layer II cells. The number-weighted selection of cells for classification using disector probes at a uniform random systematic set of sampling sites throughout the EC should be unbiased by cell size and distribution. However, methodological differences cannot easily explain why one set of numbers is so different while another set is very close, and it is likely that bats differ from rats and humans in the cellular composition of MEA layer II. To pinpoint the nature of differences, a design-based stereological assessment of the cellular composition in the other species is needed.

Neuron number in the rat was estimated to 6.6×10^4 in MEA layer II (Mulders et al. 1997). This is almost twice the count in Wahlberg's epauletted fruit bat, which has approximately the same brain weight (2 g) as a rat, and although comparable to the straw-coloured fruit bat, the brain weight (4 g) is about twice that of the rat. It would be of interest to establish if the input from layer II is shared by the dentate gyrus and CA2/3 region of the hippocampus in the ratio (~17.7) reported in the primates and rat (Mulders et al. 1997). In the dentate gyrus, the straw-coloured fruit bat has an estimated mean total granule cell count of ~1,200,000 and that of Wahlberg's epauletted fruit bat is ~900,000 (C. Gatome, unpublished observations). The ratios granule cells:MEA layer II of ~19 (straw-coloured fruit bat) or ~29 (Wahlberg's epauletted fruit bat) show that large differences in the divergence of the projection

from the MEA layer II to the dentate gyrus can occur in closely related species. The estimated ratio in the rat of about ~18 (Mulders et al. 1997; West et al. 1991) distinctly differs from Wahlberg's epauletted fruit bat. This difference in divergence may well explain the increase in the size of some neuronal phenotypes, likely to be hippocampal projecting in Wahlberg's epauletted fruit bat, which is the smaller species.

Functional implications

Stellate cells are, in the entorhinal cortex as elsewhere, considered modified pyramidal cells (Germroth et al. 1989b, 1991; Klink and Alonso 1997a; Peters and Jones 1984) and share with them a number of electrophysiological properties (Alonso and Klink 1993; Alonso and Llinas 1989; van der Linden and Lopes da Silva 1998). However, the two cell types differ from their morphological complements in layer III (Erchova et al. 2004; van der Linden and Lopes da Silva 1998), and, for example, in their modulation by cholinergic inputs also from each other (Klink and Alonso 1997b). This may imply two parallel channels that act differently on the hippocampus (Alonso and Klink 1993; Klink and Alonso 1997a). The physiological properties of non-stellate or non-pyramidal neurons are not reported, although it is known that some phenotypes, such as the horizontal bipolar and tripolar cells also contribute to the perforant pathway (Germroth et al. 1989a).

The medial EC contains grid cells that fire selectively in specific locations in the environment (Brun et al. 2008; Fyhn et al. 2004; Hafting et al. 2005). Although correlational evidence based on dynamic membrane properties points towards the stellate cell as the anatomical equivalent of the grid cell (Garden et al. 2008; Giocomo and Hasselmo 2008), other morphological phenotypes cannot be ruled out. The current knowledge on grid cells supports a two-dimensional representation of the environment (Hafting et al. 2005). If and how grid cells represent dimensions that not only reflect movement across a surface but also above a surface is a question that, in mammals, can most easily be addressed in bats. It is tempting to speculate that the relative proportions of cell types within layer II are associated with the representation of a three-dimensional environment. Alternatively, the proportions observed in bats may be a trait reflecting the phylogenetic history of the Chiroptera, which must accommodate, but is not necessarily specific to a three-dimensional representation.

Acknowledgments We thank Prof. Menno Witter for a critical reading of the manuscript. We are grateful for the help of Mr. Ben Agwanda (National Museums of Kenya, Nairobi), and Dr. Robert Kityo (Makerere University, Kampala) for guidance on the species biology and ecology and logistical support, Mr. Francis Muchemi (National Museums of Kenya, Nairobi), and Dr. Joseph M. Bukenya (Rubaga Hospital, Kampala) for assistance in the capture. Dr. Urs Ziegler (ZMB, Zürich) kindly introduced us to the 3D modelling software. This work was supported by grants from Rita Levi Montalcini Fellowship for African Women in Neuroscience, International Brain Research Organisation, National Centre for Competence in Research (NCCR) Neural Plasticity and Repair, and Swiss National Science Foundation.

References

Alonso A, Klink R (1993) Differential electroresponsiveness of stellate and pyramidal-like cells of medial entorhinal cortex layer II. J Neurophysiol 70:128–143

Alonso A, Llinas RR (1989) Subthreshold Na^+-dependent theta-like rhythmicity in stellate cells of entorhinal cortex layer II. Nature 342:175–177

Amaral DG, Insausti R, Cowan WM (1987) The entorhinal cortex of the monkey: I. Cytoarchitectonic organization. J Comp Neurol 264:326–355

Ashwell KW, Zhang LL, Marotte LR (2005) Cyto- and chemoarchitecture of the cortex of the tammar wallaby (*Macropus eugenii*): areal organization. Brain Behav Evol 66:114–136

Baron G, Stephan H, Frahm HD (1996a) Atlases of a Megachiroptera brain. In: Baron G, Stephan H, Frahm HD (eds) Comparative neurobiology of Chiroptera: macromorphology, brain structures, tables and atlases, vol 1. Birkhäuser Verlag, Basel, pp 433–529

Baron G, Stephan H, Frahm HD (1996b) Comparative brain characteristics. In: Baron G, Stephan H, Frahm HD (eds) Comparative neurobiology of Chiroptera: macromorphology, brain structures, tables and atlases, vol 1. Birkhäuser Verlag, Basel, 529 pp

Beall MJ, Lewis DA (1992) Heterogeneity of layer II neurons in human entorhinal cortex. J Comp Neurol 321:241–266

Blaizot X, Martinez-Marcos A, Arroyo-Jimenez MdM, Marcos P, Artacho-Perula E, Munoz M, Chavoix C, Insausti R (2004) The parahippocampal gyrus in the Baboon: anatomical, cytoarchitectonic and magnetic resonance imaging (MRI) Studies. Cereb Cortex 14:231–246

Brodmann K (1909) Vergleichende Lokalisationslehre der Grosshirnrinde in ihren Prinzipien dargestellt auf Grund des Zellenbaues. Barth, Leipzig

Brodmann K (1925) Vergleichende Lokalisationslehre der Grosshirnrinde. C. G. Leipzig, Röder GmbH, pp 177–183

Brun VH, Solstad T, Kjelstrup KB, Fyhn M, Witter MP, Moser EI, Moser MB (2008) Progressive increase in grid scale from dorsal to ventral medial entorhinal cortex. Hippocampus 18:1200–1212

Buhl EH, Dann JF (1991) Cytoarchitecture, neuronal composition, and entorhinal afferents of the flying fox hippocampus. Hippocampus 1:131–152

Burwell RD, Amaral DG (1998) Perirhinal and postrhinal cortices of the rat: interconnectivity and connections with the entorhinal cortex. J Comp Neurol 391:293–321

Campbell MJ, Morrison JH (1989) Monoclonal antibody to neurofilament protein (SMI-32) labels a subpopulation of pyramidal neurons in the human and monkey neocortex. J Comp Neurol 282:191–205

DeFelipe J, Hendry SH, Jones EG (1989) Visualization of chandelier cell axons by parvalbumin immunoreactivity in monkey cerebral cortex. Proc Natl Acad Sci USA 86:2093–2097

Dorph-Petersen KA, Nyengaard JR, Gundersen HJG (2001) Tissue shrinkage and unbiased stereological estimation of particle number and size. J Microsc 204:232–246

Erchova I, Kreck G, Heinemann U, Herz AV (2004) Dynamics of rat entorhinal cortex layer II and III cells: characteristics of

membrane potential resonance at rest predict oscillation properties near threshold. J Physiol 560:89–110
Fonseca M, Soriano E, Ferrer I, Martinez A, Tunon T (1993) Chandelier cell axons identified by parvalbumin-immunoreactivity in the normal human temporal cortex and in Alzheimer's disease. Neuroscience 55:1107–1116
Frederickson CJ, Koh JY, Bush AI (2005) The neurobiology of zinc in health and disease. Nat Rev Neurosci 6:449–462
Fyhn M, Molden S, Witter MP, Moser EI, Moser M-B (2004) Spatial representation in the entorhinal cortex. Science 305:1258–1264
Fyhn M, Hafting T, Witter MP, Moser EI, Moser M-B (2008) Grid cells in mice. Hippocampus 18:1230–1238
Garden DL, Dodson PD, O'Donnell C, White MD, Nolan MF (2008) Tuning of synaptic integration in the medial entorhinal cortex to the organization of grid cell firing fields. Neuron 60:875–889
Geneser-Jensen FA, Haug FM, Danscher G (1974) Distribution of heavy metals in the hippocampal region of the guinea pig. A light microscope study with Timm's sulfide silver method. Z Zellforsch Mikrosk Anat 147:441–478
Germroth P, Schwerdtfeger WK, Buhl EH (1989a) GABAergic neurons in the entorhinal cortex project to the hippocampus. Brain Res 494:187–192
Germroth P, Schwerdtfeger WK, Buhl EH (1989b) Morphology of identified entorhinal neurons projecting to the hippocampus. A light microscopical study combining retrograde tracing and intracellular injection. Neuroscience 30:683–691
Germroth P, Schwerdtfeger WK, Buhl EH (1991) Ultrastructure and aspects of functional organization of pyramidal and nonpyramidal entorhinal projection neurons contributing to the perforant path. J Comp Neurol 305:215–231
Giocomo LM, Hasselmo ME (2008) Time constants of h current in layer ii stellate cells differ along the dorsal to ventral axis of medial entorhinal cortex. J Neurosci 28:9414–9425
Goldstein ME, Sternberger LA, Sternberger NH (1983) Microheterogeneity ("neurotypy") of neurofilament proteins. Proc Natl Acad Sci USA 80:3101–3105
Gundersen HJG, Jensen EB, Kiêu K, Nielsen J (1999) The efficiency of systematic sampling in stereology–reconsidered. J Microsc 193:199–211
Hafting T, Fyhn M, Molden S, Moser MB, Moser EI (2005) Microstructure of a spatial map in the entorhinal cortex. Nature 436:801–806
Hamam BN, Amaral DG, Alonso AA (2000) Morphological and electrophysiological characteristics of layer V neurons of the rat medial entorhinal cortex. J Comp Neurol 418:457–472
Hamam BN, Amaral DG, Alonso AA (2002) Morphological and electrophysiological characteristics of layer V neurons of the rat lateral entorhinal cortex. J Comp Neurol 451:45–61
Hassiotis M, Paxinos G, Ashwell KW (2004) Cyto- and chemoarchitecture of the cerebral cortex of the Australian echidna (*Tachyglossus aculeatus*). I. Areal organization. J Comp Neurol 475:493–517
Hassiotis M, Paxinos G, Ashwell KW (2005) Cyto- and chemoarchitecture of the cerebral cortex of an echidna (*Tachyglossus aculeatus*). II. Laminar organization and synaptic density. J Comp Neurol 482:94–122
Hendry SH, Jones EG, Emson PC, Lawson DE, Heizmann CW, Streit P (1989) Two classes of cortical GABA neurons defined by differential calcium binding protein immunoreactivities. Exp Brain Res 76:467–472
Hof P, Sherwood C (2005) Morphomolecular neuronal phenotypes in the neocortex reflect phylogenetic relationships among certain mammalian orders. Anat Rec A Discov Mol Cell Evol Biol 287A:1153–1163
Hof PR, Cox K, Morrison JH (1990) Quantitative analysis of a vulnerable subset of pyramidal neurons in Alzheimer's disease: I. Superior frontal and inferior temporal cortex. J Comp Neurol 301:44–54
Hof PR, Glezer II, Nimchinsky EA, Erwin JM (2000) Neurochemical and cellular specializations in the mammalian neocortex reflect phylogenetic relationships: evidence from primates, cetaceans, and artiodactyls. Brain Behav Evol 55:300–310
Holm IE, Geneser FA (1989) Histochemical demonstration of zinc in the hippocampal region of the domestic pig: I. Entorhinal area, parasubiculum, and presubiculum. J Comp Neurol 287: 145–163
Iñiguez C, Gayoso MJ, Carreres J (1985) A versatile and simple method for staining nervous tissue using Giemsa dye. J Neurosci Methods 13:77–86
Insausti R, Tuñón T, Sobreviela T, Insausti AM, Gonzalo LM (1995) The human entorhinal cortex: a cytoarchitectonic analysis. J Comp Neurol 355:171–198
Insausti R, Herrero MT, Witter MP (1997) Entorhinal cortex of the rat: cytoarchitectonic subdivisions and the origin and distribution of cortical efferents. Hippocampus 7:146–183
Jeffery KJ (2007) Integration of the sensory inputs to place cells: what, where, why, and how? Hippocampus 17:775–785
Johnson JI, Kirsch JA, Reep RL, Switzer RC 3rd (1994) Phylogeny through brain traits: more characters for the analysis of mammalian evolution. Brain Behav Evol 43:319–347
Jones G, Teeling EC (2006) The evolution of echolocation in bats. Trends Ecol Evol 21:149–156
Kerr KM, Agster KL, Furtak SC, Burwell RD (2007) Functional neuroanatomy of the parahippocampal region: the lateral and medial entorhinal areas. Hippocampus 17:697–708
Kingdon J (1984) Bats: fruit bats. In Kingdon J (ed) East African mammals: an atlas of evolution in Africa: Part A Insectivores and bats, vol 2. The University of Chicago Press, Hampshire, pp 117–174
Klink R, Alonso A (1997a) Morphological characteristics of layer II projection neurons in the rat medial entorhinal cortex. Hippocampus 7:571–583
Klink R, Alonso A (1997b) Muscarinic modulation of the oscillatory and repetitive firing properties of entorhinal cortex layer II neurons. J Neurophysiol 77:1813–1828
Kruska D (1975) Comparative quantitative study on brains of wild and laboratory rats. II. Comparison of size of allocortical brain centers. J Hirnforsch 16:485–496
Lapointe F, Baron G, Legendre P (1999) Encephalization, adaptation and evolution of chiroptera: a statistical analysis with further evidence for bat monophyly. Brain Behav Evol 54:119–126
Lorente de Nó R (1933) Studies on the structure of the cerebral cortex. J Psychol Neurol 45:381–438
Maseko BC, Manger PR (2007) Distribution and morphology of cholinergic, catecholaminergic and serotonergic neurons in the brain of Schreiber's long-fingered bat, *Miniopterus schreibersii*. J Chem Neuroanat 34:80–94
Maseko BC, Bourne JA, Manger PR (2007) Distribution and morphology of cholinergic, putative catecholaminergic and serotonergic neurons in the brain of the Egyptian rousette flying fox, *Rousettus aegyptiacus*. J Chem Neuroanat 34:108–127
Mikkonen M, Pitkänen A, Soininen H, Alafuzoff I, Miettinen R (2000) Morphology of spiny neurons in the human entorhinal cortex: intracellular filling with lucifer yellow. Neuroscience 96:515–522
Morrison JH, Lewis DA, Campbell MJ, Huntley GW, Benson DL, Bouras C (1987) A monoclonal antibody to non-phosphorylated neurofilament protein marks the vulnerable cortical neurons in Alzheimer's disease. Brain Res 416:331–336
Moser EI, Kropff E, Moser MB (2008) Place cells, grid cells, and the brain's spatial representation system. Annu Rev Neurosci 31:69–89

Mulders WH, West MJ, Slomianka L (1997) Neuron numbers in the presubiculum, parasubiculum, and entorhinal area of the rat. J Comp Neurol 385:83–94

O'Keefe J, Burgess N (2005) Dual phase and rate coding in hippocampal place cells: theoretical significance and relationship to entorhinal grid cells. Hippocampus 15:853–866

Paoletti P, Vergnano AM, Barbour B, Casado M (2009) Zinc at glutamatergic synapses. Neuroscience 158:126–136

Perez-Clausell J, Danscher G (1985) Intravesicular localization of zinc in rat telencephalic boutons. A histochemical study. Brain Res 337:91–98

Peters A, Jones EG (1984) Classification of cortical neurons. Classification of cortical neurons. In: Jones EG, Peters A (eds) Cerebral Cortex, vol 1. Plenum Press, New York, pp 107–121

Pettigrew JD, Jamieson BG, Robson SK, Hall LS, McAnally KI, Cooper HM (1989) Phylogenetic relations between microbats, megabats and primates (Mammalia: Chiroptera and Primates). Philos Trans R Soc Lond B Biol Sci 325:489–559

Pettigrew JD, Maseko BC, Manger PR (2008) Primate-like retinotectal decussation in an echolocating megabat, *Rousettus aegyptiacus*. Neuroscience 153:226–231

Pitkänen A, Amaral DG (1993) Distribution of parvalbumin-immunoreactive cells and fibers in the monkey temporal lobe: the hippocampal formation. J Comp Neurol 331:37–74

Ramón y Cajal S (1988) On a special ganglion of the spheno-occipital cortex. In: DeFelipe J, Jones EG (eds) Cajal on the cerebral cortex. An annoted translation of the complete writings. Oxford University Press, New York, pp 363–376

Rose M (1912) Histologische lokalisation der Grosshirnrinde bei Kleinen Saugetierein (Rodentia, Insectivora, Chiroptera). J Psychol Neurol 19:119–207

Rose M (1926) Der Allocortex bei Tier und Mensch. I. Teil. J Psychol Neurol 34:1–110

Rosene DL, Van Hoesen GW (1987) The hippocampal formation of the primate brain. A review of some comparative aspects of cytoarchitecture and connections. In: Jones EG, Peters A (eds) Cerebral cortex, vol 6. Plenum, New York, pp 345–456

Saleem KS, Price JL, Hashikawa T (2007) Cytoarchitectonic and chemoarchitectonic subdivisions of the perirhinal and parahippocampal cortices in macaque monkeys. J Comp Neurol 500:973–1006

Schwartz SP, Coleman PD (1981) Neurons of origin of the perforant path. Exp Neurol 74:305–312

Simmons NB, Seymour KL, Habersetzer J, Gunnell GF (2008) Primitive early Eocene bat from Wyoming and the evolution of flight and echolocation. Nature 451:818–821

Slomianka L (1992) Neurons of origin of zinc-containing pathways and the distribution of zinc-containing boutons in the hippocampal region of the rat. Neuroscience 48:325–352

Slomianka L, Geneser FA (1991) Distribution of acetylcholinesterase in the hippocampal region of the mouse: I. Entorhinal area, parasubiculum, retrosplenial area, and presubiculum. J Comp Neurol 303:339–354

Slomianka L, West MJ (1989) Comparative quantitative study of the hippocampal region of two closely related species of wild mice: interspecific and intraspecific variations in volumes of hippocampal components. J Comp Neurol 280:544–552

Slomianka L, West MJ (2005) Estimators of the precision of stereological estimates: an example based on the CA1 pyramidal cell layer of rats. Neuroscience 136:757–767

Stephan H, Baron G, Frahm HD, Stephan M (1986) Comparison of the size of brains and brain structures of mammals. Z Mikrosk Anat Forsch 100:189–212

Sternberger LA, Sternberger NH (1983) Monoclonal antibodies distinguish phosphorylated and nonphosphorylated forms of neurofilaments in situ. Proc Natl Acad Sci USA 80:6126–6130

Suzuki W, Amaral DG (1994) Topographic organization of the reciprocal connections between the monkey entorhinal cortex and the perirhinal and parahippocampal cortices. J Neurosci 14:1856–1877

Swanson LW, Cowan WM (1977) An autoradiographic study of the organization of the efferent connections of the hippocampal formation in the rat. J Comp Neurol 172:49–84

Swanson LW, Köhler C (1986) Anatomical evidence for direct projections from the entorhinal area to the entire cortical mantle in the rat. J Neurosci 6:3010–3023

Tandrup T (1993) A method for unbiased and efficient estimation of number and mean volume of specified neuron subtypes in rat dorsal root ganglion. J Comp Neurol 329:269–276

Teeling EC, Scally M, Kao DJ, Romagnoli ML, Springer MS, Stanhope MJ (2000) Molecular evidence regarding the origin of echolocation and flight in bats. Nature 403:188–192

Tuñón T, Insausti R, Ferrer I, Sobreviela T, Soriano E (1992) Parvalbumin and calbindin D-28K in the human entorhinal cortex. An immunohistochemical study. Brain Res 589:24–32

Ulanovsky N, Moss CF (2007) Hippocampal cellular and network activity in freely moving echolocating bats. Nat Neurosci 10:224–233

Uva L, Grüschke S, Biella G, De Curtis M, Witter MP (2004) Cytoarchitectonic characterization of the parahippocampal region of the guinea pig. J Comp Neurol 474:289–303

van der Linden S, Lopes da Silva FH (1998) Comparison of the electrophysiology and morphology of layers III and II neurons of the rat medial entorhinal cortex in vitro. Eur J Neurosci 10:1479–1489

van Groen T (2001) Entorhinal cortex of the mouse: cytoarchitectonical organization. Hippocampus 11:397–407

van Groen T, Miettinen P, Kadish I (2003) The entorhinal cortex of the mouse: organization of the projection to the hippocampal formation. Hippocampus 13:133–149

van Hoesen G, Pandya DN (1975) Some connections of the entorhinal (area 28) and perirhinal (area 35) cortices of the rhesus monkey. I. Temporal lobe afferents. Brain Res 95:1–24

West MJ, Slomianka L, Gundersen HJG (1991) Unbiased stereological estimation of the total number of neurons in thesubdivisions of the rat hippocampus using the optical fractionator. Anat Rec 231:482–497

Wouterlood FG, Hartig W, Bruckner G, Witter MP (1995) Parvalbumin-immunoreactive neurons in the entorhinal cortex of the rat: localization, morphology, connectivity and ultrastructure. J Neurocytol 24:135–153

Woźnicka A, Malinowska M, Kosmal A (2006) Cytoarchitectonic organization of the entorhinal cortex of the canine brain. Brain Res Rev 52:346–367

NUMBER ESTIMATES OF NEURONAL PHENOTYPES IN LAYER II OF THE MEDIAL ENTORHINAL CORTEX OF RAT AND MOUSE (IN REVIEW)

Title

Number estimates of neuronal phenotypes in layer ll of the medial entorhinal cortex of rat and mouse

Authors

Catherine W. Gatome, Lutz Slomianka, Hans-Peter Lipp, Irmgard Amrein

Institute of Anatomy, University of Zurich, Winterthurerstrasse 190, 8057 Zurich, Switzerland

Section Editor

Dr. M. Witter

Text pages 19

Figures 4

Tables 4

Corresponding author

Irmgard Amrein

Institute of Anatomy, University of Zürich, Winterthurerstrasse 190, 8057 Zürich, Switzerland

Phone +41 44 635 53 42; Fax +41 44 635 57 02, Mail: i.amrein@anatom.uzh.ch

Abbreviations

Entorhinal cortex	EC
Medial entorhinal area	MEA
Caudal entorhinal field	CE
Medial entorhinal field	ME

Abstract

Modelling entorhinal function or evaluating the consequences of neuronal losses which accompany neurodegenerative disorders requires detailed information on the quantitative cellular composition of the normal entorhinal cortex. Using design-based stereological methods, we estimated the numbers, proportions, densities and sectional areas of layer II cells in the medial entorhinal area (MEA), and its constituent caudal entorhinal (CE) and medial entorhinal (ME) fields, in the rat and mouse. We estimated layer II of the MEA to contain ~58,000 neurons in the rat and ~24,000 neurons in the mouse. Field CE accounted for more than three-quarters of the total neuron population in both species. In the rat, layer II of the MEA is comprised of 38% ovoid stellate cells, 29% polygonal pyramidal cells and 17% pyramidal cells. The remainder is comprised of much smaller populations of e.g. horizontal bipolar, tripolar, oblique pyramidal and small round cells. In the mouse, MEA layer II is comprised of 52% ovoid stellate cells, 22% polygonal stellate cells and 14% pyramidal cells. Significant species differences in the proportions of ovoid and polygonal stellate cells suggest differences in physiological and functional properties. The majority of MEA layer II cells contribute to the entorhinal-hippocampal pathways. The degree of divergence from MEA layer II cells to the dentate granule cells was similar in the rat and mouse. In both rat and mouse, the only dorsoventral difference we observed is a gradient in polygonal stellate cell sectional area, which may relate to the dorsoventral increase in the size and spacing of individual neuronal firing fields. In summary, we found species-specific cellular compositions of MEA layer II, while, within a species, quantitative parameters other than cell size are stable along the dorsoventral and mediolateral axis of the MEA.

Key words: species differences; caudal entorhinal field; medial entorhinal field; stellate cells; nucleator; optical fractionator

Layer II of the medial entorhinal area (MEA) contains a morphological, physiological, chemical and functional heterogeneous population of cells. Morphologically, based on the shape and size

of the soma and dendritic arbour and spine characteristics, subtypes of stellate (Klink and Alonso, 1997a), pyramidal (Lorente de Nó, 1933, Klink and Alonso, 1997a) and horizontal (Schwartz and Coleman, 1981) cells have been identified. Multipolar cells that closely resemble the stellate cell (Tamamaki and Nojyo, 1993) have also been reported. Parvalbumin is expressed by two types of GABAergic multipolar interneurons, which differ in soma size and dendritic length (Wouterlood et al., 1995). Calretinin labels few GABAergic and non-GABAergic bipolar and multipolar interneurons (Wouterlood et al., 2000) and calbindin identifies GABAergic multipolar interneurons that do not co-express parvalbumin or calretinin (Rogers, 1992, Tuñón et al., 1992). Neurofilament markers also give a staining pattern that suggests different subpopulations of cells (Beall and Lewis, 1992). Physiologically, hippocampally projecting cells are broadly classified as stellate, pyramidal and horizontal, distinguished by their active and passive membrane properties (Alonso and Klink, 1993) and differential responses to cholinergic innervation (Klink and Alonso, 1997b). Spatial firing patterns of the MEA layer II cells have established at least four functional neuronal phenotypes in the mouse (Fyhn et al., 2008).

In a recent study of the EC of megachiropteran bats (Gatome et al., 2010) we observed species differences in the cellular makeup of MEA layer II – both between the bat species and, based on the data currently available, also between bats, rats and mice. While there are design-based estimates of cell numbers in the layers of the EC (Irizarry et al., 1997, Mulders et al., 1997, Merrill et al., 2001, Rapp et al., 2002) the phenotypic composition of MEA layer II is only available from electrophysiological (Alonso and Klink, 1993) and tract-tracing studies (Schwartz and Coleman, 1981) with their inherent cell selection biases. We therefore decided to apply design-based estimators to the rat and mouse MEA layer II and describe quantitative species differences. Earlier findings of the MEA layer II species differences include projections of layer II cells to the contralateral dentate gyrus in the rat but not in the mouse (van Groen et al., 2002), and projections to CA3 that originate predominantly from layer II in the rat but from layer III in the mouse (van Groen, 2001). Functional phenotypes may differ too, with the grid, head-direction, conjunctive grid-head direction and border cells in layer II of the mouse (Fyhn

et al., 2008), while only grid and border cells have been identified in layer II in the rat (Fyhn et al., 2004, Solstad et al., 2008).

Furthermore we investigated dorsoventral differences within the MEA fields CE and ME in the densities, proportions and sectional areas of neuronal phenotypes. Dorsoventral gradients have been described in the physiological properties of MEA layer II stellate cells (Giocomo et al., 2007, Garden et al., 2008). The scale of the grid representation of the environment increases along the dorsoventral axis of the MEA (Brun et al., 2008), which by means of topographically organised projections to the hippocampus (Dolorfo and Amaral, 1998, Witter, 2007) is likely to relate to a similar dorsoventral expansion of hippocampal place fields (Kjelstrup et al., 2008). A relationship between the scale of the grid and the number of cells necessary to represent the environment has been suggested (Brun et al., 2008). We compared the same parameters between the CE and ME to investigate if the quantitative morphological makeup of layer II may provide information on a possible functional differentiation between the two fields.

This information will be valuable in studies of entorhinal-hippocampal information processing and as a basis for the evaluation of histopathological changes associated with laboratory rodent models of diseases such as Alzheimer's disease and schizophrenia (McGowan et al., 2006) which impact on layer II of the EC (Gomez-Isla et al., 1996).

EXPERIMENTAL PROCEDURES

Nissl staining

Twenty micron thick glycolmethylacrylate-embedded Giemsa-stained horizontal sections prepared in previous studies on five 30-day old female Wistar rats (West et al., 1991, Mulders et al., 1997) and six 4-month old female C57BL/6 mice (Ben Abdallah et al., 2010) were used.

Stereology

Layer II of the MEA was delineated at a 360x final magnification. Using the StereoInvestigator® software (MicroBrightfield Inc, Colchester, Vermont), total cell numbers were estimated using the optical fractionator (West et al., 1991) with a 40x oil-immersion objective (N.A. 1.3) in every 10th (mouse) or 18th (rat) section with a counting frame sized 40 by 40 μm, a disector height (h) of 10 μm and x, y-steps of 100 μm. The guard zone above the disector sample was 2 μm thick, and section thickness (t) was measured at every 6th sampling site. On average, 9 sections per rat (8 - 10) and 10 sections per mouse (9 - 11) were used in field CE. In field ME, 5 sections per rat (4 - 5) and 5 sections per mouse (5 - 7) were studied. Cell number (N) estimates were calculated using

$$N = \frac{1}{ssf} \times \frac{1}{asf} \times \frac{1}{hsf} \times \sum Q^{-} \qquad hsf = \frac{h}{t}$$

where *ssf* is the section sampling fraction, *asf* is the area sampling fraction, *hsf* is the height sampling fraction and $\sum Q^{-}$ is the total number of cells counted in the disector samples. Number-weighed section thickness (Dorph-Petersen et al., 2001) was used for *t*.

Proportions of cell types were obtained by dividing the count per phenotype with the overall count. The density for each phenotype was estimated by dividing the count per phenotype with the number of disectors that fell within the region of interest.

The sectional area of neuronal somata was estimated using the Nucleator method (Gundersen, 1988, Tandrup, 1993) for cells counted in the disector samples. The nucleolus was used as the cell's reference point. The sectional area of a cell (A_N) was calculated using $A_N = 4\pi {l_n}^2$, where l_n represents the mean distance from the nucleolus to the cell membrane.

The tracings of layer II with the markers of cells counted were used to determine the locations of ovoid and polygonal stellate cells and pyramidal cells.

Fields within the MEA

The MEA has been divided into two fields, CE and ME (Insausti et al., 1997). Field CE (rat: Fig. 1a, d; mouse: Fig. 1e, h) has a distinct layer II, distinguished by the presence of large, densely staining cells, a broad and homogenous layer III and a well-developed layer IV. Layers V and VI are densely populated and have a radial columnar organisation. Field ME (rat: Fig. 1a, c; mouse: Fig. e, g) is a narrow strip of cortex parallel and lateral to CE. It has a distinct layer II that is separate from a bilaminar layer III, wide layer IV, and distinct and wide layers V and VI. The ventromedial extreme of the MEA is not included in our analysis because layer II cannot be reliably distinguished from layer III.

To compare estimates of cell density and cell sectional area between the dorsal and ventral parts of MEA fields CE and ME, sections of each animal containing the subfields were divided midway to give equally sized dorsal and ventral batches. Measurements from sections in each batch were averaged. When the sections were odd-numbered, measurements from the middle section were used in both the dorsal and ventral batch.

---- insert figure 1 approximately here ----

Neuronal Types

Stellate cells have been defined based on their shape (Schwartz and Coleman, 1981), size, and structure of dendritic (Lorente de Nó, 1933, Ramón y Cajal, 1988, Klink and Alonso, 1997a) and axonal arbours (Lorente de Nó, 1933). Those with large, polygonal and often trapezoid somata that are either transversely or vertically oriented are referred to as polygonal stellate cells (Fig. 2a, c, e – g, j - l). Four or more thick primary dendrites emerge from the soma in a radial or bi-tufted pattern. The term polygonal encompasses a variety of somal shapes, of which the ones we most commonly observed correspond best with cells Ia and Ib of Klink and Alonso (1997a), the cell illustrated by Tamamaki and Nojyo (1993) in their figure 1A, vertical stellate cells shown by Schwartz and Coleman (1981) in their figure 2 and type I spinous stellate cell illustrated by Jones (1994). Ovoid stellate cells are smaller in size and have round or elongated somata (Fig. 2a – h, i). Multiple small calibre dendrites and typically one or two somewhat larger dendritic trunks emerge from the soma. Often, they are oriented vertically. Cell Ic of Klink and Alonso (1997a) or the type II stellate cell illustrated by Jones (1994) would represent commonly observed ovoid stellate cells in our material.

Pyramidal cells (Schwartz and Coleman, 1981, Ramón y Cajal, 1988, Klink and Alonso, 1997a) are medium-sized to large cells with conical or triangular somata (Fig. 2a, d, f, I; cell IIa of Klink and Alonso, 1997a). They have a large apical process oriented perpendicular to the pial surface, which may bifurcate at the border between layers I and II. Oblique pyramidal cells (Klink and Alonso, 1997a) resemble the pyramidal cells but their apical process is oblique to the pial surface.

Horizontal bipolar (Fig. 2b, g, h; Germroth et al., 1989, their figure 1) and tripolar (Fig. 2d, e, k; Schwartz and Coleman, 1981, their figure 1; Klink and Alonso, 1997a, their figure 9) cells have round or horizontally elongated somata and are usually located at the border between layers I and II.

Other types include small round cells (Fig. 2c, e, h; Jones and Buhl, 1993, their figure 1), and those of fusiform appearance (Wouterlood et al., 2000, their figure 3B).

Biotin dextran amine (BDA) labeling

To compare cellular characteristics visible in the Giemsa stained sections with the extended dendritic trees visible after retrograde BDA labelling, four 7-month old female C57BL/6 mice were anaesthetized with ketamine (100 mg/kg) and xylaxine (15 mg/kg). Pressure injections of 0.5 µl of 10% BDA (MW 10,000; B9139, Sigma-Aldrich, Missouri) in 0.9% saline were made at two sites (bregma 2.0, 1.0 lateral and 2.0 ventral; bregma 3.75, 2.5 lateral and 3.25 ventral) (Franklin and Paxinos, 1997). After 3 days survival, the animals were deeply anaesthetized with sodium pentobarbital (50 mg/kg) and perfused with 0.9% saline followed by 4% paraformaldehyde. Brains were removed, post-fixed for 1 hour and cryoprotected in 30% sucrose.

Forty micron thick horizontal sections were cut, rinsed in tris-triton buffer (pH 7.4), and incubated for 2 hours at room temperature with avidin-biotin-peroxidase complex (Vectastain® Elite ABC Kit). BDA labelled neurons were stained using diaminobenzidine as a chromogen, rinsed, cleared and coverslipped (Fig. 2 i-l).

---- insert figure 2 approximately here ----

Statistics

The coefficients of error of number estimates were calculated according to Gundersen et al. (1999) using the conservative m = 0 approach (Slomianka and West, 2005). Statistical analyses used SPSS Statistics version 17.0.0 (SPSS Inc., Chicago, Illinois).

One-way analysis of variance (ANOVA) and paired *t*-tests were used to compare dorsoventral and mediolateral differences in frequencies and sectional areas. Independent two-sample *t*-tests were used to analyse species differences in cell frequencies and sectional areas. A $p < 0.05$ was considered significant in all tests.

Image Processing

Images were adjusted in brightness and contrast to resemble the appearance of the sections under the microscope. No local image manipulations were performed in Fig. 1 and panels i - l of Fig. 2. For panels a - h of Fig. 2, most of the marked cells have been composited from images taken at several focal planes to illustrate at least some of the detail visible in the sections at high magnification.

RESULTS

Cell numbers, proportions and densities

We compared the total number of cells in layer II of the MEA (Table 1) with those obtained previously by Mulders et al. (1997) in the same animals. A paired *t*-test showed no significant difference in layer II total numbers (p = 0.117). The correlation between the two datasets was however weak (r = 0.2) and non-significant (p = 0.747).

Species comparison. Estimates of the total cell numbers in MEA layer II and its constituent fields CE and ME are given in table 1. The estimated total numbers of the neuronal phenotypes, their proportions and *p*-values for the comparisons of rat and mouse are listed in table 2. In the mouse, MEA layer II mean cell number was approximately half of that in the rat. Ovoid and polygonal stellate cells and pyramidal cells were the most frequent cell types and together accounted for ~84% and ~83% in the CE and ME of the rat, and for ~87% and ~91% in the CE and ME of the mouse.

Estimates of the numbers and proportions of individual cell types are given in table 2. Ovoid stellate cells comprise a significantly greater portion of CE and ME layer II cells in the mouse (CE: 51.8%, ME: 50.8%) than in the rat (CE: 37.9%, ME: 38.6%). Instead, the proportion of polygonal stellate cells is significantly smaller in the CE of the mouse (22.2%) than in the rat (28.8%). Numerically, differences in the proportions of ME polygonal stellate cells in mouse (23.6%) and rat (28.5%) are similar to the CE but did not reach statistical significance. The frequencies of other cell types did not differ between the rat and mouse.

The contribution of the variance generated by the estimation procedures to the group variance ($\overline{CE}^2/CV^2$) was less than 0.5 for all major cell types of the CE. The ratio exceeded 0.5 for ovoid stellate cells and pyramidal cells of the ME and variance induced by the sampling is likely to contribute significantly to the observed group variances. This did however not obscure

significant species differences in the proportion of ME ovoid stellate cells, and proportions of ME pyramidal cells are so close that they would be unlikely to reach statistical significance had the variance generated by the estimation procedures been lower.

Comparison of CE and ME. Cell numbers in the ME amount to just short of one-quarter of that in the CE. Proportions of the most common cell types did not differ between the ME and CE in the rat or mouse (Table 2).

Comparison of cell densities. In the rat and mouse, we found no significant differences in cell densities between the CE and ME, or between the dorsal and ventral parts of the CE and ME (Table 3). Collated cell densities for the MEA are provided in table 4.

Cell sectional areas

In the rat field CE, comparisons of sectional areas within individual animals (ANOVA) show a significant dorsoventral difference in polygonal stellate cells within all animals (F = 7.2, p = 0.10; F = 6.3, p = 0.015; F = 11.5, p < 0.001; F = 6.7, p = 0.012; F = 7.7, p = 0.007). Across the group (Table 3), a paired two-tailed t-test also shows significant dorsoventral differences in polygonal stellate and pyramidal cell sectional areas (Fig. 3).

In the rat field ME, dorsoventral differences were found within only one animal for ovoid stellate (F = 8.2, p = 0.018) and polygonal stellate cells (F = 6.2; p = 0.034). Paired t-tests across the group only showed significant dorsoventral differences in polygonal stellate cell sectional area (Table 3 and Fig. 3).

In the mouse field CE (Table 3), within animal comparisons show a significant dorsoventral difference in ovoid stellate cell sectional area in only one animal (F = 6.5, p = 0.013), polygonal stellate cell sectional area within all animals (F = 8.1, p = 0.008; F = 10.0, p = 0.004; F = 5.23, p = 0.031; F = 9.3, p = 0.005; F = 5.4, p = 0.026) except one, and pyramidal cell sectional area in two

animals (F = 13.0, p = 0.009; F = 9.8, p = 0.017). Paired t-tests across the group for dorsoventral differences in sectional areas show a significant difference in polygonal stellate cell sectional area (Table 3 and Fig. 3).

In the mouse field ME, individual animal comparisons showed significant dorsoventral differences in polygonal stellate cell sectional area in two animals (F = 8.7, p = 0.032; F = 25.0, p = 0.004). Paired comparisons show no significant dorsoventral differences in sectional areas for all cell types (Table 3 and Fig. 3).

Collated cell areas for the MEA are provided in table 4.

---- insert figure 3 approximately here ----

Locations of cells

In the rat, 41% of ovoid stellate cells were located superficially and 59% deep in layer II. 56% of polygonal stellate cells were located superficially and 44% deep in the layer. 12% of pyramidal cells were located superficially and 88% deep in the layer. In the mouse, 48% of ovoid stellate cells were located superficially and 53% deep in layer II, and they tended to occur in clusters. 53% of polygonal stellate cells were located superficially and 47% deep in the layer. 23% of pyramidal cells were located superficially and 77% deep in the layer. In both species, horizontal tripolar and bipolar cells were located superficially in the layer. The round and fusiform cell types were located superficially or deep in the layer, and usually in close contact with the soma of stellate and pyramidal cells, or primary dendrites of stellate cells.

DISCUSSION

In this study we estimated cell numbers, distributions and sectional areas of neuronal populations in layer II of the MEA, and its fields, CE and ME, in the rat and mouse (main findings are summarized in Fig.4). Species-specific differences were observed in the proportions of the stellate cell populations. We also found dorsoventral variations in cell sectional areas in both species but not in densities and proportions. Fields CE and ME cannot be distinguished by the parameters we investigated.

---- insert figure 4 approximately here ----

Methodological considerations

The design of our study is similar to other studies investigating neuronal numbers and sizes (Merrill et al., 2001, Dorph-Petersen et al., 2004, Stark et al., 2007, Gatome et al., 2010). Characteristics that have been used to distinguish between various morphological phenotypes in cell-labelling studies that are recognisable in Nissl stains include the somal shape and size, number, root and calibre of primary dendrites. There are phenotypes that share somal characteristics and are best distinguished on the basis of the sparsely spinous to aspinous nature of their dendrites, and axon targeting – features not discernable in our material. These include several types of interneurons, for example basket, chandelier and bipolar cells, which may contribute less than 10% to the entorhinal cell population (Kumar and Buckmaster, 2006). Their proportions could not be assessed by us.

The number-weighted selection of cells for counting and classification using disector probes at a uniform random systematic set of sampling sites throughout the EC should be unbiased by cell size and distribution (Dorph-Petersen et al., 2001). However, cell densities have to be treated with caution, because we did not control for tissue shrinkage and because they will be affected by the definition of the reference volume. Densities can, with confidence, only be treated as

relative values. Also, unbiased estimates of cell volume require isotropic or vertical designs when methods like the Nucleator are employed. Preparing isotropic or vertical sections means sacrificing the information provided by a specific orientation of the sections. In the horizontal series used in this study, the Nucleator can therefore not provide unbiased estimates of cell volume. Instead, we used sectional areas, which can only be used for the comparison of objects of similar shape and orientation, i.e. for comparisons within particular cell types.

Comparison with previous studies

Cell numbers. Our estimate of ~58,000 MEA layer II cells is comparable to an earlier stereological estimate of ~59,000 in young Fischer 344 rats (Merrill et al., 2001). In a previous study of the animals used in our study (Mulders et al., 1997), the estimate was ~66,000 neurons. About one-third of the difference is explained by differences between the section thicknesses used previously (mean 18.5 μm) and the number-weighed estimates used here (mean 17.5 μm). Taking section thickness into account, the datasets differ by only 9% (paired t-test p = 0.36), which includes both estimator variance and possible changes in anatomical definitions between the investigators that performed the estimates.

Considering the use of different mouse strains and of the disector instead of the optical fractionator, our estimate of ~24,000 cells for the MEA is low, but within a range that can be expected from an earlier estimate of ~60,000 cells for the entire EC layer II (Irizarry et al., 1997).

Proportions. Intracellular labelling studies in the rat have shown layer II stellate cells to constitute 65 - 81% of the neuronal population while pyramidal cells contribute between 17 - 32% (Schwartz and Coleman, 1981, Klink and Alonso, 1997a). These estimates tightly bracket ours. The contribution of various hippocampally projecting stellate phenotypes to the overall

population differs from our estimates (Schwartz and Coleman, 1981), which may be due to methodological differences.

Cell Sectional Areas. A stereological estimate of a mean layer II cell area of 150 μm^2 (Merrill et al., 2001) is very close to our estimate. Dimensions provided by Klink and Alonso (1997a) for pyramidal and stellate cells also correspond reasonably well with our estimates. A dorsoventral decrease of somal surface area was also observed (Garden et al., 2008), although different stellate cell phenotypes were not distinguished.

Locations. In agreement with Klink and Alonso (1997a) over 75% of pyramidal cells were located deep in layer II. Overall, stellate cells were evenly distributed within the layer with polygonal stellate cells showing a slight preference for a superficial location, which was also reported (Klink and Alonso, 1997a).

Species comparisons

Cell numbers and proportions. As expected, the mouse has fewer neurons in the MEA layer II than the rat. Although the same general types of cells are found in MEA layer II of the rat and mouse, the proportions varied between the species. We have previously found that cell types appear preserved across species while proportions can vary between species (Gatome et al., 2010). In fruit bats, ovoid stellate cells comprised 35 – 40%, polygonal stellate cells comprised 5 – 13%, and pyramidal cells, 17 – 18%. We suggested that this may confer differences in neural activity in line with species-specific stimulus processing in the EC. The ratio between dentate granule cells and the MEA layer II cells is ~18 in the rat (Mulders et al., 1997) and ~21 in the mouse (granule cell numbers from Ben Abdallah et al., 2010), showing a little more divergence of the layer II projections in the mouse. Following the approach of Amaral et al., (1990), if a rat granule cell provides about ~2500 axospinous synaptic sites in the middle molecular layer (Geinisman et al., 1996, Weeks et al., 1998, Eyre et al., 2003), the extent of divergence suggests

that each rat MEA layer II cell contacts about ~43,000 sites – more than twice as much as originally proposed. This wide influence of the EC may provide the capacity for the summation of differently scaled grids (McNaughton et al., 2006) over large segments along the septotemporal axis of the dentate gyrus and for the global remapping of place fields associated with coordinate shifts of the grid cell frame (Fyhn et al., 2007).

Relationship between structure and function

Cell Sectional Areas. The overall cell sectional area and that of particular phenotypes such as the polygonal stellate cell is similar in the rat and mouse. Other similarities include the MEA cytoarchitecture and projection pattern to the dentate gyrus (van Groen et al., 2003). This correlates well with grid cell spatial firing properties, such as size and spacing of spatial fields, which were found to be similar in the rat and mouse (Fyhn et al., 2008).

Cell types. Physiological investigations (Klink and Alonso, 1993, Erchova et al., 2004, Hamam et al., 2007) have only been able to discern between the two major classes of cells, i.e. pyramidal and stellate cells. Within the subtypes of principal cells in layer II of the MEA, variations of somal shapes and sizes, and dendritic and axonal projection patterns suggest a further functional differentiation between these cells (Lingenhohl and Finch, 1991, Tamamaki and Nojyo, 1993, Klink and Alonso, 1997a). Additionally, differences in membrane oscillation properties have been found in layer II stellate cells at the same dorsoventral level (Giocomo et al., 2007). Different functional phenotypes (cells with localised and multiple firing fields, border cells, conjunctive head-direction cells) that represent a range of metric information may be related to the morphological and physiological diversity of stellate cells. It is not clear if the finding of conjunctive cells in the mouse MEA layer II (Fyhn et al., 2008) may be associated with the prominence of the ovoid stellate cell in the mouse.

Dorsoventral differences. Grid cell spacing and field size increase from the dorsal to ventral MEA (Hafting et al., 2005, Brun et al., 2008). This change is accompanied by a dorsoventral gradient in synaptic and membrane properties of MEA layer II stellate cells (Garden et al., 2008, Giocomo and Hasselmo, 2009). Also, the decrease of polygonal stellate cell size along the dorsoventral axis in the MEA layer II is likely to be accompanied by a change in the complexity of their dendritic trees (Garden et al., 2008). Not only do morphological changes suggest that the contextual representation of smaller spatial fields is functionally more demanding, but the spatial domain is also gradually replaced by different functional domains towards the ventral MEA. While the dorsocaudal MEA is sufficient and necessary to mediate spatial learning and memory (Moser et al., 1993, Steffenach et al., 2005), lesions to the ventromedial MEA preferentially affect fear-related behaviour (Steffenach et al., 2005). Concerted changes in the sectional areas of pyramidal cells in the rat suggest similar functional changes.

Conclusion

While the density of dentate gyrus granule cells, to which entorhinal layer II cells project, has been known to decrease from septal to temporal in rats (Gaarskjaer, 1978), we do not observe corresponding changes in the cellular composition of the MEA layer II. We also did not observe differences between the CE and ME in either rat or mouse. We could only confirm a decrease in cell sectional areas along the dorsoventral axis, which appears modest in view of considerable physiological and functional differences observed along this axis. Our data suggest that changes in function along the axes of the MEA have to be accommodated by MEA layer II cell assemblies that do not change in composition, but that do change in composition between rat and mouse. We hope that the quantitative data presented here will be useful for simulations of information processing within the MEA grid cell network and its transformation between the MEA and hippocampus.

ACKNOWLEDGEMENTS

The materials of this study were used with the kind permissions of Mark J West and Nada MB Ben Abdallah. This work was supported by the NCCR 'Neural Plasticity and Repair', Swiss National Science Foundation and an IBRO Rita Levi Montalcini Fellowship for African Women in Neuroscience to CWG.

Table 1

Neuron numbers (unilateral, rounded to the next 100) in fields CE and ME of the MEA. Standard deviations of the group means are given in parentheses.

		CE		ME		MEA	
	Animal	Cell number	$\overline{CE}$	Cell number	$\overline{CE}$	Cell number	$\overline{CE}$
Rat	1	55000	0.08	13100	0.13	68100	0.07
	2	37400	0.11	7800	0.16	45300	0.10
	3	44900	0.09	9400	0.16	54300	0.08
	4	51100	0.08	8000	0.16	59100	0.07
	5	52300	0.07	10600	0.13	62900	0.06
	Mean	48100 (7000)	0.09	9800 (2200)	0.15	57700 (8500)	0.08
Mouse	1	13900	0.09	4200	0.16	18100	0.08
	2	13600	0.09	3700	0.18	17300	0.08
	3	23200	0.07	5100	0.19	28400	0.06
	4	13900	0.12	3700	0.21	17600	0.12
	5	22100	0.08	4900	0.17	27000	0.07
	6	20300	0.09	11000	0.10	31900	0.07
Mean		18300 (4200)	0.09	5400 (2800)	0.17	23800 (6100)	0.08

Table 2

Mean cell counts (unilateral) and proportions (%) in fields CE and ME of the MEA. $\overline{CE}$ is the mean coefficient of error of the estimates for m = 0. $P_{Prop\ Species}$ denotes the p value of comparisons of proportions between rat and mouse (two-tailed t-tests). $P_{Prop\ CE,\ ME}$ denotes the p value of comparisons of proportions between the CE and ME. No $\overline{CE}$ or P values are presented if meaningful estimates could not be calculated due to small sample sizes.

	Cell type	Number (SD)		CE		Proportion (SD)		$P_{Prop\ CE,\ ME}$		$P_{Prop\ Species}$
		Rat	Mouse	Rat	Mouse	Rat	Mouse	Rat	Mouse	
CE	ovoid stellate	18095	8982	0.13	0.13	37.9	51.8	0.849	0.751	**0.007**
		(3407)	(1742)			(7.6)	(5.6)			
	polygonal	13901	3959	0.13	0.17	28.8	22.2	0.957	0.622	**0.027**
	stellate	(2813)	(1539)			(2.6)	(5.0)			
	pyramidal	8390	2573	0.16	0.24	17.7	12.9	0.397	0.209	0.083
		(1044)	(1473)			(2.9)	(4.7)			
	oblique	1015	158			2.0	0.8			
	pyramidal	(499)	(55)			(0.8)	(0.2)			
	horizontal	966	98			1.5	0.7			
	tripolar	(506)	(72)			(1.2)	(0.5)			
	horizontal	282	38			0.6	0.2			
	bipolar	(343)	(52)			(0.7)	(0.3)			
	round	2498	1099	0.31	0.32	5.0	6.2	0.598	0.161	0.343
		(1105)	(489)			(1.7)	(2.0)			
	others	3181	978	0.28	0.34	6.4	5.3	0.144	0.256	0.356
		(1366)	(297)			(2.1)	(1.9)			
ME	ovoid stellate	3797	2166	0.24	0.21	38.6	50.8			**0.018**
		(1208)	(279)			(9.0)	(4.9)			
	polygonal	2696	768	0.28	0.30	28.5	23.6			0.213
	stellate	(466)	(420)			(7.8)	(4.1)			
	pyramidal	1585	1054	0.38	0.40	15.6	16.5			0.820
		(909)	(228)			(5.5)	(7.0)			
	oblique	155	17			1.4	0.7			
	pyramidal	(251)	(38)			(2.4)	(1.1)			
	horizontal	246	37			2.1	0.8			
	tripolar	(188)	(51)			(2.0)	(1.2)			
	horizontal	100	20			1.0	0.7			
	bipolar	(115)	(44)			(1.4)	(1.0)			
	round	472	155			4.5	3.4			
		(326)	(115)			(2.8)	(2.8)			
	others	794	541			8.3	3.5			
		(246)	(747)			(2.2)	(2.5)			

Table 3

Dorsal (D) and ventral (V) mean densities and cell sectional areas (μm^2) in fields CE and ME.

	Cell Type	Density						Sectional Area					
		Rat			Mouse			Rat			Mouse		
		Dorsal	Ventral	$P_{D,V}$	Dorsal	Ventral	$P_{D,V}$	Dorsal	Ventral	$P_{D,V}$	Dorsal	Ventral	$P_{D,V}$
CE	ovoid stellate	0.42 (0.06)	0.44 (0.05)	0.70	0.54 (0.11)	0.61 (0.05)	0.09	158 (16)	149 (14)	0.233	135 (13)	128 (15)	0.192
	polygonal stellate	0.32 (0.15)	0.35 (0.08)	0.68	0.24 (0.09)	0.28 (0.08)	0.43	239 (33)	207 (31)	**0.015**	227 (19)	187 (18)	**<0.001**
	pyramidal	0.19 (0.05)	0.21 (0.04)	0.26	0.15 (0.07)	0.21 (0.1)	0.30	208 (26)	181 (18)	**0.003**	185 (15)	161 (22)	0.058
ME	ovoid stellate	0.41 (0.12)	0.43 (0.07)	0.64	0.67 (0.12)	0.65 (0.15)	0.85	154 (20)	148 (18)	0.484	130 (13)	135 (9)	0.159
	polygonal stellate	0.28 (0.13)	0.36 (0.09)	0.36	0.28 (0.09)	0.29 (0.06)	0.85	224 (40)	205 (29)	**0.048**	240 (26)	208 (26)	0.053
	pyramidal	0.17 (0.17)	0.19 (0.06)	0.70	0.18 (0.12)	0.23 (0.09)	0.43	193 (26)	165 (27)	0.091	184 (33)	166 (23)	0.182

Table 4

MEA layer II overall mean cell densities, sectional areas (μm²) and proportions (%). Areas and proportions were rounded to the next integer. Standard deviations are given in parentheses.

Cell type	Density		Area		Proportion	
	Rat	Mouse	Rat	Mouse	Rat	Mouse
ovoid stellate	0.43	0.62	152	132	38	52
	(0.01)	(0.06)	(16)	(12)	(7.3)	(4.6)
polygonal stellate	0.33	0.27	219	215	29	22
	(0.04)	(0.02)	(34)	(29)	(2.3)	(4.0)
pyramidal	0.19	0.19	187	174	17	14
	(0.02)	(0.04)	(28)	(24)	(3.0)	(4.4)

FIGURE LEGENDS

Figure 1

Horizontal sections at a dorsal (**a**, **c**, **d**, **e**, **g** and **h**) and ventral (**b** and **f**) level showing the MEA (delimited by open arrowheads) and the fields CE and ME (border indicated by grey arrows), in the rat (**a**-**d**) and mouse (**e**-**h**). Stippled lines in c, d, g and h indicate the border between layer II and III. Scale bar in a, b, e, f: 200 μm, c, d, g, h: 100 μm.

Figure 2

Neuronal phenotypes in MEA layer II. (**a** – **h**) Nissl-stained sections of rat (**a** - **d**) and mouse (**e - h**). (**i** – **l**) Retrogradely BDA labelled neurons. 1: ovoid stellate cell, 2: pyramidal cell, 3: polygonal stellate cell, 4: tripolar cell, 5: bipolar cell, 6: small round cell.

Polygonal stellate cells have a polygonal soma with at least four thick primary dendrites emerging from the poles, in Giemsa material (a, c, e, f, and g) and BDA labelling (j, k, and l). In comparison, ovoid stellate cells are often smaller, with a rounded soma and less prominent dendritic processes in Giemsa material (a, c, f, g) and BDA labelling (i). Pyramidal cells are characterised by a triangular soma with a prominent thick ascending process and thin basal dendrites, evident in Giemsa stain (a, d, f) and BDA labelling (i). The triangular-shaped horizontal tripolar has three dendritic processes originating from its poles (e, k), and like the bipolar cell (b, h) is often located superficially in the layer. Many of the small round cells were found closely associated with cell soma (h) or processes (c) of the principal cells.

Scale bars a -h: 10 μm, i – l: 20 μm.

Figure 3

Cell area estimates of stellate and pyramidal cells in the MEA in the rat and mouse. The somal area of polygonal stellate cells in CE and ME, and pyramidal cells in CE decreased ventrally in the rat. In the mouse, the somal area of the polygonal stellate cells decreased ventrally in CE, while the decrease in ME is similar in magnitude but only suggesting that ther may be a true effect different from zero. Bars represent mean cell area ± SD. *$p < 0.05$; **$p < 0.01$; ***$p < 0.001$.

Figure 4

Schematic representation of the main findings of our study. Cell sectional areas of pyramidal and polygonal stellate cells are smaller ventrally. The proportion of ovoid stellate cells is increased in both fields of the mouse at the expense of polygonal stellate cells. Each cell symbol represents ~10% of the total cell population of layer II in fields CE and ME. MEA outlines represent a posterior view (adapted from Slomianka and Geneser, (1991) and Insausti et al., (1997)).

REFERENCES

Alonso A, Klink R (1993) Differential electroresponsiveness of stellate and pyramidal-like cells of medial entorhinal cortex layer II. J Neurophysiol 70:128-143.

Amaral DG, Ishizuka N, Claiborne B (1990) Neurons, numbers and the hippocampal network. Prog Brain Res 83:1-11.

Beall MJ, Lewis DA (1992) Heterogeneity of layer II neurons in human entorhinal cortex. J Comp Neurol 321:241-266.

Ben Abdallah NMB, Slomianka L, Vyssotski AL, Lipp H-P (2010) Early age-related changes in adult hippocampal neurogenesis in C57 mice. Neurobiol Aging 31:151-161.

Brun VH, Solstad T, Kjelstrup KB, Fyhn M, Witter MP, Moser EI, Moser MB (2008) Progressive increase in grid scale from dorsal to ventral medial entorhinal cortex. Hippocampus 18:1200-1212.

Dolorfo CL, Amaral DG (1998) Entorhinal cortex of the rat: Topographic organization of the cells of origin of the perforant path projection to the dentate gyrus. J Comp Neurol 398:25-48.

Dorph-Petersen KA, Nyengaard JR, Gundersen HJG (2001) Tissue shrinkage and unbiased stereological estimation of particle number and size. J Microsc 204:232-246.

Dorph-Petersen KA, Pierri JN, Sun Z, Sampson AR, Lewis DA (2004) Stereological analysis of the mediodorsal thalamic nucleus in schizophrenia: volume, neuron number, and cell types. J Comp Neurol 472:449-462.

Erchova I, Kreck G, Heinemann U, Herz AV (2004) Dynamics of rat entorhinal cortex layer II and III cells: characteristics of membrane potential resonance at rest predict oscillation properties near threshold. J Physiol 560:89-110.

Eyre MD, Richter-Levin G, Avital A, Stewart MG (2003) Morphological changes in hippocampal dentate gyrus synapses following spatial learning in rats are transient. Eur J Neurosci 17:1973-1980.

Franklin KB, Paxinos G (1997) The mouse brain in stereotaxic coordinates. San Diego CA: Academic press.

Fyhn M, Hafting T, Treves A, Moser MB, Moser EI (2007) Hippocampal remapping and grid realignment in entorhinal cortex. Nature 446:190-194.

Fyhn M, Hafting T, Witter MP, Moser EI, Moser M-B (2008) Grid cells in mice. Hippocampus 18:1230-1238.

Fyhn M, Molden S, Witter MP, Moser EI, Moser M-B (2004) Spatial Representation in the entorhinal cortex. Science 305:1258-1264.

Gaarskjaer FB (1978) Organization of the mossy fiber system of the rat studied in extended hippocampi. I. Terminal area related to number of granule and pyramidal cells. J Comp Neurol 178:49-72.

Garden DL, Dodson PD, O'Donnell C, White MD, Nolan MF (2008) Tuning of synaptic integration in the medial entorhinal cortex to the organization of grid cell firing fields. Neuron 60:875-889.

Gatome CW, Slomianka L, Mwangi D, Lipp H-P, Amrein I (2010) The entorhinal cortex of the Megachiroptera: a comparative study of Wahlberg's epauletted fruit bat and the straw-coloured fruit bat. Brain Struct Funct 214:375-393.

Geinisman Y, Detoledo-Morrell L, Morrell F, Persina IS, Beatty MA (1996) Synapse restructuring associated with the maintenance phase of hippocampal long-term potentiation. J Comp Neurol 368:413-423.

Germroth P, Schwerdtfeger WK, Buhl EH (1989) Morphology of identified entorhinal neurons projecting to the hippocampus. A light microscopical study combining retrograde tracing and intracellular injections. Neuroscience 30:683-691.

Giocomo LM, Hasselmo ME (2009) Knock-out of HCN1 subunit flattens dorsal-ventral frequency gradient of medial entorhinal neurons in adult mice. J Neurosci 29:7625- 7630.

Giocomo LM, Zilli EA, Fransen E, Hasselmo ME (2007) Temporal frequency of subthreshold oscillations scales with entorhinal grid cell field spacing. Science 315:1719-1722.

Gómez-Isla T, Price JL, McKeel Jr DW, Morris JC, Growdon JH, Hyman BT (1996) Profound loss of layer II entorhinal cortex neurons occurs in very mild Alzheimer's disease. J Neurosci 16:4491-4500.

Gundersen HJ (1988) The nucleator. J Microsc 151:3-21.

Gundersen HJG, Jensen EB, Kiêu K, Nielsen J (1999) The efficiency of systematic sampling in stereology--reconsidered. J Microsc 193:199-211.

Hafting T, Fyhn M, Molden S, Moser MB, Moser EI (2005) Microstructure of a spatial map in the entorhinal cortex. Nature 436:801-806.

Hamam BN, Sinai M, Poirier G, Chapman CA (2007) Cholinergic suppression of excitatory synaptic responses in layer II of the medial entorhinal cortex. Hippocampus 17:103- 113.

Insausti R, Herrero MT, Witter MP (1997) Entorhinal cortex of the rat: cytoarchitectonic subdivisions and the origin and distribution of cortical efferents. Hippocampus 7:146-183.

Irizarry MC, Soriano F, McNamara M, Page KJ, Schenk D, Games D, Hyman BT (1997) Aβ deposition is associated with neuropil changes, but not with overt neuronal loss in the human amyloid precursor protein V717F (PDAPP) transgenic mouse. J Neurosci 17:7053-7059.

Jones, RSG (1994) Synaptic and intrinsic properties of neurons of origin of the perforant path in layer II of the rat entorhinal cortex in vitro. Hippocampus 4:335-353.

Jones RSG, Buhl EH (1993) Basket-like interneurones in layer II of the entorhinal cortex exhibit a powerful NMDA-mediated synaptic excitation. Neurosci Lett 149:35-39.

Kjelstrup KB, Solstad T, Brun VH, Hafting T, Leutgeb S, Witter MP, Moser EI, Moser MB (2008) Finite scale of spatial representation in the hippocampus. Science 321:140-143.

Klink R, Alonso A (1993) Ionic mechanisms for the subthreshold oscillations and differential electroresponsiveness of medial entorhinal cortex layer II neurons. J Neurophysiol 70:144-157.

Klink R, Alonso A (1997a) Morphological characteristics of layer II projection neurons in the rat medial entorhinal cortex. Hippocampus 7:571-583.

Klink R, Alonso A (1997b) Muscarinic modulation of the oscillatory and repetitive firing properties of entorhinal cortex layer II neurons. J Neurophysiol 77:1813-1828.

Kumar SS, Buckmaster PS (2006) Hyperexcitability, interneurons, and loss of GABAergic synapses in entorhinal cortex in a model of temporal lobe epilepsy. J Neurosci 26:4613-4623.

Lingenhohl K, Finch DM (1991) Morphological characterization of rat entorhinal neurons in vivo: soma-dendritic structure and axonal domains. Exp Brain Res 84:57-74.

Lorente de Nó R (1933) Studies on the structure of the cerebral cortex. J Psychol Neurol 45:381-438.

McGowan E, Eriksen J, Hutton M (2006) A decade of modeling Alzheimer's disease in transgenic mice. Trends Genet 22:281-289.

McNaughton BL, Battaglia FP, Jensen O, Moser EI, Moser MB (2006) Path integration and the neural basis of the 'cognitive map'. Nat Rev Neurosci 7:663-678.

Merrill DA, Chiba AA, Tuszynski MH (2001) Conservation of neuronal number and size in the entorhinal cortex of behaviorally characterized aged rats. J Comp Neurol 438:445-456.

Moser E, Moser MB, Andersen P (1993) Spatial learning impairment parallels the magnitude of dorsal hippocampal lesions, but is hardly present following ventral lesions. J Neurosci 13:3916-3925.

Mulders WH, West MJ, Slomianka L (1997) Neuron numbers in the presubiculum, parasubiculum, and entorhinal area of the rat. J Comp Neurol 385:83-94.

Ramón y Cajal S (1988) On a special ganglion of the spheno-occipital cortex. In: Cajal on the cerebral cortex. An annoted translation of the complete writings. (DeFelipe J, Jones EG, eds), pp 363-376. New York: Oxford University Press.

Rapp PR, Deroche PS, Mao Y, Burwell RD (2002) Neuron number in the parahippocampal region is preserved in aged rats with spatial learning deficits. Cereb Cortex 12:1171-1179.

Rogers JH (1992) Immunohistochemical markers in rat cortex: co-localization of calretinin and calbindin-D28k with neuropeptides and GABA. Brain Res 587:147-157.

Schwartz SP, Coleman PD (1981) Neurons of origin of the perforant path. Exp Neurol 74:305-312.

Slomianka L, Geneser FA (1991) Distribution of acetylcholinesterase in the hippocampal region of the mouse: I. entorhinal area, parasubiculum, retrosplenial area and presubiculum. J Comp Neurol 303:359-354.

Slomianka L, West MJ (2005) Estimators of the precision of stereological estimates: an example based on the CA1 pyramidal cell layer of rats. Neuroscience 136:757-767.

Solstad T, Boccara CN, Kropff E, Moser MB, Moser EI (2008) Representation of geometric borders in the entorhinal cortex. Science 322:1865-1868.

Stark AK, Toft MH, Pakkenberg H, Fabricius K, Eriksen N, Pelvig DP, Møller M, Pakkenberg B (2007) The effect of age and gender on the volume and size distribution of neocortical neurons. Neuroscience 150:121-130.

Steffenach HA, Witter M, Moser MB, Moser EI (2005) Spatial memory in the rat requires the dorsolateral band of the entorhinal cortex. Neuron 45:301-313.

Tamamaki N, Nojyo Y (1993) Projection of the entorhinal layer II neurons in the rat as revealed by intracellular pressure-injection of neurobiotin. Hippocampus 3:471-480.

Tandrup T (1993) A method for unbiased and efficient estimation of number and mean volume of specified neuron subtypes in rat dorsal root ganglion. J Comp Neurol 329:269-276.

Tuñón T, Insausti R, Ferrer I, Sobreviela T, Soriano E (1992) Parvalbumin and calbindin D-28K in the human entorhinal cortex. An immunohistochemical study. Brain Res 589:24-32.

van Groen T (2001) Entorhinal cortex of the mouse: cytoarchitectonical organization. Hippocampus 11:397-407.

van Groen T, Kadish I, Wyss JM (2002) Species differences in the projections from the entorhinal cortex to the hippocampus. Brain Res Bull 57:553-556.

van Groen T, Miettinen P, Kadish I (2003) The entorhinal cortex of the mouse: organization of the projection to the hippocampal formation. Hippocampus 13:133-149.

Weeks AC, Ivanco TL, LeBoutillier JC, Racine RJ, Petit TL (1998) The degree of potentiation is associated with synaptic number during the maintenance of long-term potentiation in the rat dentate gyrus. Brain Res 798:211-216.

West MJ, Slomianka L, Gundersen HJG (1991) Unbiased stereological estimation of the total number of neurons in the subdivisions of the rat hippocampus using the optical fractionator. Anat Rec 231:482-497.

Witter MP (2007) The perforant path: projections from the entorhinal cortex to the dentate gyrus. Prog Brain Res 163:43-61.

Wouterlood FG, Hartig W, Bruckner G, Witter MP (1995) Parvalbumin-immunoreactive neurons in the entorhinal cortex of the rat: localization, morphology, connectivity and ultrastructure. J Neurocytol 24:135-153.

Wouterlood FG, van Denderen JC, van Haeften T, Witter MP (2000) Calretinin in the entorhinal cortex of the rat: distribution, morphology, ultrastructure of neurons, and co-localization with γ-aminobutyric acid and parvalbumin. J Comp Neurol 425:177-192.

Figure 1

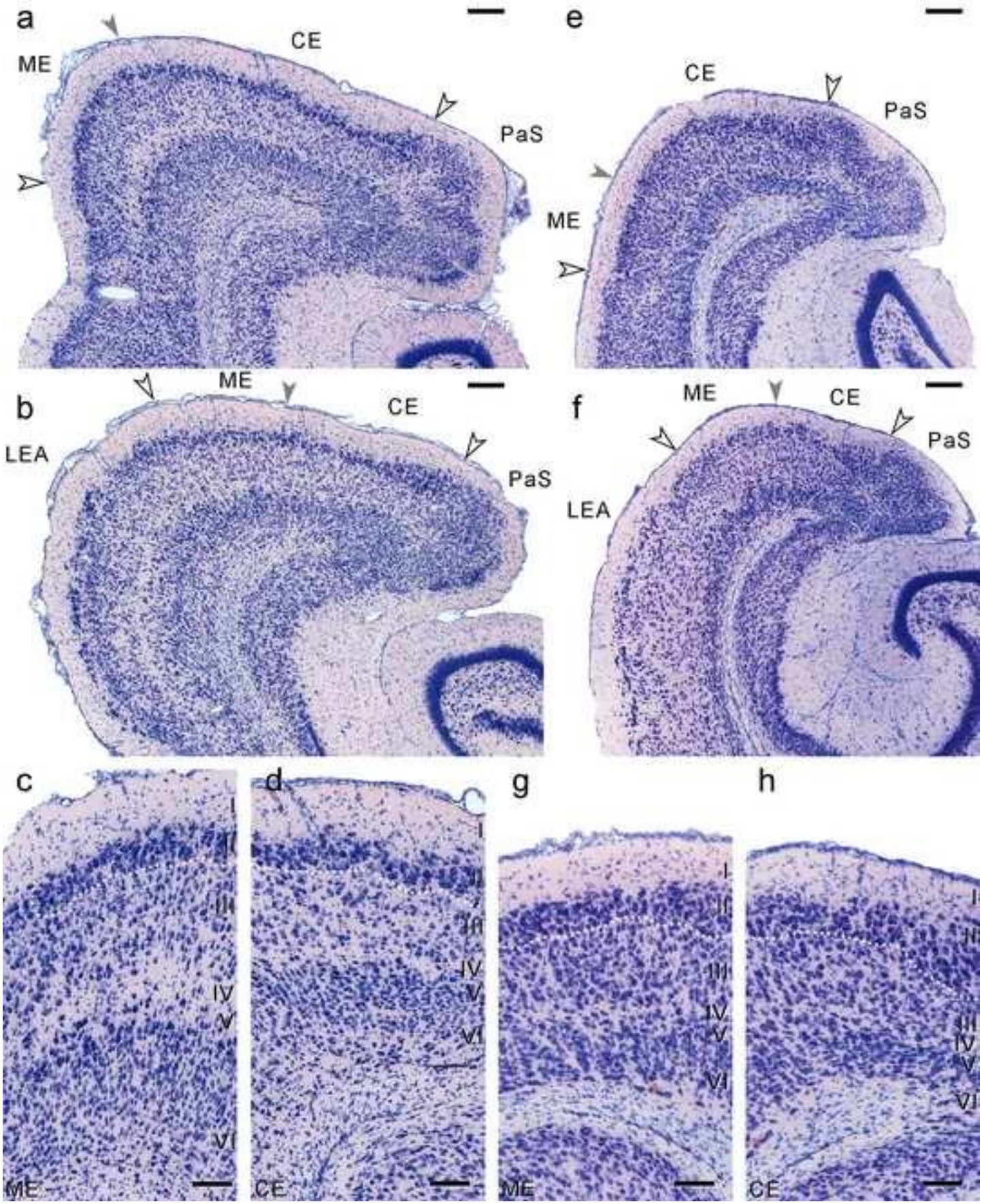
a
ME
CE
PaS
e
CE
PaS
ME
b
ME
CE
LEA
PaS
f
ME
CE
PaS
LEA
c
I
II
III
IV
V
VI
ME
d
I
II
III
IV
V
VI
CE
g
I
II
III
IV
V
VI
ME
h
I
II
III
IV
V
VI
CE

Figure 2

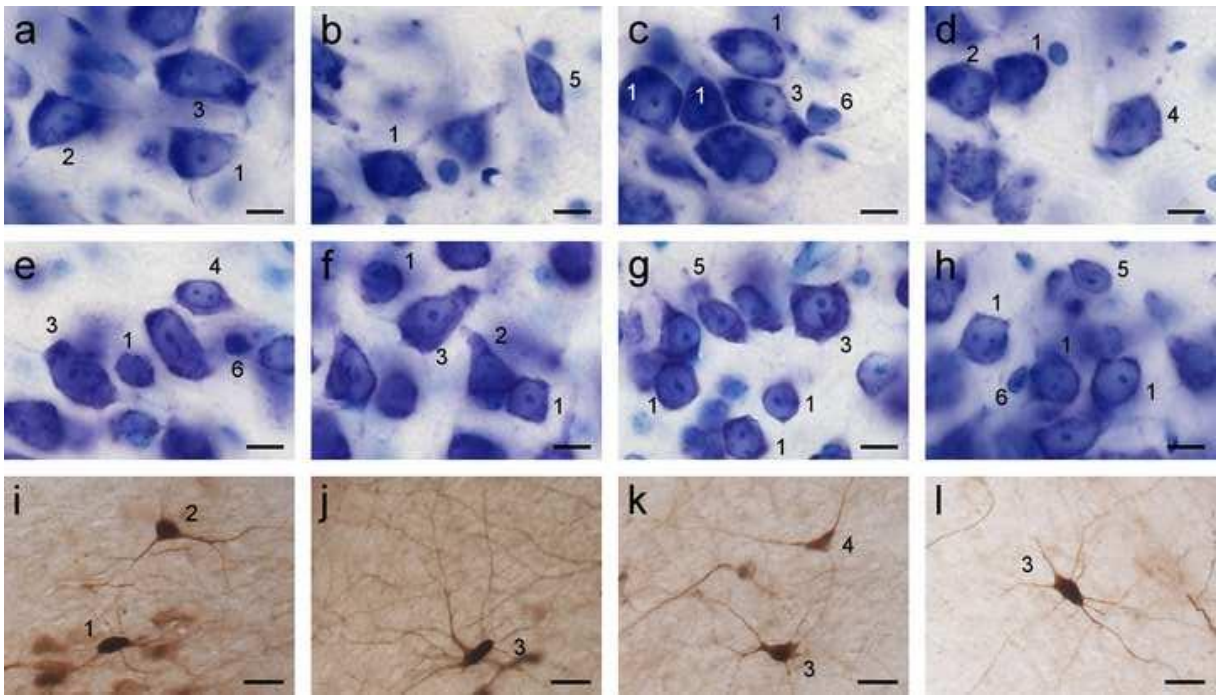

Figure 3

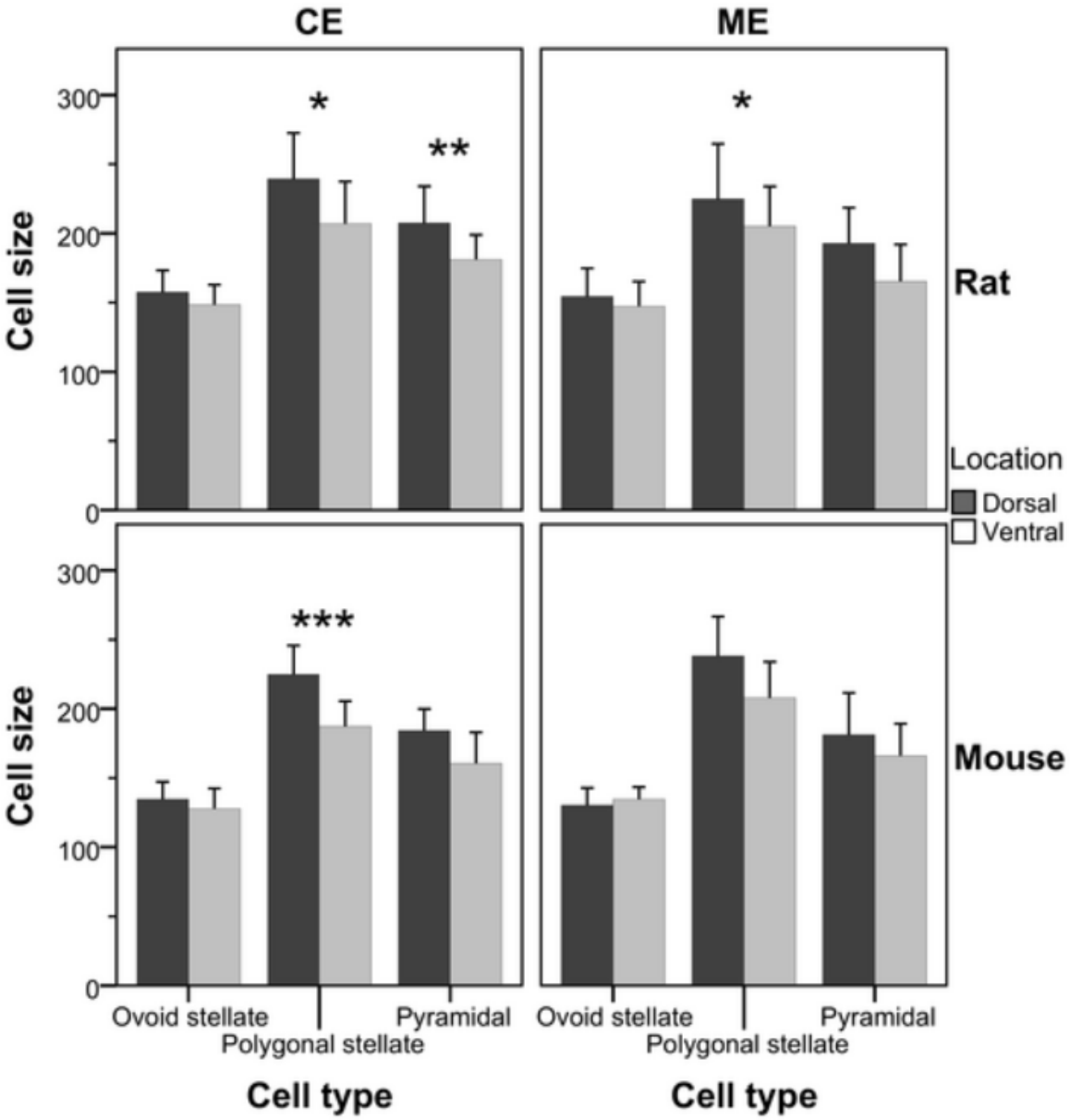
CE
ME
Cell size
300
200
100
0
*
**
*
Rat
Location
Dorsal
Ventral
***
Mouse
Ovoid stellate
Polygonal stellate
Pyramidal
Cell type

Figure 4

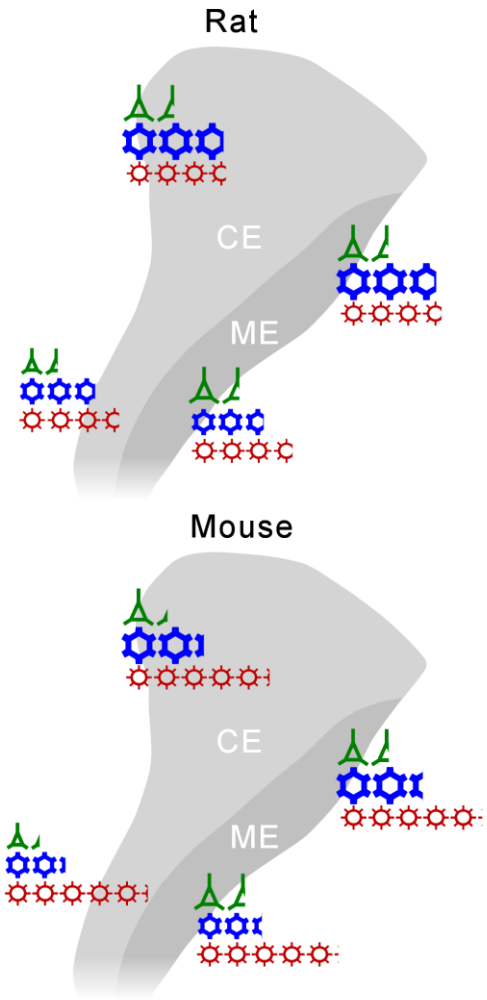

Title

Hippocampal neurogenesis and cortical cellular plasticity in Wahlberg's epauletted fruit bat: A qualitative and quantitative study

Authors

Catherine W. Gatome[1], Deter K. Mwangi[2], Hans-Peter Lipp[1], Irmgard Amrein[1]

[1]Institute of Anatomy, University of Zurich, Winterthurerstrasse 190, 8057 Zurich, Switzerland

[2]Department of Veterinary Anatomy and Physiology, University of Nairobi, PO Box 30107-00100 Nairobi, Kenya

Running title

Neurogenesis in fruit bats

Keywords

Epomophorus wahlbergi, hippocampus, olfactory bulb, piriform cortex, immunohistochemistry, optical fractionators, plasticity

Figures 5, Tables 2

Corresponding author

Irmgard Amrein, Institute of Anatomy, University of Zurich, Winterthurerstrasse 190, CH-8057 Zurich, Switzerland

Phone +41 44 635 53 42; Fax +41 44 635 57 02 ; Mail: i.amrein@anatom.uzh.ch

ABSTRACT

Species-specific characteristics of neuronal plasticity emerging from comparative studies can address the functional relevance of hippocampal or cortical plasticity in light of ecological adaptation and evolutionary history of a given species. Here, we present a quantitative and qualitative analysis of neurogenesis in young and adult free-living Wahlberg's epauletted fruit bat. Using PCNA, BrdU, DCX and PSA-NCAM, we describe our findings in the hippocampus, olfactory and cortical regions and compare them to reports in other mammals. Expressed as a percentage of the total number of granule cells, PCNA- and BrdU-positive cells account for 0.04 in young (y) to 0.01% in adult (a) animals; DCX-positive cells for 0.05 (y) to 0.01% (a); PSA-NCAM-positive cells for 0.1 (y) to 0.02% (a); and pyknotic cells for 0.007 (y) to 0.005% (a). The numbers are comparable to other long-lived, late maturing mammals such as primates. A significant increase of total granule cell number from young to adult animals demonstrates the successful formation and integration of new cells. In adulthood, granule cell number appears stable and is surprisingly low in comparison to other species. Observations in the olfactory bulb and rostral migratory stream are qualitatively similar to descriptions in other species. In the ventral horn of the lateral ventricle, we note a prominent expression of DCX and PSA-NCAM forming a temporal migratory stream targeting the piriform cortex, possibly reflecting the importance of olfaction to these species.

Low, but persistent hippocampal neurogenesis in non-echolocating fruit bats contrasts the findings in echolocating microbats, in which hippocampal neurogenesis is largely absent. Together with the observed intense cortical plasticity in the olfactory system of fruit bats we suggest a differential influence of sensory modalities on hippocampal and cortical plasticity in this mammalian order.

INTRODUCTION

Adult neurogenesis has been reported across several species living under laboratory conditions or in their natural habitats [Amrein et al. 2008]. Similarities and differences have been described in proliferative zones and rates of neuron formation [Kaslin et al. 2008] with species-specific differences attributed to lifespan and age [Kornack and Rakic 1999; Lindsey and Tropepe 2006; Ben Abdallah et al. 2010]. The functional relevance of adult-born neurons is still intensively investigated, and studying natural populations with a wide range of ecological and behavioural demands is an advocated approach in the functional investigation of adult neurogenesis [Nottebohm 2002; Treves et al. 2008; Barnea 2009; Barnea 2010].

Bats occupy an unique ecological niche among mammals, and initial investigations in echolocating microbats (Microchiroptera) [Amrein et al. 2007] have demonstrated neurogenesis in the olfactory bulb and subventricular zone common to also rodents [Lois et al. 1996] and primates [Pencea et al. 2001]. However, hippocampal neurogenesis in microbats was observed to be largely absent and, when present, occurred at a low rate [Amrein et al. 2007]. Microbats and the non-echolocating fruit bats (Megachiroptera) share an evolutionary history with an unique adaptation to flight and longevity [Teeling et al. 2000; Shen et al. 2010; Wilkinson and South 2002] and fruit-eating microbats and fruit bats have a common ecological niche [Thies et al. 1998; Hutcheon et al. 2002; Hodgkison et al. 2007]. Fruit bats use olfactory and visual senses for spatial orientation and navigation, as shown for locating ripe fruit [Hodgkison et al. 2007; Raghuram et al. 2009]. Indeed, brain regions processing visual and olfactory information are prominent in fruit bats [Barton et al. 1995; Hutcheon et al. 2002]. Most interesting is that nectar- and fruit eating lifestyles evolved independently in micro- and fruit bats, leading to convergent clustering of brain proportions in these species [de Winter and Oxnard 2001]. Nectar- and fruit eating microbats lack adult

hippocampal neurogenesis [Amrein et al. 2007], and investigating fruit bats can therefore reveal if cellular plasticity in these species is subservient to phylogenetic constraints characterising the Chiroptera or, if present, is a trait reflecting a mosaic organization caused by selective adaptation as proposed by de Winter & Oxnard (2001).

Descriptions of cellular plasticity as inferred from cortical doublecortin (DCX) staining include almost the entire brain if compounded across the investigated mammalian species [Gould et al. 2001; Nacher et al. 2001; Bernier et al. 2002; Nacher et al. 2002; Shapiro et al. 2007; Xiong et al. 2008; Luzzati et al. 2009]. The presence of DCX-positive cells in the piriform cortex appears common to several species, perhaps indicative of the shared importance of olfaction. The piriform cortex in its role of olfactory discrimination and autoassociative learning [Barnes et al. 2008; Linster et al. 2009] displays a high degree of synaptic plasticity, and it appears that a need for structural plasticity is reflected in the persistent expression of proteins such as DCX or PSA-NCAM. Given that fruit bats rely on precise olfactory discrimination, we therefore expect a high demand for plasticity in the piriform cortex to be reflected by the expression of markers of cellular plasticity.

Additionally, fruit bats are relatively long-lived (~20 years) [Wilkinson and South 2002] and mature late; Wahlberg's epauletted fruit bat achieves sexual maturity at 15 months of age [Acharya 1992]. Fruit bats therefore provide the opportunity to test the hypothesis that long-lived and late maturing species have lower rates of adult hippocampal neurogenesis [Kornack and Rakic 1999; Amrein and Lipp 2009]. We present here a qualitative and quantitative assessment of neurogenesis in young and adult, free-living Wahlberg's

epauletted fruit bat. For this, we used antibodies against proliferating cells (PCNA and BrdU) and immature neurons (DCX and PSA-NCAM) and identified dying cells by their morphological appearance. We discuss our findings in relation to the ecology and behaviour of this species, and compare the rate of neurogenesis of fruit bats with rodents and primates.

MATERIALS AND METHOD

Animals and Treatment

The original research reported herein was performed under guidelines established by the National Museums of Kenya and University of Nairobi. Wahlberg's epauletted fruit bats (n=14) were captured in Nairobi, Kenya, and licences were granted by the National Museums of Kenya. The animals were assigned to one of two age groups (young and adult, Table 1) based on the following criteria: closure of the femoral and humeral epiphyseal plate, body weight, forearm length and sexual maturity (evidence of lactation or pregnancy). Young animals were flying and feeding independently of adults.

Five animals (three young, two adults) were injected with a single dose (100 mg/kg i.p.) of BrdU (BD Biosciences, San Diego, CA) and perfused 12 h later.

Histology

Tissue preparation: Animals were deeply anaesthetized 12 h post-capture with sodium pentobarbital (Nembutal®, 50 mg/kg) and transcardially perfused first with heparinised 0.9% saline, followed by phosphate-buffered 0.6% sodium sulphide solution and then cold 4% paraformaldehyde in 0.1 M phosphate buffer with 15% picric acid. Brains were removed and post-fixed overnight at 4°C and transferred to 30% sucrose for 24 h.

Immunohistochemistry:

From frozen right hemispheres, forty micron coronal, horizontal and sagittal sections were cut and collected in twelve series. For each antibody, sections were run in a single batch with mouse brain tissue as controls. Antibody concentrations that gave the best signal to background ratio were determined by dilution series. Anti-proliferating cell nuclear antigen (PCNA) rabbit polyclonal antibody (1:30,000, Delta Biolabs, Gilroy, CA), anti-BrdU rat monoclonal antibody (1:400, Harlan Sera-Laboratories, Indianapolis, IN), anti-doublecortin (DCX) goat polyclonal antibody (1:1,000, Santa Cruz Biotechnology, Santa Cruz, CA) and anti-polysialic acid neural cell adhesion molecule (PSA-NCAM) mouse monoclonal antibody (1:5,000, Chemicon, Temecula, CA) were used to demonstrate proliferation and neurogenesis. One series was used for each marker. Sections were rinsed in tris-triton buffered saline (TBS, pH 7.4), and pre-treated in 0.6% hydrogen peroxide. Epitope retrieval in citrate buffer (ChemMate, DAKO, Glostrup, Denmark) at 94°C was done for PCNA immunolabelling. Sections were pre-incubated in normal serum for 1 h at room temperature, before overnight incubation in primary antibodies at 4°C. This was followed by rinsing with TBS (pH 7.4), incubation for 2 h at room temperature with biotinylated secondary antibodies (1:1000, goat anti-rabbit IgG (PCNA); rabbit anti-goat IgG (DCX); 1:500, donkey anti-mouse (PSA-NCAM)), rinses in TBS, and incubation for 35 min with avidin-biotin complex (ABC) (Vectastain® Elite ABC Kit, Vector Laboratories, Burlingame, CA). Immunoreaction was detected using 3, 3'-diaminobenzidinetrahydrochloride (DAB) staining. DCX and PSA-NCAM stained sections were counterstained with haematoxylin (51275 Fluka, Buchs, Switzerland).

For BrdU immunolabelling, sections were incubated overnight at 4°C with primary antibody following DNA denaturation (2 h incubation in 50% formamide/ 2X SSC (0.3 M sodium

chloride, 0.03 M sodium citrate) at 65°C), 15 min rinse in 2X SSC, 30 min incubation in 2 N hydrochloric acid at 37°C, and 10 min rinse in 0.1 M boric acid (pH 8.5). Detection with DAB followed incubation with a secondary goat anti-rat IgG (1:300, Jackson ImmunoResearch Laboratories, West Grove, PA) and ABC as described above.

Nissl staining: Left hemispheres were processed as described in detail before [Gatome et al. 2010]. Briefly, tissue was dehydrated, infiltrated and embedded with glycolmethylacrylate solution (Technovit 7100, Kulzer GmbH, Wehrheim, Germany). Twenty micron horizontal sections were Nissl-stained with Giemsa solution (Merck, Darmstadt, Germany).

Quantitative analysis of cell numbers: Estimates of total granule cell numbers were made in every twelfth glycolmethylacrylate-embedded Nissl-stained horizontal sections. Using the StereoInvestigator® software (MicroBrightfield Inc, Colchester, VT), total granule cell numbers were estimated using the Optical Fractionator method [West et al. 1991] with a 40x oil-immersion objective (N.A. 1.3) and a counting frame of 15 µm x 15 µm, a disector height of 10 µm and x, y-steps of 210 µm. Section thickness was measured at every 6^{th} sampling site. Cell numbers were estimated using number-weighed section thickness [Dorph-Petersen et al. 2001]. The same sections were also used for absolute counts of pyknotic cells [Amrein et al. 2004] in the subgranular layer (SGL). Dying cells were counted throughout the thickness of the sections, omitting cells in the top focal plane. Cell numbers were multiplied with the inverse of the section sampling fraction, e.g. 12. In every twelfth immunostained section, PCNA- and BrdU- positive cells were counted in the SGL while DCX -

and PSA-NCAM-positive cells were counted in both SGL and granular cell layer (GCL) following the rules described above for pyknotic cells.

Qualitative analysis of staining intensity: Analysis was performed in the same series of section used for the quantitative analysis for hippocampal neurogenesis. Staining pattern of PCNA, BrdU, DCX and PSA-NCAM was analysed in olfactory bulb, sub-ventricular zone (SVZ), temporal migratory stream and piriform cortex and scored as absent (0), weak staining with few, scattered immune-positive cells (1; e.g. Fig. 3i), moderate number of intensively immune-positive cells (2; e.g. Fig. 3k), intense staining with single and clustered, intensively immune-positive cells (3; e.g. Fig. 3d), or very intense staining with clusters and chains of heavily immune-positive cells (4; e.g. Fig. 3c, h).

Statistics: Statistical analyses were done using PASW Statistics version 17.0.0 (SPSS Inc., Chicago, IL). Age-dependent variations were tested with general linear model (GLM), correlations with Pearson's *r*. Coefficients of error (CE) for cell number estimates were calculated according to Gundersen et al. [Gundersen et al. 1999] using the conservative m = 0 approach [Slomianka and West 2005], and the ratio CE^2/CV^2 (CV=coefficient of variance) was calculated to test if variance resulting from the estimation procedures was a major contributor to group variance [Gundersen and Jensen 1987].

Image processing: Images were captured at 40 x – 100 x magnifications using a MBF CX9000 camera (MicroBrightField Inc., Colchester, VT). Adjustments were made to the brightness and colour of the images to restore the original optical clarity.

RESULTS

Animal details and number of brain sections analysed are shown in table 1. Adult animals had a higher body weight ($p = 0.0001$). Brain weight did not vary between the age groups.

Hippocampal region

We noted that PCNA-, BrdU- , DCX- , and PSA-NCAM-positive stained cells were mostly located in the infrapyramidal blade of the dentate gyrus. For all markers, few stained cells were also observed in the hilus and molecular layer of the dentate gyrus. Estimates of immunoreactive cell numbers and their relative proportions as a percentage of the resident granule cell population are shown in table 2 for both age groups.

Proliferation: PCNA and BrdU labelling pattern were typical compared to mouse tissue (Fig. 1a-d). The number of PCNA-positive cells was higher in young animals than in adults ($p < 0.0001$, Figs. 1c, d, 2). The number of BrdU-positive cells did not differ significantly between the age groups although a trend towards lower numbers in adults was evident ($p = 0.07$, Figs. 1a, b, 2). Overall, the numbers of BrdU-positive cells correlated with PCNA-positive cells ($r = 0.89$, $p = 0.046$). In young fruit bats, proliferating cells (BrdU and PCNA) accounted for 0.039% of the total granule cell number. In adults, this number decreased to 0.009%.

Neuronal differentiation: PSA-NCAM labelling pattern was typical compared to mouse tissue (Fig. 1e, f). The DCX-positive cells in the hippocampus (Fig. 1g, h) and in the brain regions described below stained considerably weaker in comparison to PSA-NCAM. The age-

dependent down-regulation in staining intensity was more pronounced for DCX than PSA-NCAM (Fig. 1e-h). In both age groups, some DCX-positive cells showed an atypical staining, with brownish stained somata that had no obvious processes. The numbers of DCX- and PSA-NCAM-positive cells were not significantly different between the age groups (Fig. 2). Overall, a strong correlation was noted between the numbers of DCX- and PSA-NCAM-positive cells (r = 0.89, p = 0.003). Across both age groups, DCX cell counts correlate with PCNA-positive cell counts, r = 0.54, p = 0.048, as do PSA-NCAM cell counts (r = 0.73, p = 0.039).

Pyknotic cells: The age groups did not differ in the number of pyknotic cells (Fig. 2). Pyknotic cell numbers were highly correlated to PCNA-positive cell numbers in adult (r = 0.909; p = 0.005), but not in young animals (r = 0.229; p = 0.62). Pyknotic cells were also observed in the hilus and molecular layer of the dentate gyrus.

Granule cell number: Mean granule cell number in young animals accounts for 86% of the mean total number in adult animals. The granule cell number was higher in adult animals (p = 0.047).

CE^2/CV^2: Ratio CE^2/CV^2 shown in table 2 indicates that the variation in the data introduced through the methodology is a minor contributor to the observed group variances. The only exception is total granule cell number in adults; however, in this case the average of CE estimates was 11% only.

Olfactory bulb and sub-ventricular zone (SVZ)

Staining was typical to that observed in the mouse tissue. We observed newly born neurons migrating to the olfactory bulb from the lateral ventricle through the rostral migratory stream (RMS) as shown in rodents and primates (Fig. 3a-d) [Lois et al. 1996; Kornack and Rakic 2001]. There were individual clusters and chains of cells labelled for PCNA, BrdU, DCX and PSA-NCAM in the SVZ. DCX- and PSA-NCAM-positive cells displayed soma that extended stumpy dendritic processes resembling filopodia. In the olfactory bulb, proliferating cells appeared in small clusters in young animals, and as individual cells in young and adult animals (Fig. 3j, k). The olfactory bulb showed lower reactivity compared to the SVZ. A patent olfactory ventricle is present in the olfactory bulb of fruit bats, unlike in primates and mice. DCX- and PSA-NCAM-positive cells were observed in the bulbar ventricle wall and some spread radially towards the granule cells, extending fine processes. Scored staining intensities for PCNA, and BrdU (Fig. 4), and DCX and PSA-NCAM (Fig. 5) showed that immunoreactivity decreased significantly with age (all measurements $p < 0.01$) except for a marginally non-significant decrease of PSA-NCAM in the olfactory bulb ($p = 0.055$).

Piriform cortex

In young animals, a temporal stream of DCX- and PSA-NCAM positive cells is apparent from the ventral horn of the lateral ventricle and lines the external capsule in an apparent rostrodorsal direction towards the anterior piriform cortex (Fig. 3 e, f). More caudally, the migrating chain surrounds the amygdala targeting the posterior piriform cortex. At the caudal end, DCX- and PSA-NCAM positive dendrites appear perpendicular to the ventricle wall, ending in the posterior piriform cortex. The appearance of DCX- and PSA-NCAM-

positive cells in the migratory stream resembled that described in the SVZ above. DCX- and PSA-NCAM-positive cells located in layers II and III were mostly oriented perpendicular to the pial surface (Fig. 3h, i). Cell clustering was more obvious in the young animals, and stained cells were of round, pyramidal and fusiform morphology. Most cells had several fine, elongated branching processes extending into the molecular layer above and white matter below. PCNA- and BrdU-positive cells along the ventricle walls were present in young animals, but scarce in adults (Fig. 3, insert in e). Scored staining intensities for PCNA, BrdU, DCX and PSA-NCAM in the temporal migratory stream and in the piriform cortex were significantly higher in young than adult animals (all measurements $p < 0.01$) except for PCNA in the piriform cortex ($p = 0.15$) (Figs. 4, 5). Pyknotic cells were also observed in the piriform cortex layer II, more frequently in young animals.

DISCUSSION

We provide quantitative data and a description of neurogenesis in Wahlberg's epauletted fruit bat, a member of the non-echolocating, fruit- and nectar feeding Megachiroptera. We report for this species a low hippocampal neurogenesis, but extensive presence of markers for young neurons in other brain areas such as piriform cortex. We discuss our findings in relation to possible functional implications within the context of other mammalian species.

Hippocampal neurogenesis

We present the first report of cellular plasticity and neurogenesis in a fruit bat species using immunohistochemical markers. We applied two different antibodies for proliferating cells (PCNA, BrdU) and differentiating neuronal cells (DCX, PSA-NCAM) and observed good correlations between the markers. This indicates that, within the limits of explanatory power of immunohistochemical techniques, proteins specific for proliferating cells and differentiating neurons are expressed in Wahlberg's epauletted fruit bat, as they are in rodents. Comparison of neurogenesis across studies and species has to deal with differences in methodology and species life spans [Kempermann 2006]. We use life-stages i.e. young and adult, in comparing our age groups with those in other species. We also express the number of proliferation and neurogenesis-related cell counts as a percentage of the resident granule cell number. This is necessary to assess the relative importance of the newly formed cells in relation to the functions subserved by the resident granule cells. The relationship between estimates of cell proliferation, neuronal differentiation and cell death provide valuable insights into species- or higher order specific regulatory mechanisms of adult neurogenesis.

Comparative assessment

Proliferation: In two month old C57 mice, proliferating, PCNA-positive cells [Snyder et al. 2009] amount to ~0.9% of the total granule cell number [Ben Abdallah et al. 2010], BrdU–positive cells in a 2h survival paradigm amount to ~0.6% [Chitra et al. 2004]. In primates, BrdU-positive cells [Leuner et al. 2007] amount to 0.03% (Kozorovitskiy 2005) in adult marmosets. In the fruit bat, the number for PCNA- positive cells is 0.04 to 0.01% of the total granule cell number in young and adult animals respectively, cell counts for BrdU reveal the same numbers. Thus, fruit bats show a low level of proliferation in the SGL that is comparable to primates. Our observation of equal number of BrdU- and PCNA-positive cells contrasts with two-fold higher number of PCNA-positive cells in comparison to BrdU-positive cell counts in mice [Chitra et al. 2004; Snyder et al. 2009]. However, it fits well with others, reporting only minor differences [Gil et al. 2005; Valero et al. 2005]. Cell cycle duration is not known in fruits bats, but our survival time of 12 h might have allowed cells to incorporate BrdU and complete mitosis resulting in two daughter cells [Cameron and McKay 2001].

Neuronal differentiation: With regard to neuronal differentiation, our findings fall below those of rodents indicating a low level of neurogenic activity in the dentate gyrus of fruit bats. In mice, DCX-positive cells drop from ~2.1% in two month to 0.2% in seven to nine month old animals [Ben Abdallah et al. 2010]. In adult Sprague-Dawley rats, the PSA-NCAM-positive cells amount to 1.6% of total granule cells [Pham et al. 2003]. In fruit bats, PSA-NCAM- positive cells account only for 0.1 to 0.02% of the total number of granule cells in young and adult animals. The percentages of DCX-positive cells are even lower (0.05 to 0.01%). DCX and PSA-NCAM have an overlapping window of expression in rodents [Ming and Song 2005; Lledo et al. 2006]. In fruit bats we find that the number of PSA-NCAM-positive cells in the dentate gyrus is twice as high as DCX. Although staining intensity of DCX was in

general weaker than PSA-NCAM, which might be due to a species-specific regulation or different antigenicity, both markers overlap in their regional staining and age-dependent down-regulation.

Cell death: In fruit bats, the pyknotic cells amount to 0.007 and 0.005% of the total granule cells in young and adult animals respectively, again closer to the numbers in primates [Jabès et al. 2010] than to mice [Ben Abdallah et al. 2010].

Young fruit bats show significantly more proliferating cells and, albeit not significantly, higher numbers of young cells of the neuronal lineage. The net increase of total granule cells at the transition from young to adult animals supports the assumption of an experience-dependent addition of new cells [Tashiro et al. 2007]. Behaviourally, this corresponds with the exposure to increasingly novel sensory stimuli in early flight periods. In adults, cell proliferation and cell death are tightly linked in rodents [Amrein et al. 2004] and fruit bats, suggesting similarities in the regulation of adult hippocampal neurogenesis in mammals. In fruit bats, the number of dentate gyrus granule cells is unlikely to increase in adulthood, as granule cell number, proliferation and pyknosis show low variation in the adults, despite the likely large range in ages of the animals studied. Essentially, we observe the same age-dependent decrease of proliferation as shown in other mammals [Kuhn et al. 1996]. The decrease in proliferative activity may be due to a drop in the number of dividing precursors in the dentate gyrus [Olariu et al. 2007].

We found a low total number of granule cells in fruit bats, which we did not expect because the hippocampal size index in a sister species of Wahlberg's epauletted fruit bat is by a

factor two larger than that of rats and corresponds well to that of primates [Gatome et al. 2010]. However, the mean number of granule cells in adult fruit bats of 950'000 is *below* the reported total granule cells of 1'200'000 in rats [West et al. 1991; Rapp and Gallagher 1996]. Fruit bats have the largest hippocampus among the Chiroptera [Baron et al. 1996b; Hutcheon et al. 2002], and its functional relevance has been linked to the use of complex habitats and large territories [Safi and Dechmann 2005], high demands for spatio-temporal memory processing in locating food sources [Hutcheon et al. 2002] and high alertness needed for species roosting in open space [Baron et al. 1996a]. The efficiency of hippocampal processing in Wahlberg's epauletted fruit bat is not mirrored in high numbers of resident or newly born granule cells, but might be linked to other cellular adjustments such as a highly differentiated entorhinal cortex [Gatome et al. 2010].

Olfactory system

In young fruit bats, we find a prominent rostral migratory stream leading to the olfactory bulb, as well as a temporal stream of young neurons originating from the ventral horn of the lateral ventricle targeting the piriform cortex. Inspection of coronal, horizontal and sagittal DCX- and PSA-NCAM stained series of sections indicate that DCX and PSA-NCAM positive cells in anterior and posterior piriform cortex originate from the temporal migratory stream as shown in rabbits [Luzzati et al. 2009] and primates [Bernier et al. 2002], there is no indication of a caudoventral migratory stream targeting the anterior piriform cortex as shown in rats [Shapiro et al. 2007].

The staining pattern of immunoreactive cells in layer II of the piriform cortex with their dendrites extending in layer I and deep layers resemble closest to what has been shown in

cats [Cai et al. 2009]. However, Cai and co-authors do not advocate that these cells migrate from the ventricles into the cortical areas, stating that DCX-positive cells in the piriform cortex are resident. We argue that the DCX- and PSA-NCAM-positive cells in this area are not likely to be progeny of resident precursor cells, but migrate from the ventricle walls to their final destination as shown in other species [Luzzati et al. 2009; Bernier et al. 2002], indicated by the strong proliferation activity in the ventricle walls of the temporal horn seen in BrdU and PCNA stained sections and the intense migratory stream towards the cortical area. We observed an age-related decrease in DCX and PSA-NCAM expression in the piriform cortex of the bat as described in the rat [Shapiro et al. 2007] with adult animals displaying weak immunoreactivity in the temporal stream and piriform cortex.

Relationship between sensory modalities and neuronal plasticity?

Expression of DCX and PSA-NCAM in the piriform cortex appears to be a common feature across several species for whom olfaction is important. The olfactory bulb sends direct input to the piriform cortex where several forms of plasticity have been reported in response to odour experiences [Wilson et al. 2004]. Olfactory discrimination and autoassociative learning in the piriform cortex [Barnes et al. 2008; Linster et al. 2009] might dependent on the expression of NCAM as shown in young rats [Knafo et al. 2005]. Integration of new neurons, which in the olfactory bulb is necessary in readapting to ongoing environmental changes and to maintain maximal discrimination [Petreanu and Alvarez-Buylla 2002; Rochefort et al. 2002], could represent an adaptive process in the piriform cortex as well. The flower-visiting and fruit eating microbats do not express DCX in the piriform cortex (Amrein, unpublished observations) possibly because they have not developed their olfactory system to the same

extent, relying more on echolocation for food detection (Hutcheon et al. 2002). Therefore, DCX and probably also PSA-NCAM expression in the piriform cortex appears to be confined to the fruit bats. This cellular plasticity in response to sensory processing requirements thus reflects mosaic trait of brain organization, despite the shared ecological niche and the common evolutionary ancestry of the two bat groups.

The abilities of the microbats to discriminate between group members and perform spatial tasks are aided by auditory mechanisms [Mueller and Emlen 1957; Mueller and Mueller 1979; Boughman and Wilkinson 1998], which modulate the hippocampus in a manner different from rodents [Ulanovsky and Moss 2007]. Possibly, the adaptive value of the auditory system [O'Neill and Suga 1979; Suga and O'Neill 1979] takes precedence over other structures involved in spatial and olfactory tasks (Hutcheon et al. 2002). Olfactory sensory stimulation may be linked to hippocampal neurogenesis as olfactory bulbectomy in rats leads to decreased hippocampal neurogenesis [Jaako-Movits and Zharkovsky 2005; Pope and Wilson 2007]. If foraging demands and sensory modalities influence the occurrence and nature of hippocampal plasticity in fruit bats (as well), it is worth undertaking an investigation in a species such as *Rousettus*. This fruit bat species faces similar foraging demands as Wahlberg's epauletted fruit bat and uses all three sensory modalities, olfaction, vision and echolocation. A further approach would be to investigate hippocampal neurogenesis in *Eidolon helvum*, a closely related species which uses larger home ranges and shows migratory behaviour.

Acknowledgement

This work was supported by the NCCR 'Neural Plasticity and Repair', Swiss National Science Foundation and an IBRO Rita Levi Montalcini Fellowship for African Women in Neuroscience to CWG. We are grateful to Ben Agwanda (National Museums of Kenya, Nairobi) for guidance on the species biology, ecology and logistical support, Francis Muchemi (National Museums of Kenya, Nairobi) for assistance in the capture, and Lutz Slomianka for assistance with the pictures.

References

Acharya L (1992) *Epomophorus wahlbergi*. Mammalian Species 394:1-4.

Amrein I, Boonstra R, Lipp H-P, Wojtowicz JM (2008) Adult neurogenesis in natural populations of mammals. In Adult neurogenesis (FH Gage, G Kempermann, H Song (eds)). New York: Cold Spring Harbor Laboratory Press, pp645-659.

Amrein I, Dechmann DKN, Winter Y, Lipp H-P (2007) Absent or low rate of adult neurogenesis in the hippocampus of bats (Chiroptera). Plos One 2:e455.

Amrein I, Lipp HP (2009) Adult hippocampal neurogenesis of mammals: evolution and life history. Biol Lett 5:141-144.

Amrein I, Slomianka L, Lipp HP (2004) Granule cell number, cell death and cell proliferation in the dentate gyrus of wild-living rodents. Eur. J. Neurosci. 20:3342-3350.

Barnea A (2009) Interactions between environmental changes and brain plasticity in birds. Gen. Comp. Endocrinol. 163:128-134.

Barnea A (20101) Wild neurogenesis. Brain Behav. Evol. 75:86-87.

Barnes DC, Hofacer RD, Zaman AR, Rennaker RL, Wilson DA (2008) Olfactory perceptual stability and discrimination. Nat. Neurosci. 11:1378-1380.

Baron G, Stephan H, Frahm HD (1996a) Comparative Neurobiology in Chiroptera: Brain Characteristics in Functional Systems, Ecoethological Adaptation, Adaptive Radiation and Evolution. Basel: Birkhäuser Verlag.

Baron G, Stephan H, Frahm HD (1996b) Comparative Neurobiology in Chiroptera: Macromorphology, brain structures, tables and atlases. Basel: Birkhäuser Verlag.

Barton RA, Purvis A, Harvey PH (1995) Evolutionary radiation of visual and olfactory brain systems in primates, bats and insectivores. Philosophic Trans. R. So. Lond. B 348:381-392.

Ben Abdallah NMB, Slomianka L, Vyssotski AL, Lipp H-P (2010) Early age-related changes in adult hippocampal neurogenesis in C57 mice. Neurobiol. Aging 31:151-161.

Bernier PJ, Bédard A, Vinet J, Lévesque M, Parent A (2002) Newly generated neurons in the amygdala and adjoining cortex of adult primates. Proc. Natl. Acad. Sci. 99:11464-11469.

Boughman JW, Wilkinson GS (1998) Greater spear-nosed bats discriminate group mates by vocalizations. Anim. Behav. 55:1717-1732.

Cai Y, Xiong K, Chu Y, Luo D-W, Luo X-G, Yuan X-Y, Struble RG, Clough RW, Spencer DD, Williamson A, Kordower JH, Patrylo PR, Yan X-X (2009) Doublecortin expression in adult cat and primate cerebral cortex relates to immature neurons that develop into GABAergic subgroups. Exp. Neurol. 216:342-356.

Cameron H, McKay R (2001) Adult neurogenesis produces a large pool of new granule cells in the dentate gyrus. J. Comp. Neurol. 435:406-417.

Chitra DM, Rebekah DN, Amelia JE (2004) Chronic morphine induces premature mitosis of proliferating cells in the adult mouse subgranular zone. J. Neurosci. Res. 76:783-794.

de Winter W, Oxnard CE (2001) Evolutionary radiations and convergences in the structural organization of mammalian brains. Nature 409:710-714.

Dorph-Petersen KA, Nyengaard JR, Gundersen HJG (2001) Tissue shrinkage and unbiased stereological estimation of particle number and size. J. Microsc. 204:232-246.

Gatome C, Slomianka L, Mwangi D, Lipp H-P, Amrein I (2010) The entorhinal cortex of the Megachiroptera: a comparative study of Wahlberg's epauletted fruit bat and the straw-coloured fruit bat. Brain Structure Funct. 214:375-393.

Gil JMAC, Mohapel P, Araújo IM, Popovic N, Li J-Y, Brundin P, Petersén Å (2005) Reduced hippocampal neurogenesis in R6/2 transgenic Huntington's disease mice. Neurobiol. Dis. 20:744-751.

Gould E, Vail N, Wagers M, Gross CG (2001) Adult-generated hippocampal and neocortical neurons in macaques have a transient existence. Proc. Natl. Acad. Sci. 98:10910-10917.

Gundersen HJ, Jensen EB (1987) The efficiency of systematic sampling in stereology and its prediction. J. Microsc. 147:229-263.

Gundersen HJG, Jensen EB, Kiêu K, Nielsen J (1999) The efficiency of systematic sampling in stereology--reconsidered. J. Microsc. 193:199-211.

Hodgkison R, Ayasse M, Kalko E, Häberlein C, Schulz S, Mustapha W, Zubaid A, Kunz T (2007) Chemical ecology of fruit bat foraging behavior in relation to the fruit odors of two species of paleotropical bat-dispersed figs (Ficus hispida and Ficus scortechinii). J. Chem. Ecol. 33:2097-2110.

Hutcheon JM, Kirsch JA, Garland Jr T (2002) A comparative analysis of brain size in relation to foraging ecology and phylogeny in the Chiroptera. Brain Behav. Evol. 60:165-180.

Jaako-Movits K, Zharkovsky A (2005) Impaired fear memory and decreased hippocampal neurogenesis following olfactory bulbectomy in rats. Eur. J. Neurosci. 22:2871-2878.

Jabès A, Lavenex PB, Amaral DG, Lavenex P (2010) Quantitative analysis of postnatal neurogenesis and neuron number in the macaque monkey dentate gyrus. Eur. J. Neurosci. 31:273-285.

Kaslin J, Ganz J, Brand M (2008) Proliferation, neurogenesis and regeneration in the non-mammalian vertebrate brain. Philosophic Trans. R. So. Lond. B 363:101-122.

Kempermann G (2006) Adult neurogenesis in different animal species. In G. Kempermann (ed.), Adult neurogenesis: stem cells and neuronal development in the adult brain. New York: Oxford University Press, Inc.

Knafo S, Barkai E, Herrero AI, Libersat F, Sandi C, Venero U (2005) Olfactory learning-related NCAM expression is state, time, and location specific and is correlated with individual learning capabilities. Hippocampus 15:316-325.

Kornack DR, Rakic P (1999) Continuation of neurogenesis in the hippocampus of the adult macaque monkey. Proc. Natl. Acad. Sci. 96:5768-5773.

Kornack DR, Rakic P (2001) The generation, migration, and differentiation of olfactory neurons in the adult primate brain. Proc. Natl. Acad. Sci. 98:4752-4757.

Kuhn HG, Dickinson-Anson H, Gage FH (1996) Neurogenesis in the dentate gyrus of the adult rat: age-related decrease of neuronal progenitor proliferation. J. Neurosci. 16:2027-2033.

Leuner B, Kozorovitskiy Y, Gross CG, Gould E (2007) Diminished adult neurogenesis in the marmoset brain precedes old age. Proc. Natl. Acad. Sci. 104:17169-17173.

Lindsey BW, Tropepe V (2006) A comparative framework for understanding the biological principles of adult neurogenesis. Prog. Neurobiol. 80:281-307.

Linster C, Menon AV, Singh CY, Wilson DA (2009) Odor-specific habituation arises from interaction of afferent synaptic adaptation and intrinsic synaptic potentiation in olfactory cortex. Learn. Memory 16:452-459.

Lledo PM, Alonso M, Grubb MS (2006) Adult neurogenesis and functional plasticity in neuronal circuits. Nature Rev. Neurosci. 7:179-193.

Lois C, García-Verdugo J-M, Alvarez-Buylla A (1996) Chain Migration of Neuronal Precursors. Science 271:978-981.

Luzzati F, Bonfanti L, Fasolo A, Peretto P (2009) DCX and PSA-NCAM expression identifies a population of neurons preferentially distributed in associative areas of different pallial derivatives and vertebrate species. Cereb. Cortex 19:1028-1041.

Ming GL, Song H (2005) Adult neurogenesis in the mammalian central nervous system. Annu. Rev. Neurosci. 28:223-250.

Mueller HC, Emlen JT, Jr. (1957) Homing in bats. Science 126:307-308.

Mueller HC, Mueller NS (1979) Sensory basis for spatial memory in bats. J. Mammal. 60:198-201.

Nacher J, Crespo C, McEwen BS (2001) Doublecortin expression in the adult rat telencephalon. Eur. J. Neurosci. 14:629-644.

Nacher J, Lanuza E, McEwen BS (2002) Distribution of PSA-NCAM expression in the amygdala of the adult rat. Neurosci. 113:479-484.

Nottebohm F (2002) Why are some neurons replaced in adult brain? J Neurosci 22:624-628.

O'Neill WE, Suga N (1979) Target range-sensitive neurons in the auditory cortex of the mustache bat. Science 203:69-73.

Olariu A, Cleaver KM, Cameron HA (2007) Decreased neurogenesis in aged rats results from loss of granule cell precursors without lengthening of the cell cycle. J. Comp. Neurol. 501:659-667.

Pencea V, Bingaman KD, Freedman LJ, Luskin MB (2001) Neurogenesis in the subventricular zone and rostral migratory stream of the neonatal and adult primate forebrain. Exp. Neurol. 172:1-16.

Petreanu L, Alvarez-Buylla A (2002) Maturation and death of adult-born olfactory bulb granule neurons: role of olfaction. J. Neurosci. 22:6106-6113.

Pham K, Nacher J, Hof PR, McEwen BS (2003) Repeated restraint stress suppresses neurogenesis and induces biphasic PSA-NCAM expression in the adult rat dentate gyrus. Eur. J. Neurosci. 17:879-886.

Pope K, Wilson DA (2007) Olfactory system modulation of hippocampal cell death. Neurosci. Lett. 422:13-17.

Raghuram H, Thangadurai C, Gopukumar N, Nathar K, Sripathi K (2009) The role of olfaction and vision in the foraging behaviour of an echolocating megachiropteran fruit bat, Rousettus leschenaulti (Pteropodidae). Mammal. Biol. 74:9-14.

Rapp PR, Gallagher M (1996) Preserved neuron number in the hippocampus of aged rat with spatial learning deficits. Proc. Natl. Acad. Sci. 93:9926-9930.

Rochefort C, Gheusi G, Vincent JD, Lledo PM (2002) Enriched odor exposure increases the number of newborn neurons in the adult olfactory bulb and improves odor memory. J. Neurosci. 22:2679-2689.

Safi K, Dechmann DK (2005) Adaptation of brain regions to habitat complexity: a comparative analysis in bats (Chiroptera). Proc. Biol. Sci. 272:179-186.

Shapiro L, Ng K, Kinyamu R, Whitaker-Azmitia P, Geisert E, Blurton-Jones M, Zhou Q-Y, Ribak C (2007) Origin, migration and fate of newly generated neurons in the adult rodent piriform cortex. Brain Structure Funct. 212:133-148.

Shen YY, Liu J, Irwin DM, Zhang YP (2010) Parallel and convergent evolution of the dim-light vision gene RH1 in bats (Order: Chiroptera). PLoS One 5:e8838.

Slomianka L, West MJ (2005) Estimators of the precision of stereological estimates: an example based on the CA1 pyramidal cell layer of rats. Neurosci. 136:757-767.

Snyder JS, Glover LR, Sanzone KM, Kamhi JF, Cameron HA (2009) The effects of exercise and stress on the survival and maturation of adult-generated granule cells. Hippocampus 19:898-906.

Suga N, O'Neill WE (1979) Neural axis representing target range in the auditory cortex of the mustache bat. Science 206:351-353.

Tashiro A, Makino H, Gage FH (2007) Experience-specific functional modification of the dentate gyrus through adult neurogenesis: a critical period during an immature stage. J. Neurosci. 27:3252-3259.

Teeling EC, Scally M, Kao DJ, Romagnoli ML, Springer MS, Stanhope MJ (2000) Molecular evidence regarding the origin of echolocation and flight in bats. Nature 403:188-192.

Thies W, Kalko EKV, Schnitzler H-U (1998) The roles of echolocation and olfaction in two Neotropical fruit-eating bats, *Carollia perspicillata* and *C. castanea*, feeding on Piper. Behav. Ecol. Sociobiol. 42:397-409.

Treves A, Tashiro A, Witter MP, Moser EI (2008) What is the mammalian dentate gyrus good for? Neurosci. 154:1155-1172.

Ulanovsky N, Moss CF (2007) Hippocampal cellular and network activity in freely moving echolocating bats. Nat. Neurosci. 10:224-233.

Valero J, Weruaga E, Murias AR, Recio JS, Alonso JR (2005) Proliferation markers in the adult rodent brain: bromodeoxyuridine and proliferating cell nuclear antigen. Brain Res. Protoc. 15:127-134.

West MJ, Slomianka L, Gundersen HJ (1991) Unbiased stereological estimation of the total number of neurons in the subdivisions of the rat hippocampus using the optical fractionator. Anat. Rec. 231:482-497.

Wilkinson GS, South JM (2002) Life history, ecology and longevity in bats (supplementary material). Aging Cell 1:124-131.

Wilson DA, Best AR, Sullivan RM (2004) Plasticity in the olfactory system: Lessons for the neurobiology of memory. Neuroscientist 10:513-524.

Xiong K, Luo DW, Patrylo PR, Luo XG, Struble RG, Clough RW, Yan XX (2008) Doublecortin-expressing cells are present in layer II across the adult guinea pig cerebral cortex: partial colocalization with mature interneuron markers. Exp. Neurol. 211:271-282.

Table 1: Animal and section characteristics

Age group	N, gender	Mean body weight (g), SD	Mean brain weight (g), SD	Cryosections mean, range	Plastic sections mean, range
Young	2M, 5F	53.5 (11)	1.7 (0.2)	8.7 (7-10)	19.4 (18-21)
Adult	1M, 6F	85.6 (7)	1.9 (0.1)	8.8 (7-10)	19.7 (18-23)

Table 2: Hippocampal proliferation and neurogenesis

	Young				Adult				Age differences
	N	Cell numbers mean, (SD)	In % to GC	CE^2/CV^2	N	Cell numbers mean, (SD)	In % to GC	CE^2/CV^2	p-values
PCNA	7	324 (80)	0.04	0.23	7	84 (48)	0.009	0.33	<0.0001
BrdU	3	292 (59)	0.04	0.71	2	90 (110)	0.01	0.10	0.07
DCX	7	422 (613)	0.05	0.03	7	72 (40)	0.008	0.22	0.158
PSA-NCAM	4	1188 (1070)	0.14	0.02	3	244 (288)	0.02	0.03	0.196
Pyknotic cells	7	54 (24)	0.007	0.33	7	44 (33)	0.005	0.26	0.528
Granule cells GC	7	819674 (117196)		0.39	7	945273 (94363)		1.57	0.047

Figure 1

Proliferation and neurogenesis in the hippocampus of young (a,c,e,g) and adult (b,d,f,h) fruit bats. In young animals (a), more cells in the subgranular layer (SGL) of the dentate gyrus having incorporated BrdU are visible than in adults (b). PCNA immunopositive cells in the SGL show a staining intensity similar to mouse tissue. PSA-NCAM (e,f) and DCX (g,h) immunopositive cells in the dentate gyrus stain considerably weaker than cortical and subventricular regions (see Fig 3) and in comparison to rodents. Scale bars: a,b 50μm; c-f 20μm; g,h 10μm; insert in b 5μm.

Figure 2

Stereologically estimated cell numbers in the dentate gyrus of young and adult fruit bats differ only for PCNA, all other cell numbers are not statistically different. Note the large individual variation in markers for young differentiating neurons (DCX and PSA-NCAM) in young animals. Bars = standard deviation SD

Figure 3

Proliferation and cellular neuronal plasticity in the SVZ, olfactory bulb, temporal migratory stream and piriform cortex in young and adult fruit bats.

Proliferating cells visualized with BrdU in the SVZ decrease from young (a) to adult (b) fruit bats. The age-dependent down-regulation is obvious for DCX positive cells in the SVZ as well (c young, d adult). Proliferating cells (BrdU, insert in e) in the temporal horn of the lateral ventricle are likely to be the founder population of migrating, PSA-NCAM positive cells

surrounding the amygdala and targeting the piriform cortex layer ll (PSA-NCAM in sagital (e) and coronal (f) sections of a young fruit bat. In the piriform cortex, PSA-NCAM-positive cell bodies are located in layer ll, abundant in young (h) and scarce in adult (i) animals. Close up of a PSA-NCAM positive, radially migrating neuron in piriform layer ll is shown in g. In the olfactory bulb, DCX positive cells forming extensive dendritic trees are abundant in young (j) and rare in adults (k).

BLA: basolateral amygdala; HIP: hippocampus; LV: lateral ventricle; ec: external capsule. Scale bars: a,b,e,f 500μm; c,d,h,I,j,k and inserts in a and b 50μm; g 5mm; insert in e 100μm.

Figure 4

Scored staining intensity for proliferation (PCNA and BrdU) in the subventricular zone (SVZ), olfactory bulb, piriform cortex and temporal migratory stream (TMS) reveal an age-dependent down-regulation in all regions except in the piriform cortex. Score: 1 weak; 2 moderate; 3 intense; 4 very intense. Bars = SD.

Figure 5

Scored staining intensity for neuronal differentiation (DCX and PSA-NCAM) in the SVZ, olfactory bulb, piriform cortex and TMS reveal an age-dependent down-regulation in all regions except for the olfactory bulb (only PSA-NCAM). Score: 1 weak; 2 moderate; 3 intense; 4 very intense. Bars = SD.

Figure 1

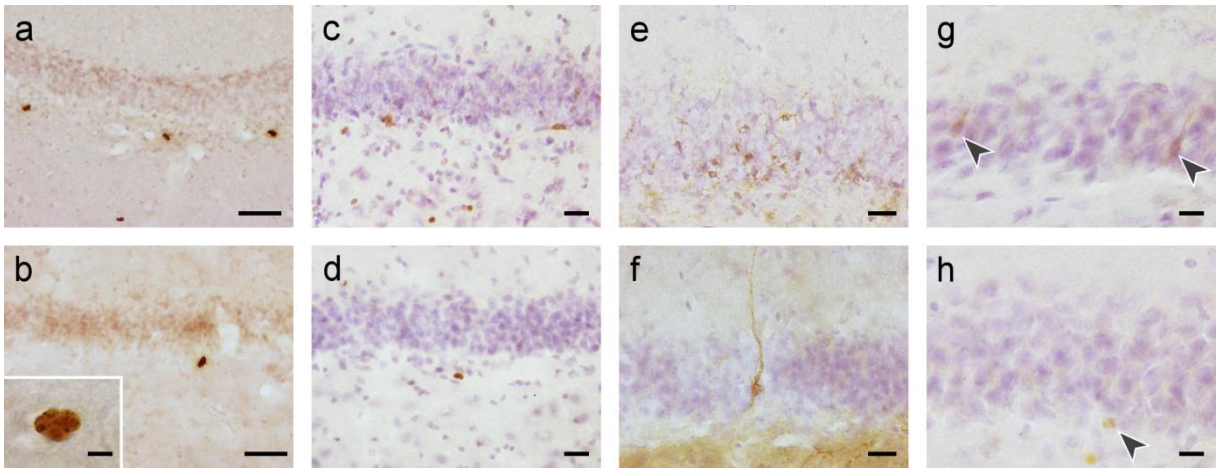

Figure 2

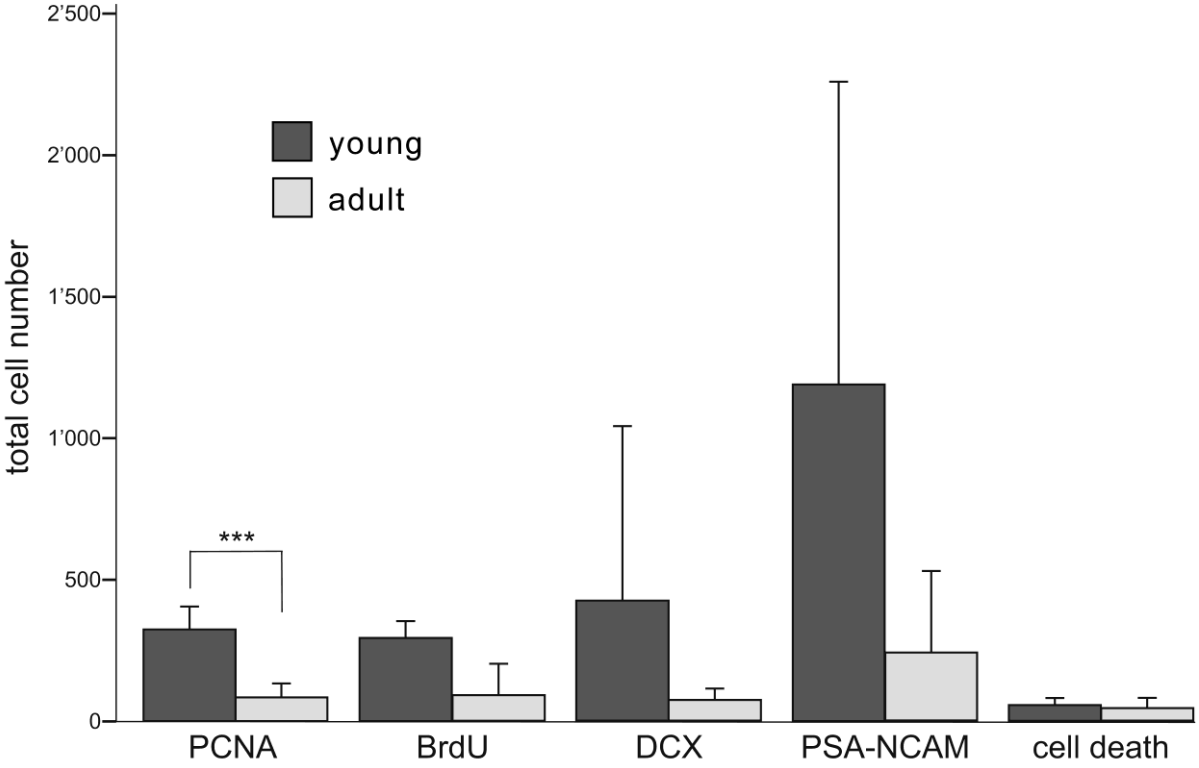
2'500
2'000
1'500
1'000
500
0
total cell number
young
adult
***
PCNA
BrdU
DCX
PSA-NCAM
cell death

Figure 3

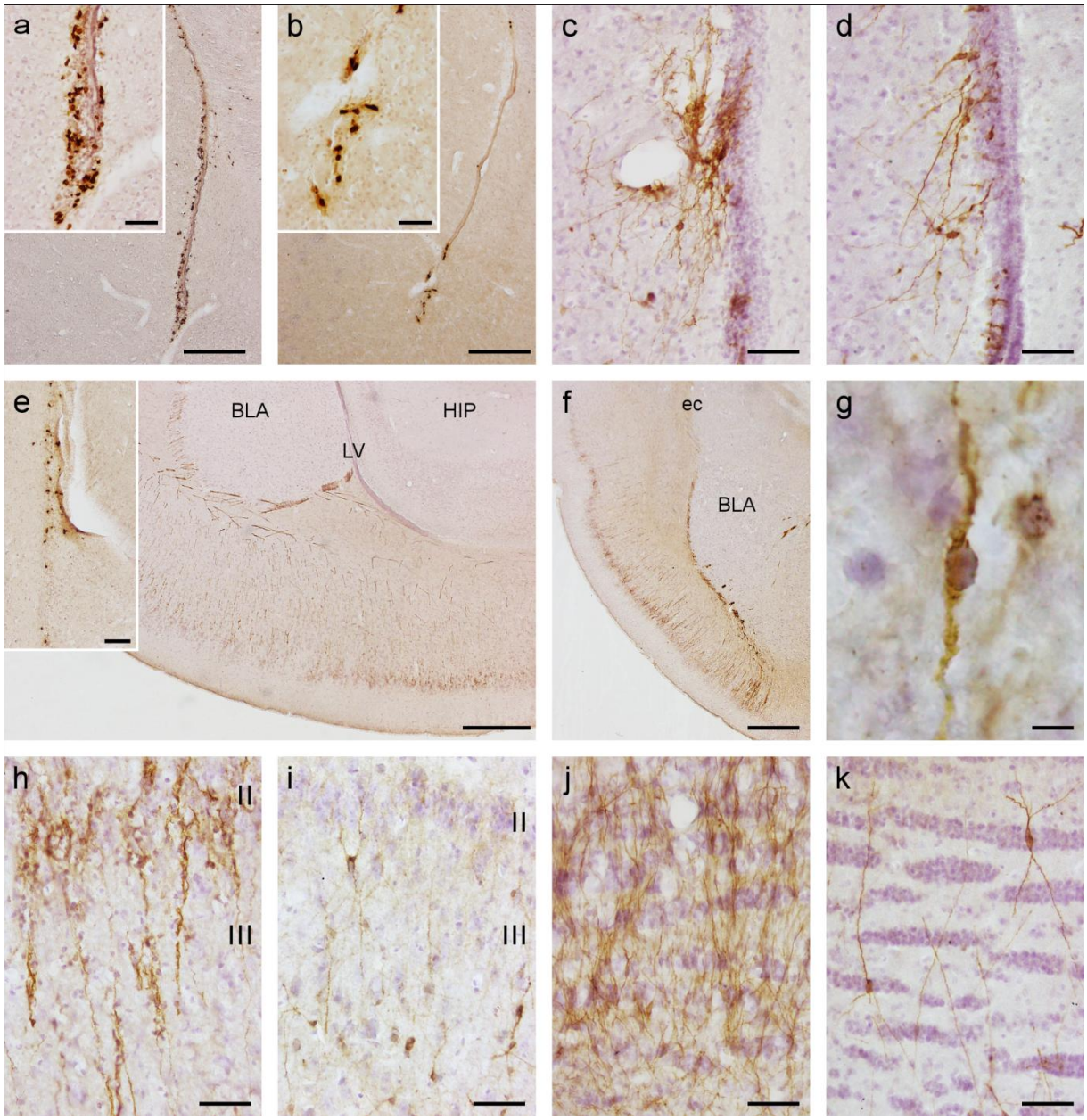

Figure 4

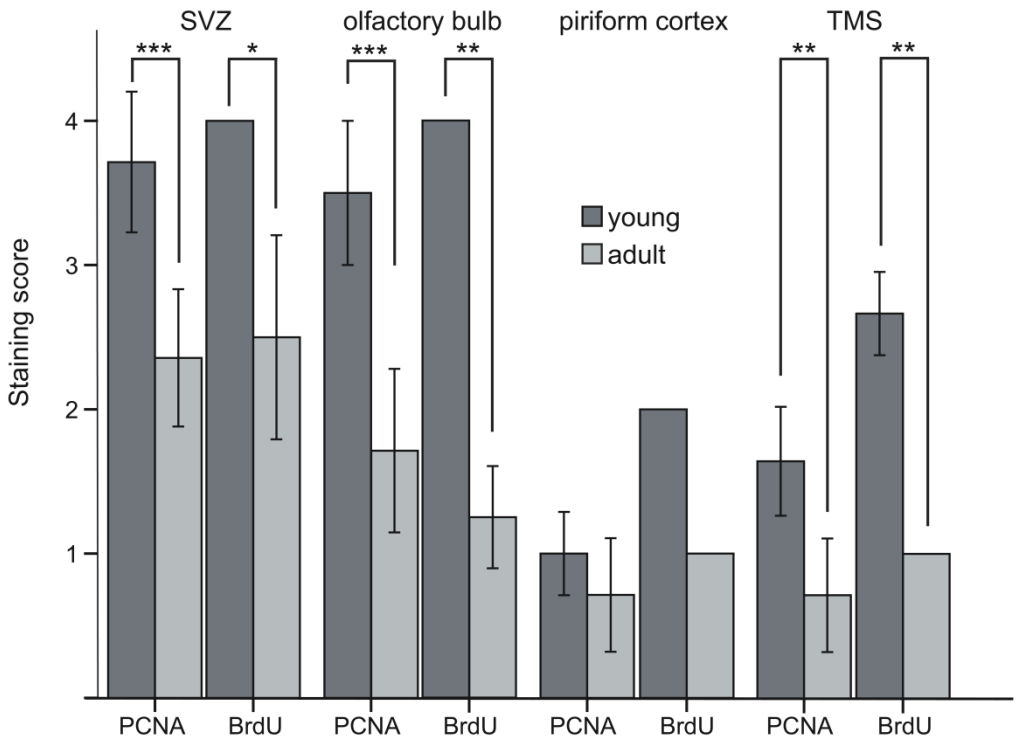
SVZ
olfactory bulb
piriform cortex
TMS
***
*
***
**
**
**
young
adult
Staining score
4
3
2
1
PCNA
BrdU
PCNA
BrdU
PCNA
BrdU
PCNA
BrdU

Figure 5

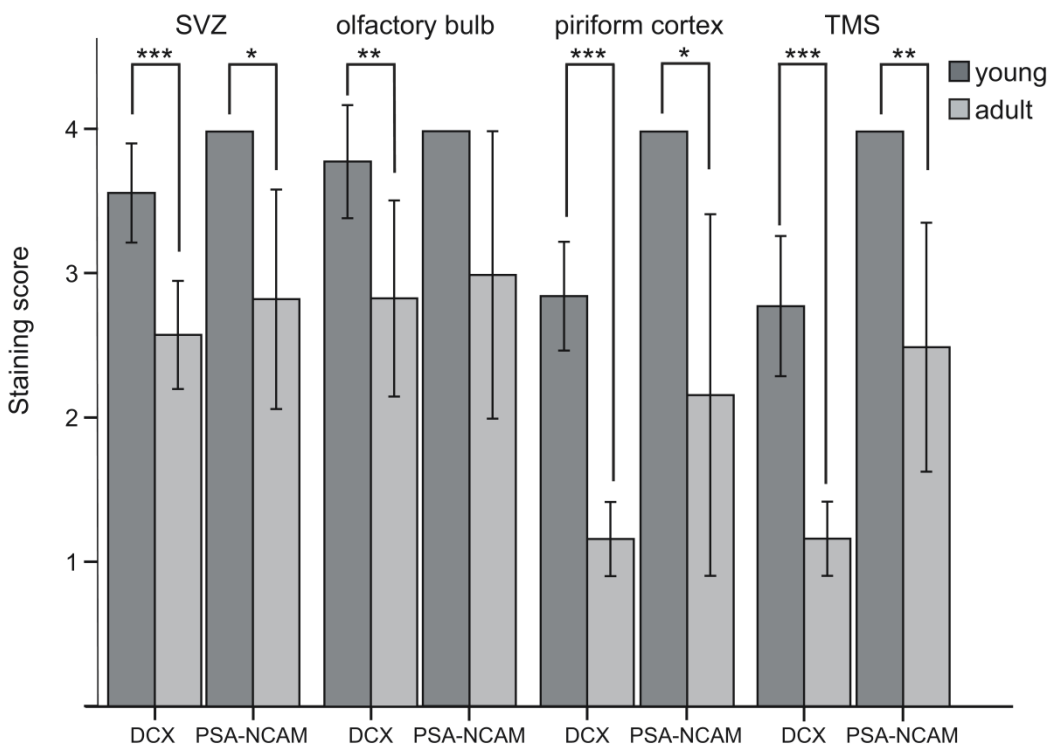
SVZ
olfactory bulb
piriform cortex
TMS
***
*
**
***
*
***
**
young
adult
Staining score
4
3
2
1
DCX
PSA-NCAM
DCX
PSA-NCAM
DCX
PSA-NCAM
DCX
PSA-NCAM

Layer II cell size estimates were made in four adult animals of each bat species as previously described [Gatome et al. 2010b, in review]. Prof. Peter Macdonald (McMaster University, Canada) assisted in performing a MIX (mixture) distribution analysis [Leys et al. 2005] of layer II cell sectional area (size) estimates. Without assigning a bin size for each cell type, there was too much overlap between different cell types, and although 3 lognormal distributions could be fitted, these did not correspond to any particular cell type. We therefore binned the cells according to predetermined size estimates, into classes corresponding to seven cell types (Fig. 2a). Using these conditional data (size estimates), five cell types were identifiable, but with overlaps in three cell types which could not be distinguished apart (Fig. 2b).

Figure 2: Identification of MEA layer II cell phenotypes based on size estimates

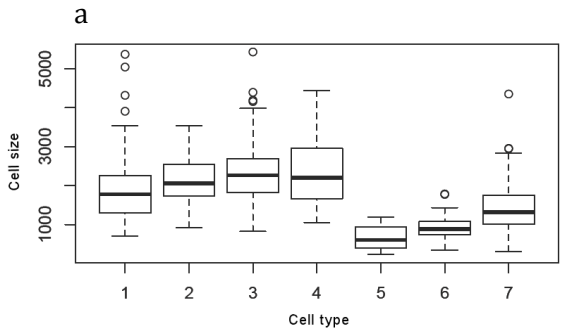

Box plots showing the size distribution of layer II cells based on identified phenotypic classes, ovoid stellate cell (1), pyramidal cell (2), polygonal stellate cell (3), oblique pyramidal cell (4), small round cell (5), fusiform cell (6) and horizontal cells (7).

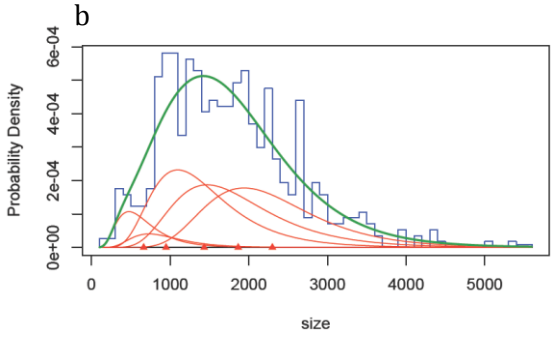

A gamma distribution of the cell mixture (green curve), and five lognormal distributions (red curves) corresponding to five cell groups (red arrows).

Conclusion: Using this method we were able to distinguish between some morphological phenotypes, but could not differentiate between the polygonal stellate cell, typical pyramidal and oblique pyramidal cell. Therefore, size alone is a poor predictor of cell type, at least for layer II MEA cells. This may also apply to MEA layers III, V and VI which have diverse cell types and the cells in the layers of the LEA.

HIPPOCAMPAL MOSSY FIBRES IN TWO SPECIES OF FRUIT BATS

Introduction: The axons of the dentate gyrus granule cells are referred to mossy fibres and they synapse with the apical and basal dendrites of CA3 pyramidal neurons. The mossy fibres have species-specific characteristics, and can be defined into suprapyramidal (SP-MF), intra- and infrapyramidal (IIP-MF) projections in the rodents and bats, but not in primates [Kondo et al. 2008]. The distribution of the mossy fibres shows variability across and within species particularly in the intra- and infrapyramidal projections formed by the terminal boutons of the granule cell axons synapsing upon basal dendrites of cells in the CA3 region. In rodents the size of the IIP-MF projections has been correlated to hippocampal-mediated behaviours, for example, spatial abilities [Schwegler and Crusio 1995], and to habitat and lifestyle [Pleskacheva et al. 2000]. Larger IIP-MF appear to be associated with superior spatial performance [Schwegler and Crusio 1995] in species living in complex environments that require smooth sensory integration of many stimuli in activities such as foraging [Pleskacheva et al. 2000]. Species with low ecological demands have small IIP-MF projections [Pleskacheva et al. 2000].

Materials and methods: Brains from adult fruit bats were glycolmethylacrylate-embedded, cut at 20 μm and processed in Timm's solution, as previously described [Gatome et al. 2010c]. Using the StereoInvestigator® software (MicroBrightfield Inc., Colchester, Vermont), measurements of the hilus and mossy fibres were done using the Cavalieri estimator at 20 x objective (N.A. 0.50) in every 12th (Wahlberg's epauletted fruit bat) and 24th (straw-coloured fruit bat) section. X, y steps of 100 μm were made and the section thickness was set at 20 μm. Statistical analysis was done using PASW Statistics 18 (SPSS Inc., Chicago, Illinois). Areas and volumes of the hilus, SP-MF and IIP-MF projections (Fig. 3a - d) were divided by the granule cell count to normalise the data and compared using independent samples *t*-test at a significance level of $p < 0.05$. Granule cell counts were divided by brain weight and compared using independent samples *t*-test at a significance level of $p < 0.05$.

Results: Normalised area and volume estimates of the hilus, SP-MF and IIP-MF projections are shown in table 1. The area of the hilar ($t = -0.32$; $p = 0.77$), SP-MF ($t = -1.03$; $p = 0.34$) and IIP-MF ($t = 0.85$; $p = 0.43$) projections are not different between the species. The volume of the hilar ($t = -3.58$; $p = 0.01$) and SP-MF ($t = -4.81$; $p = 0.003$) projections are larger in the straw-coloured fruit bat. The volume of the IIP-MF projections ($t = -0.35$; $p = 0.739$) shows no difference between the species. The normalised granule cell numbers are higher (table 1) ($t = 3.686$; $p = 0.010$) in Wahlberg's epauletted fruit bat. The Gundersen's coefficient of error (CE) for measurements of the hilar, SP-MF and IIP-projections are 0.06, 0.05 and 0.10 respectively, in Wahlberg's epauletted fruit bat. The Gundersen's CE for measurements of the hilar, SP-MF and IIP-MF projections are 0.07, 0.05 and 0.08 respectively, in the straw-coloured fruit bat.

Figure 3: The hippocampal region of fruit bats

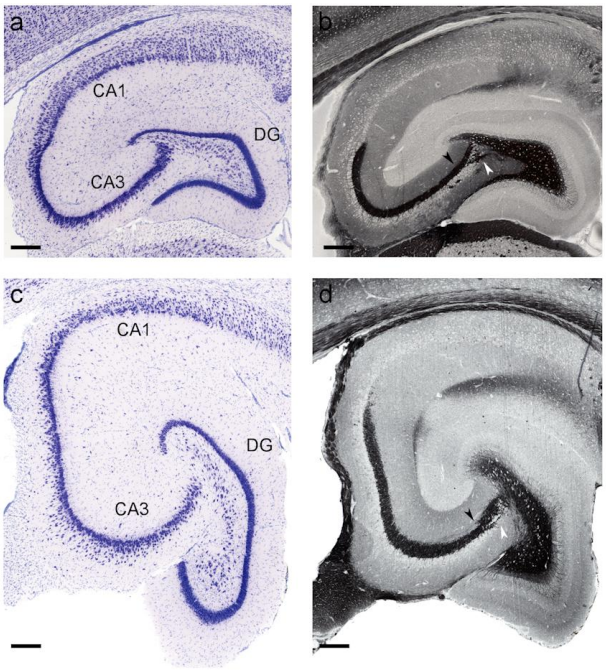

Wahlberg's epauletted fruit bat (a, b)

Straw-coloured fruit bat (c, d)

Nissl (a, c) and Timm's (b, d) stained sections showing the SP-MF projections (black arrow) and IIP-MF projections (white arrow).

The dentate gyrus (DG), CA1 and CA3 regions of the hippocampus are indicated. Scale bar a – d, 300 µm.

Table 1: Area and volume estimates of the hilar and mossy fibre projections

Species	Body weight (g)	Brain weight (g)	Section no.	Granule cells / Brain weight	Hilus area / GC	Hilus vol. / GC	SP-MF area / GC	SP-MF vol. / GC	IIP-MF area / GC	IIP-MF vol. / GC
Wahlberg's epauletted fruit bat (n = 4)	66	2	24	480180 (61446)	1.52 (0.28)	359.64 (67.31)	1.12 (0.17)	265.38 (41.08)	0.25 (0.09)	57.39 (21.46)
Straw-coloured fruit bat (n = 4)	275	4	20§	323075 (59092)	1.64 (0.75)	507.87 (48.19)	1.39 (0.51)	451.63 (65.63)	0.19 (0.08)	61.29 (6.43)

GC refers to granule cell count and standard deviation is indicated in brackets
§ Every 24th section in 2 animals and every 12th in 3 animals

Figure 4: Area and volume estimates of the hilar, SP-MF and IIP-MF projections

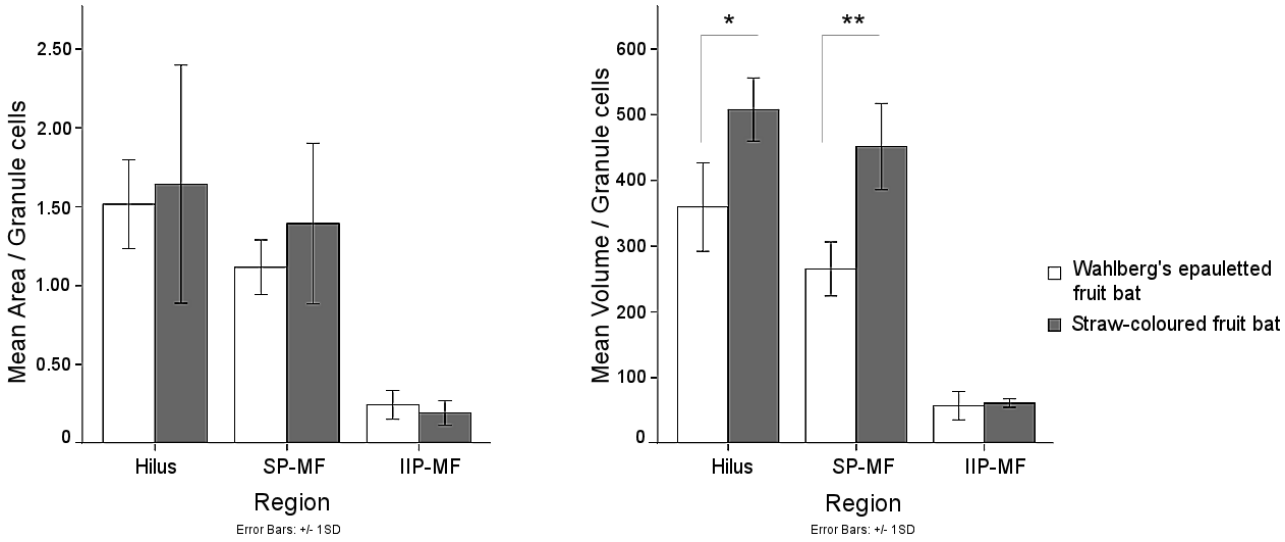

No species differences are observed for area estimates, but volume estimates are higher for hilar and SP-MF projections in the straw-coloured fruit bat (* $p < 0.05$; ** $p < 0.01$)

Discussion: The volume of the hilar and SP-MF projections are probably scaling to brain size, with the smaller Wahlberg's epauletted fruit bat having the smaller volumes. The IIP-MF projections have a scattered distribution and similar size in the two species, and appear less developed in comparison to the larger IIP-MF projections in rodents [Slomianka and West 1989; Pleskacheva et al. 2000]. Going by findings in rodents, we expected Wahlberg's epauletted fruit bat which flies in a cluttered environment [Baron et al. 1996a] to have better developed IIP-MF. There may therefore be other determinants of the size of the IIP-MF projections, such as genetics within species [Pleskacheva et al. 2000] or the less developed IIP-MF may be a feature of fruit bats or bats in general, possibly related to a largely prenatal ontogenesis of the hippocampus [Pleskacheva et al. 2000]. The relevance in bats would then require an analysis of several species. We would also expect a comparable rate of hippocampal neurogenesis between the two fruit bat species, based on the IIP-MF projections [Pleskacheva et al. 2000].

Introduction: Descriptions of cellular plasticity as inferred from cortical doublecortin (DCX) staining include almost the entire brain if compounded across the investigated mammalian species [Gould et al. 2001; Nacher et al. 2001; Bernier et al. 2002; Nacher et al. 2002b; Shapiro et al. 2007; Xiong et al. 2008; Luzzati et al. 2009].

Material and methods: In the fruit bats, we applied proliferation (PCNA, BrdU) and immature neuronal (DCX, PSA-NCAM) markers as previously described [Gatome et al. 2010a, in review].

Results: PCNA-, BrdU-, PSA-NCAM- and DCX-positive cells were observed in the somatosensory cortex. The staining of DCX and other markers in the somatosensory cortex (Fig. 5) is more prominent in the young (Fig. 5 a, c) compared to adult (Fig 5b, d) animals. In comparison to the subventricular zone and piriform cortex [Gatome et al. 2010a, in review], the stained cells, mostly in layer II (Fig. 5c, d) were fewer, stained weaker and extended less processes. PCNA- and BrdU-positive cells were rare.

Figure 5: DCX-positive cells in the somatosensory cortex

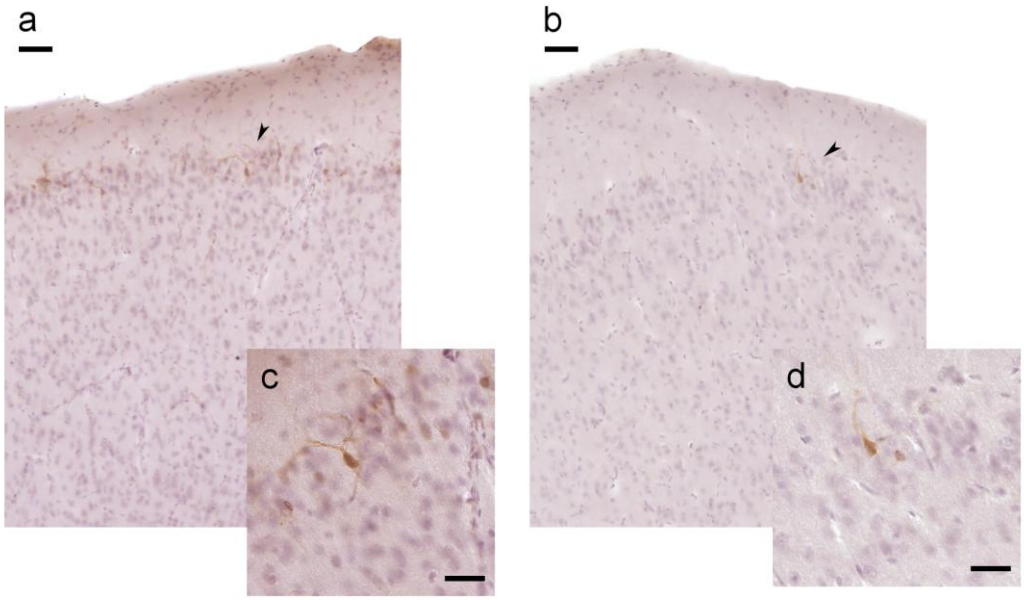

Somatosensory cortex of Wahlberg's epauletted fruit bat in young (a, c) and adult (b, d) animals. More reactivity was noted in the young animals. Arrows (a, b) indicate DCX-positive cells which are shown at higher magnification in inserts (c, d). Scale bars in a, b: 300 µm; c, d: 250 µm.

Positively stained cells to all markers were also observed in the striatum, and rarely amygdala in both young and adult bats. In the hippocampus, proliferative and neurogenic activity included the hilus, stratum radiatum, and stratum moleculare. Reports of similar hippocampal regional reactivity have been made in the rat [Rietze et al. 2000; Nacher et al. 2002a].

Discussion: Currently, investigations show that cell proliferation (BrdU and PCNA-positive cells) in the cortex, such as we observed in the somatosensory areas, is non-neuronal [Kornack and Rakic 2001; Koketsu et al. 2003; Bhardwaj et al. 2006]. Cortical PSA-NCAM and DCX immunostaining still need further clarification [Bhardwaj et al. 2006] as these proteins can be expressed in neurons undergoing synaptogenesis or neurite outgrowth [Nacher et al. 2001; Ming and Song 2005] that is experience-dependent [Cremer et al. 2000].

Even though the nature and role of the cellular plasticity is not clear, it suggests a dynamic process. Fruit bats have a well developed trigeminal nerve and nucleus and their facial vibrissae have a large representation in the cortex. It has been suggested that they provide tactile information about group members and air streams which enable the bat to adjust its head position during flight [Baron et al. 1996c]. The cellular plasticity suggests further investigations in the organisation of the somatosensory receptors in the orofacial region, and tactile information processing in fruit bats.

DISCUSSION

Flight has allowed the bats to use their space in three-dimensions, occupy diverse niches and develop a unique sensory modality, echolocation. Most fruit bat species do not use echolocation and have instead invested in their visual and olfactory systems. Flight is likely to produce immense demands on acquisition of sensory stimuli useful in the processing of location-related information. In guiding spatial behaviour, some of the structures involved include the EC, hippocampus, olfactory bulb and piriform cortex. The EC is essential for providing spatial (metric information) and contextual representations (odour, colour, emotional information) related to a location within the environment. The hippocampus links discrete events within memory, associated with an object (spatial and contextual representations) and a location and related to a behavioural episode (flight). The piriform cortex provides some of the contextual representation, in the form of olfactory information, which is dominant in foraging.

The piriform cortex and hippocampus are characterised by structural plasticity into adulthood, manifested as adult neurogenesis in fruit bats, also noted in rodents and primates. Relatively more reactivity is observed in the piriform cortex than hippocampus in fruit bats. The entorhinal cortex does not show this cellular plasticity, but shows differences in its cytoarchitecture within the fruit bats and between bats and rodents, which may be related to the diversity and complexity of its inputs and outputs. Our main findings are the inter- and intraspecies differences in the overall organisation of the EC and the cellular composition in the MEA layer II. Similarities include the organisation of the deep layers of the EC and cellular elements in the MEA layer II. Unpublished observations in the straw-coloured fruit bat on hippocampal neurogenesis suggest a low rate that is comparable to Wahlberg's epauletted fruit bat and piriform neurogenesis that is qualitatively also comparable. The use of two closely related fruit bat species allows us to examine the ecological and behavioural adaptations of brain structure.

Ecological considerations

We consider our main findings in the light of phylogenetic, ecological and behavioural adaptations. We also consider the functional implications of our findings.

Phylogenetic relationship: Although the fruit bats are phylogenetically close, there is diversification in their brain structures [Baron et al. 1996a], which may account for the noted differences in the cytoarchitecture of the EC and MEA layer II [Gatome et al. 2010c]. This has been observed in rodents where the cytoarchitecture of the EC of the rat and mouse appears rather similar [Insausti et al. 1997; van Groen 2001], but has differences with the MEA fields of the guinea pig [Uva et al. 2004].

Early investigations suggest that the rate of neurogenesis in the two fruit bat species is comparable, suggesting that the process is tightly regulated in these species. The differences in hippocampal features between the fruit bats include the higher granule cell number in Wahlberg's epauletted fruit bat which may be related to species-specific differences or habitat complexity. These hippocampal features, and particularly those associated with the dentate gyrus (DG), are highly variable among rodents, and even closely related species [Slomianka and West 1989; Pleskacheva et al. 2000; Amrein et al. 2004a]. Hilar and suprapyramidal mossy fibre (SP-MF) projections that are larger in the straw-coloured fruit bat possibly scale to brain size. It could also be that the granule cells in the straw-coloured fruit bat send a greater number of projections to CA3 hippocampal region, suggesting a need to analyse intrinsic hippocampal circuitry. The intra- and infrapyramidal mossy fibre (IIP-MF) projections are comparable between the fruit bats suggesting that they are a less useful comparative feature. Information on the phylogenetic distance between the two fruit bat species would be useful to further discussions on evolutionary relationships in brain structure.

Flight behaviour and habitat complexity: The low flying behaviour of Wahlberg's epauletted fruit bat and navigation through vegetation (complex habitat) [Baron et al. 1996a], suggests higher spatial demands, and is supported by a more granule cells and a better differentiated MEA. Wahlberg's epauletted fruit bat has a smaller home range than the straw-coloured fruit bat. In rodents, large home ranges [Amrein et al. 2004a] and high habitat complexity [Pleskacheva et al. 2000] have been associated with high granule cell counts. Therefore, habitat complexity appears to be a selection pressure for hippocampal traits in both rodents and bats. Migratory behaviour apparently neither requires more granule cells nor a well-differentiated MEA in the straw-coloured fruit bat [Gatome et al. 2010c]. In passerines, the size of the hippocampus is not influenced by migratory behaviour [Healy et al. 1991].

Dietary specialisations: If the dietary preference influences the size of the hippocampus, then specialisations to particular fruit that may require greater searching and locating behaviour may be relevant. Foraging for seeds over large territories in bank voles [Pleskacheva et al. 2000] requires more granule cells [Amrein et al. 2004a]. From literature, the two species favour similar fruits of the *Ficus* species [Kingdon 1984b; Acharya 1992], but the overlap in diet is not complete, and it is not clear if the foraging demands of Wahlberg's epauletted fruit bat are higher.

Social factors: Social factors such as group size, complexity of the social structure, and social learning have been known to influence size of the neocortex in bats [Baron et al. 1996c], primates [Reader and Laland 2002] and other taxa [Shultz and Dunbar 2007]. Large group sizes and the complexity of social interactions in the straw-coloured fruit bat are suggested to be responsible for the increased neocorticalisation [Baron et al. 1996c], suggesting as in primates a greater importance of behavioural flexibility and cognitive abilities [Reader and Laland 2002]. This may be at the expense of the hippocampus, and hence the finding of low granule cell count compared to similarly sized rodents. Large flock size may be related to the larger home ranges of the straw-coloured fruit bat, with possibly an advantage of flock 'effort' in locating food resources. This may lower the challenge on spatial demands and impact on the size of the DG and differentiation of the MEA. The better developed LEA in the straw-coloured fruit bat may signify the greater importance of non-spatial input, possibly to address cognitive demands.

Sensory modality, longevity, and hippocampal ontogeny: From a comparative perspective, the finding of absent to low hippocampal neurogenesis in microbats [Amrein et al. 2007] and low rates in fruit bats suggests that it may not be related to social organisation, complexity of environment, home range, and dietary preference which are shared between the two clades. It may be influenced by the 'echolocation priority', and investigations in *Rousettus* would help to clarify this. The fruit bats are long-lived late-maturing species and as predicted have a low rate of hippocampal neurogenesis. From a comparison of features in young and adult animals, the hippocampus of the fruit bats is expected to undergo a largely pre-natal development, which is also associated with a low rate of hippocampal neurogenesis [Kornack and Rakic 1999].

Functional implications

Functionally related subsystems have evolved together [Barton et al. 1995] and therefore the finding that a well-differentiated MEA layer II is related to a more populated DG seems consistent. The MEA and up to three-quarters of the DG are associated with spatial processing [Moser and Moser 1998], and it is therefore possible that Wahlberg's epauletted fruit bat has higher spatial processing demands. The poorly differentiated LEA layer II in Wahlberg's epauletted fruit bat may suggest a greater input of olfactory information from its well-developed olfactory bulbs, which has also been associated with poorly differentiated superficial layers in the primate field E_0 [Amaral et al. 1987]. It can also be inferred from our findings in rodents and bats that species-specific characteristics are largely restricted to the EC layer II [Gatome et al. 2010c], related to species sensory inputs in line with functional demands. Of benefit would be investigations of the LEA and EC extrinsic and intrinsic circuitry in fruit bats. Generally for all species, beneficial investigations include the relationship of inputs to the intrinsic network for which there is no data available [Canto et al. 2008] and receptor architectonics, in trying to designate particular functions to identified EC fields. More also needs to be done on the biochemical differentiation of the cellular phenotypes of MEA layer II.

The stellate cells, the likely morphological correlate of the grid cell, appear to be the most variable cell type between species [Gatome et al. 2010b, in review; Gatome et al. 2010c]. The low proportions of polygonal stellate cells in fruit bats [Gatome et al. 2010c], may suggest that they functionally rely on other morphological phenotypes. Another explanation is that there may be more than one morphological correlate of the 'grid cell'. It has been reported that layers III, V, and VI of the MEA have cells with grid cell properties [Sargolini et al. 2006]; these layers are largely populated by non-stellate cells. The investigation of spatial representation in the bat hippocampus has already revealed some informative contrasts [Ulanovsky and Moss 2007], and this is likely to be reflected upstream in the MEA layer II - an identification of the grid cell morphological phenotype is essential and may require a species by species approach.

The high size indices of the schizocortex and hippocampus of fruit bats, even compared to similarly-sized rodents are not reflected in the cellularity of the DG [Gatome et al. 2010c]. It is likely that the high indices are due to an increase in hippocampal efferent and afferent connectivity, already suggested in rodents [Slomianka and West 1989].

Hippocampal afferents may also influence the character of DG neurogenesis (low rate), but it is more likely that the selective pressure is based on phylogenetic differences, life-span and early developing hippocampus in fruit bats. From other studies, we can infer that the low rate of neurogenesis in fruit bats may be important for the maintenance of the DG perhaps important in long-lived species [Nottebohm 2002]. It could also play a role in enhancing memory processing functions of CA3, where even few cells are predicted to provide significant possibilities in memory operations [Treves et al. 2008]. Another theory is that the new cells may be required in few but complex hippocampal processing activities, for example in spatial relational memory. This requires the flexible use of geometric relationships between cues to locate a goal in a new environment [Dupret et al. 2008], perhaps suited to the foraging behaviour of fruit bats. The hippocampal neurogenesis in fruit bats may be modulated by olfactory inputs [Pope and Wilson 2007] but perhaps far less than echolocation does for bats as a group.

The overall conclusion is that the architecture and function of the EC is closely tied to phylogenetic make-up, species-specific behavioural and ecological demands. The EC input, species lifespan and hippocampal ontogeny are the overriding factors in the design and plasticity of the hippocampus. The bats undoubtedly have superior spatial abilities, but with a finding of low granule cell counts and a moderately differentiated MEA layer II, it may be possible that spatial processing is distributed to other regions, such as the well-developed CA1 hippocampal region [Buhl and Dann 1991] and EC layers III and V. Other structures that undertake spatial processing such as presubiculum, parasubiculum, anterior thalamus, retrosplenial and parietal cortex [Moser et al. 2008] may be secondarily worth analysing. Functional studies in circuitry between the cortex, EC and hippocampus would be useful to understanding information flow and the topography of spatial processing. There is a need for behavioural studies in fruit bats to test their capacity for spatial memory, which is already advanced in microbats [Winter and Stich 2005] but where the influence of the 'echolocation advantage' cannot be discounted. Investigating more species of fruit bats facing different ecological demands, would be useful to the understanding of the architecture and function of the EC and hippocampus.

Olfactory system: Fruit bats use olfactory senses for spatial orientation and navigation, as shown for locating ripe fruit [Hodgkison et al. 2007; Raghuram et al. 2009], and the structural plasticity serves to adapt to increased demands in odour discrimination and memory. This may reflect the diversity of odour inputs, but it may be that the bats additionally use olfactory stimuli in the form of an 'olfactory map', as in homing pigeon navigation where it has been suggested that the

hippocampus and piriform cortex cooperate in the navigational map learning [Gagliardo et al. 2005]. Bats already show sophisticated and complex forms of memory-based spatial behaviours which have been related to the olfactory sense in birds [Papi 1991], namely homing [Holland et al. 2006] and migration [Richter and Cumming 2008]. The similarity in the connections of the piriform cortex in birds and mammals suggests that the structures were derived from a common evolutionary ancestor and share a similar functional role [Bingman et al. 1994]. Fruit bats have large home ranges and are therefore likely to navigate into unfamiliar territory. Homing pigeons are suggested to use local environmental odours to determine the direction of displacement in unfamiliar territory, and then other cues to guide navigation back to roost [Benvenuti and Wallraff 1985]. Olfactory cues may therefore be used not just to enhance foraging efficiency but also in navigation. There may be a case for odour-guided spatial navigation in fruit bats, suggesting further research in olfactory sensitivities and qualitative odour discriminations in fruit bats. Additionally piriform characteristics in different bat species that use olfaction for different purposes, for example mother-young relationships, sexual behaviour etc [Baron et al. 1996c] would provide useful comparisons. Other useful information would come from tracking the flight of the bats, from roost to foraging sites to determine the routes followed and therefore, the cues that guide this behaviour.

The overall conclusion is that olfaction which guides foraging behaviour may play a role in spatial navigation in fruit bats, as in the homing pigeon.

Evolutionary convergences

With regard to evolutionary debates on fruit bats and primates, there is a lot of convincing evidence from molecular studies [Teeling et al. 2000] and paleontological findings [Simmons et al. 2008] that place the fruit bats firmly in Chiroptera. Shared brain characteristics between fruit bats and primates are explained by evolutionary convergences, in the mosaic organisation of the brain [de Winter and Oxnard 2001]. Various functional subsystems can respond to fairly specific natural selection [Hutcheon et al. 2002], and the well-developed deep layers of the entorhinal cortex in fruit bats and primates suggest an evolutionary convergence with respect to their ecology and biology. CA1 has also been reported to have primate-like characteristics [Buhl and Dann 1991], and this makes the fruit bats an ideal model for investigations of CA1-EC-cortical interplays. Similarities in biology with primates, such as life span may be responsible for regulation of processes, such as the rate of hippocampal neurogenesis. This suggests that fruit bats may present a small mammalian model species for investigations on the regulation of

hippocampal neurogenesis in long-lived species. The age-related decline in hippocampal and piriform neurogenesis, which is in common to all species, suggests that there are processes that are similarly tightly regulated across species.

Outlook

- Investigation of other species of fruit bats would be useful for a more representative picture and therefore exclude species-specific differences in the findings of the cytoarchitecture of the EC, and composition of EC layer II. Generally, further analysis into the spatial distributions of layer II cells may help to determine the organisation and kind of relationships between cells [Stark et al. 2007]. This may advance investigations on the attractor-based spatial representations and modularity in the organisation of the EC, thought to be important in elucidating the perception of self-location [Witter and Moser 2006].

- Gross numerical and qualitative characteristics are not adequate in explaining function, and investigations on the connective functional architecture between the EC, hippocampus and piriform cortex in fruit bats is necessary.

- Odour-guided spatial navigation in fruit bats is likely, considering the role of olfactory cues in foraging, and the prominent plasticity in the piriform cortex, and investigations in this direction would be beneficial.

- Investigations involving *Rousettus* species may determine the influence of echolocation on hippocampal plasticity, and including other fruit bat species would help to establish the character of piriform and hippocampal cellular plasticity in this taxa.

Acharya L (1992) Epomophorus wahlbergi. Mammalian Species 394:1-4.

Alonso A, Klink R (1993) Differential electroresponsiveness of stellate and pyramidal-like cells of medial entorhinal cortex layer II. J Neurophysiol 70:128-143.

Altman J, Das GD (1965) Autoradiographic and histological evidence of postnatal hippocampal neurogenesis in rats. J Comp Neurol 124:319-335.

Amaral DG, Insausti R, Cowan WM (1987) The entorhinal cortex of the monkey: I. Cytoarchitectonic organization. J Comp Neurol 264:326-355.

Amrein I, Boonstra R, Lipp H-P, Wojtowicz JM (2008) Adult neurogenesis in natural populations of mammals. In: Adult neurogenesis (Gage FH, Kempermann G, Song H, eds). New York: Cold Spring Harbor Laboratory Press.

Amrein I, Dechmann DKN, Winter Y, Lipp H-P (2007) Absent or low rate of adult neurogenesis in the hippocampus of bats (Chiroptera). Plos One 2:e455.

Amrein I, Slomianka L, Lipp H-P (2004a) Granule cell number, cell death and cell proliferation in the dentate gyrus of wild-living rodents. Eur J Neurosci 20:3342-3350.

Amrein I, Slomianka L, Poletaeva I, Bologova NV, Lipp H-P (2004b) Marked species and age-dependent differences in cell proliferation and neurogenesis in the hippocampus of wild-living rodents. Hippocampus 14:1000-1010.

Barnes DC, Hofacer RD, Zaman AR, Rennaker RL, Wilson DA (2008) Olfactory perceptual stability and discrimination. Nat Neurosci 11:1378-1380.

Baron G, Stephan H, Frahm HD (1996a) Brain characteristics and adaptive radiations: Pteropodidae. In: Comparative neurobiology of Chiroptera: Brain characteristics in functional systems, ecoethological adaptation, adaptive radiation and evolution, vol 3, pp 1246-1265. Basel: Birkhäuser Verlag.

Baron G, Stephan H, Frahm HD (1996b) Brain characteristics related to ecoethological adaptations. In: Comparative neurobiology of Chiroptera: Brain characteristics in functional systems, ecoethological adaptation, adaptive radiation and evolution, vol 3, pp 1194-1245. Basel: Birkhäuser Verlag.

Baron G, Stephan H, Frahm HD (1996c) Brain characteristics related to functional systems. In: Comparative neurobiology of Chiroptera: Brain characteristics in functional systems, ecoethological adaptation, adaptive radiation and evolution, vol 3, pp 1082-1193. Basel: Birkhäuser Verlag.

Baron G, Stephan H, Frahm HD (1996d) Size index profiles for taxonomic units. In: Comparative neurobiology of Chiroptera: Brain characteristics in taxonomic units, vol 2, pp 856-898. Basel: Birkhäuser Verlag.

Barton RA, Harvey PH (2000) Mosaic evolution of brain structure in mammals. Nature 405:1055-1058.

Barton RA, Purvis A, Harvey PH (1995) Evolutionary radiation of visual and olfactory brain systems in primates, bats and insectivores. Philos T R Soc Lond B 348:381-392.

Beall MJ, Lewis DA (1992) Heterogeneity of layer II neurons in human entorhinal cortex. J Comp Neurol 321:241-266.

Benvenuti S, Wallraff HG (1985) Pigeon navigation: Site simulation by means of atmospheric odours. J Comp Physiol A 156:737-746.

Bernier PJ, Bédard A, Vinet J, Lévesque M, Parent A (2002) Newly generated neurons in the amygdala and adjoining cortex of adult primates. Proc Natl Acad Sci USA 99:11464-11469.

Bhardwaj RD, Curtis MA, Spalding KL, Buchholz BA, Fink D, Björk-Eriksson T, Nordborg C, Gage FH, Druid H, Eriksson PS, Frisén J (2006) Neocortical neurogenesis in humans is restricted to development. Proc Natl Acad Sci USA 103:12564-12568.

Bingman VP, Casini G, Nocjar C, Jones TJ (1994) Connections of the piriform cortex in homing pigeons (*Columba livia*) studied with fast blue and WGA-HRP. Brain Behav Evol 43:206-218.

Brodmann K (1909) Vergleichende Lokalisationslehre der Grosshirnrinde in ihren Prinzipien dargestellt auf Grund des Zellenbaues. Leipzig.

Brun VH, Solstad T, Kjelstrup KB, Fyhn M, Witter MP, Moser EI, Moser MB (2008) Progressive increase in grid scale from dorsal to ventral medial entorhinal cortex. Hippocampus 18:1200-1212.

Buhl EH, Dann JF (1991) Cytoarchitecture, neuronal composition, and entorhinal afferents of the flying fox hippocampus. Hippocampus 1:131-152.

Burwell RD, Amaral DG (1998) Cortical afferents of the perirhinal, postrhinal, and entorhinal cortices of the rat. J Comp Neurol 398:179-205.

Cameron HA, Woolley CS, McEwen BS, Gould E (1993) Differentiation of newly born neurons and glia in the dentate gyrus of the adult rat. Neuroscience 56:337-344.

Canto CB, Wouterlood FG, Witter MP (2008) What does the anatomical organization of the entorhinal cortex tell us? Neural Plast.

Chaillan FA, Roman FS, Soumireu-Mourat B (1996) Modulation of synaptic plasticity in the hippocampus and piriform cortex by physiologically meaningful olfactory cues in an olfactory association task. J Physiol Paris 90:343-347.

Cremer H, Chazal G, Lledo PM, Rougon G, Montaron MF, Mayo W, Le Moal M, Abrous DN (2000) PSA-NCAM: an important regulator of hippocampal plasticity. Int J Dev Neurosci 18:213-220.

de Winter W, Oxnard CE (2001) Evolutionary radiations and convergences in the structural organization of mammalian brains. Nature 409:710-714.

DeFrees SL, Don EW (1988) Eidolon helvum. Mammalian Species 312:1-5.

Dupret D, Revest J-M, Koehl M, Ichas Fo, De Giorgi F, Costet P, Abrous DN, Piazza PV (2008) Spatial relational memory requires hippocampal adult neurogenesis. Plos One 3:e1959.

Eichenbaum H (1999) Neurobiology. The topography of memory. Nature 402:597-599.

Fanselow MS, Dong H-W (2010) Are the dorsal and ventral hippocampus functionally distinct structures? Neuron 65:7-19.

Fredens K, Stengaard-Pedersen K, Larsson LI (1984) Localization of enkephalin and cholecystokinin immunoreactivities in the perforant path terminal fields of the rat hippocampal formation. Brain Res 304:255-263.

Funmilayo O (1979) Ecology of the straw-coloured fruit bat in Nigeria. Rev. Zool. afr. 93:589-600.

Fyhn M, Hafting T, Witter MP, Moser EI, Moser MB (2008) Grid cells in mice. Hippocampus 18:1230-1238.

Gagliardo A, Odetti F, Ioale P, Pecchia T, Vallortigara G (2005) Functional asymmetry of left and right avian piriform cortex in homing pigeons' navigation. Eur J Neurosci 22:189-194.

Gatome CW, Mwangi DK, Lipp H-P, Amrein I (2010a) Hippocampal neurogenesis and cortical cellular plasticity in Wahlberg's epauletted fruit bat (In review)

Gatome CW, Slomianka L, Lipp H-P, Amrein I (2010b) Number estimates of neuronal phenotypes in layer ll of the medial entorhinal cortex of mouse and rat (In review).

Gatome CW, Slomianka L, Mwangi D, Lipp H-P, Amrein I (2010c) The entorhinal cortex of the Megachiroptera: a comparative study of Wahlberg's epauletted fruit bat and the straw-coloured fruit bat. Brain Struct Funct 214:375-393.

Gould E, Vail N, Wagers M, Gross CG (2001) Adult-generated hippocampal and neocortical neurons in macaques have a transient existence. Proc Natl Acad Sci USA 98:10910-10917.

Haberly L, Price J (1978) Association and commissural fiber systems of the olfactory cortex of the rat. II. Systems originating in the olfactory peduncle. J Comp Neurol. 1978 181:781-807.

Haberly LB (2001) Parallel-distributed processing in olfactory cortex: new insights from morphological and physiological analysis of neuronal circuitry. Chem Senses 26:551-576.

Haberly LB, Bower JM (1989) Olfactory cortex: model circuit for study of associative memory? Trends Neurosci 12:258-264.
Habets AM, Lopes Da Silva FH, Mollevanger WJ (1980) An olfactory input to the hippocampus of the cat: field potential analysis. Brain Res 182:47-64.
Hafting T, Fyhn M, Molden S, Moser MB, Moser EI (2005) Microstructure of a spatial map in the entorhinal cortex. Nature 436:801-806.
Hargreaves EL, Rao G, Lee I, Knierim JJ (2005) Major dissociation between medial and lateral entorhinal input to dorsal hippocampus. Science 308:1792-1794.
Harvey PH, Krebs JR (1990) Comparing brains. Science 249:140-146.
Harvey PH, Purvis A (1991) Comparative methods for explaining adaptations. Nature 351:619-624.
Hasselmo ME, Brandon MP (2008) Linking cellular mechanisms to behavior: entorhinal persistent spiking and membrane potential oscillations may underlie path integration, grid cell firing, and episodic memory. Neural Plast 2008:658323.
Healy SD, Krebs JR, Gwinner E (1991) Hippocampal volume and migration in passerine birds. Naturwissenschaften 78:424-426.
Hodgkison R, Ayasse M, Kalko E, Häberlein C, Schulz S, Mustapha W, Zubaid A, Kunz T (2007) Chemical ecology of fruit bat foraging behavior in relation to the fruit odors of two species of paleotropical bat-dispersed figs (*Ficus hispida* and *Ficus scortechinii*). J Chem Ecol 33:2097-2110.
Holland RA, Thorup K, Vonhof MJ, Cochran WW, Wikelski M (2006) Navigation: bat orientation using Earth's magnetic field. Nature 444:702.
Hutcheon JM, Kirsch JA, Garland Jr T (2002) A comparative analysis of brain size in relation to foraging ecology and phylogeny in the Chiroptera. Brain Behav Evol 60:165-180.
Insausti R (1993) Comparative anatomy of the entorhinal cortex and hippocampus in mammals. Hippocampus 3 19-26.
Insausti R, Herrero MT, Witter MP (1997) Entorhinal cortex of the rat: cytoarchitectonic subdivisions and the origin and distribution of cortical efferents. Hippocampus. 7:146-183.
Irizarry MC, Soriano F, McNamara M, Page KJ, Schenk D, Games D, Hyman BT (1997) Abeta deposition is associated with neuropil changes, but not with overt neuronal loss in the human amyloid precursor protein V717F (PDAPP) transgenic mouse. J Neurosci 17:7053-7059.
Jones G, Duvergé PL, Ransome RD (1993) Conservation biology of an endangered species: field studies of greater horseshoe bats. In: Racey PA, Swift SM (eds) Ecology, evolution and behaviour of bats. The proceedings of a symposium held by the Zoological Society of London and the Mammal Society, pp 309-322. London: Clarendon Press.
Kerr KM, Agster KL, Furtak SC, Burwell RD (2007) Functional neuroanatomy of the parahippocampal region: the lateral and medial entorhinal areas. Hippocampus 17:697-708.
Kingdon J (1984a) Bats. Fruit bats. In: East African mammals: an atlas of evolution in Africa, vol 2, pp 117-174. Hampshire: The University of Chicago Press.
Kingdon J (1984b) Bats. Fruit bats. *Eidolon helvum*. In J. Kingdon (ed.): East African mammals: an atlas of evolution in Africa. Volume II Part A (Insectivores and Bats), vol 2. The University of Chicago Press. Hampshire, Great Britain. pp. 145-152.
Klink R, Alonso A (1997) Morphological characteristics of layer II projection neurons in the rat medial entorhinal cortex. Hippocampus 7:571-583.
Koketsu D, Mikami A, Miyamoto Y, Hisatsune T (2003) Nonrenewal of neurons in the cerebral neocortex of adult macaque monkeys. J Neurosci 23:937-942.
Kondo H, Lavenex P, Amaral DG (2008) Intrinsic connections of the macaque monkey hippocampal formation: I. Dentate gyrus. J Comp Neurol 511:497-520.
Kornack DR, Rakic P (1999) Continuation of neurogenesis in the hippocampus of the adult macaque monkey. Proc Natl Acad Sci USA 96:5768-5773.
Kornack DR, Rakic P (2001) Cell proliferation without neurogenesis in adult primate neocortex. Science 294:2127-2130.

Krebs JR, Sherry DF, Healy SD, Perry VH, Vaccarino AL (1989) Hippocampal specialization of food-storing birds. Proc Natl Acad Sci USA 86:1388-1392.
Kumar SS, Buckmaster PS (2006) Hyperexcitability, interneurons, and loss of GABAergic synapses in entorhinal cortex in a model of temporal lobe epilepsy. J Neurosci 26:4613-4623.
Künzle H, Radtke-Schuller S (2000) The subrhinal paleocortex in the hedgehog tenrec: a multiarchitectonic characterization and an analysis of its connections with the olfactory bulb. Anat Embryol (Berl) 202:491-506.
Leuner B, Gould E, Shors TJ (2006) Is there a link between adult neurogenesis and learning? Hippocampus 16:216-224.
Leys J, McTainsh G, Koen T, Mooney B, Strong C (2005) Testing a statistical curve-fitting procedure for quantifying sediment populations within multi-modal particle-size distributions. Earth Surf Proc Land 30:579-590.
Lois C, Garcia-Verdugo JM, Alvarez-Buylla A (1996) Chain migration of neuronal precursors. Science 271:978-981.
Lorente de Nó R (1933) Studies on the structure of the cerebral cortex. J Psychol Neurol 45:381-438.
Luft S, Curio E, Tacud B (2003) The use of olfaction in the foraging behaviour of the golden-mantled flying fox, *Pteropus pumilus*, and the greater musky fruit bat, *Ptenochirus jagori* (Megachiroptera: Pteropodidae). Naturwissenschaften 90:84-87.
Luzzati F, Bonfanti L, Fasolo A, Peretto P (2009) DCX and PSA-NCAM expression identifies a population of neurons preferentially distributed in associative areas of different pallial derivatives and vertebrate species. Cereb. Cortex 19:1028-1041.
Markakis E, A. , Gage F, H. (1999) Adult-generated neurons in the dentate gyrus send axonal projections to field CA3 and are surrounded by synaptic vesicles. J Comp Neurol 406:449-460.
McGowan E, Eriksen J, Hutton M (2006) A decade of modeling Alzheimer's disease in transgenic mice. Trends Genet 22:281-289.
McNamara TP, Shelton AL (2003) Cognitive maps and the hippocampus. Trends Cogn Sci 7:333-335.
McNaughton BL, Battaglia FP, Jensen O, Moser EI, Moser MB (2006) Path integration and the neural basis of the 'cognitive map'. Nat Rev Neurosci 7:663-678.
Merrill DA, Chiba AA, Tuszynski MH (2001) Conservation of neuronal number and size in the entorhinal cortex of behaviorally characterized aged rats. J Comp Neurol 438:445-456.
Ming GL, Song H (2005) Adult neurogenesis in the mammalian central nervous system. Annu Rev Neurosci 28:223-250.
Moser EI, Kropff E, Moser MB (2008) Place cells, grid cells, and the brain's spatial representation system. Annu Rev Neurosci 31:69-89.
Moser MB, Moser EI (1998) Functional differentiation in the hippocampus. Hippocampus 8:608-619.
Nacher J, Blasco-Ibáñez JM, McEwen BS (2002a) Non-granule PSA-NCAM immunoreactive neurons in the rat hippocampus. Brain Res 930:1-11.
Nacher J, Crespo C, McEwen BS (2001) Doublecortin expression in the adult rat telencephalon. Eur J Neurosc 14:629-644.
Nacher J, Lanuza E, McEwen BS (2002b) Distribution of PSA-NCAM expression in the amygdala of the adult rat. Neuroscience 113:479-484.
Nottebohm F (2002) Neuronal replacement in adult brain. Brain Res Bull 57:737-749.
Nowak RM (1994) Old world fruit bats Pteropodidae. In: Walkers Bats of the world, pp 48-85. Maryland: The John Hopkins University Press.
O'Keefe J, Conway DH (1978) Hippocampal place units in the freely moving rat: why they fire where they fire. Exp Brain Res 31:573-590.
O'Keefe J, Nadel L (1978) The hippocampus as a cognitive map: Oxford University Press.
Papi F (1991) Orientation in birds. Olfactory navigation. EXS 60:52-85.
Petreanu L, Alvarez-Buylla A (2002) Maturation and death of adult-born olfactory bulb granule neurons: role of olfaction. J Neurosci 22:6106-6113.

Pettigrew JD, Jamieson BG, Robson SK, Hall LS, McAnally KI, Cooper HM (1989) Phylogenetic relations between microbats, megabats and primates (Mammalia: Chiroptera and Primates). Philos Trans R Soc Lond B 325:489-559.

Pleskacheva M, G. , Wolfer D, P. , Kupriyanova I, F. , Nikolenko D, L. , Scheffrahn H, Dell'Omo G, Lipp H-P (2000) Hippocampal mossy fibers and swimming navigation learning in two vole species occupying different habitats. Hippocampus 10:17-30.

Pope K, Wilson DA (2007) Olfactory system modulation of hippocampal cell death. Neurosci Lett 422:13-17.

Raghuram H, Thangadurai C, Gopukumar N, Nathar K, Sripathi K (2009) The role of olfaction and vision in the foraging behaviour of an echolocating megachiropteran fruit bat, *Rousettus leschenaulti* (Pteropodidae). Mammalian Biology - Zeitschrift fur Saugetierkunde 74:9-14.

Rapp PR, Deroche PS, Mao Y, Burwell RD (2002) Neuron number in the parahippocampal region is preserved in aged rats with spatial learning deficits. Cereb Cortex 12:1171-1179.

Reader SM, Laland KN (2002) Social intelligence, innovation, and enhanced brain size in primates. Proc Natl Acad Sci USA 99:4436-4441.

Richter HV, Cumming GS (2008) First application of satellite telemetry to track African straw-coloured fruit bat migration. J Zool 275:172-176.

Rietze R, Poulin P, Weiss S (2000) Mitotically active cells that generate neurons and astrocytes are present in multiple regions of the adult mouse hippocampus. J Comp Neurol 424:397-408.

Rochefort C, Gheusi G, Vincent JD, Lledo PM (2002) Enriched odor exposure increases the number of newborn neurons in the adult olfactory bulb and improves odor memory. J Neurosci 22:2679-2689.

Rogers JH, Resibois A (1992) Calretinin and calbindin-D28k in rat brain: patterns of partial co-localization. Neuroscience 51:843-865.

Rose M (1912) Histologische lokalisation der Grosshirnrinde bei Kleinen Saugetierein (Rodentia, Insectivora, Chiroptera). J Psychol Neurol 19:119-207.

Safi K, Dechmann DK (2005) Adaptation of brain regions to habitat complexity: a comparative analysis in bats (Chiroptera). Proc Biol Sci 272:179-186.

Sargolini F, Fyhn M, Hafting T, McNaughton BL, Witter MP, Moser MB, Moser EI (2006) Conjunctive representation of position, direction, and velocity in entorhinal cortex. Science 312:758-762.

Schwartz SP, Coleman PD (1981) Neurons of origin of the perforant path. Exp Neurol 74:305-312.

Schwegler H, Crusio WE (1995) Correlations between radial-maze learning and structural variations of septum and hippocampus in rodents. Behav Brain Res 67:29-41.

Schwerdtfeger WK, Buhl EH, Germroth P (1990) Disynaptic olfactory input to the hippocampus mediated by stellate cells in the entorhinal cortex. J Comp Neurol 292:163-177.

Shapiro L, Ng K, Kinyamu R, Whitaker-Azmitia P, Geisert E, Blurton-Jones M, Zhou Q-Y, Ribak C (2007) Origin, migration and fate of newly generated neurons in the adult rodent piriform cortex. Brain Struct Funct 212:133-148.

Shen YY, Liu J, Irwin DM, Zhang YP (2010) Parallel and convergent evolution of the dim-light vision gene RH1 in bats (Order: Chiroptera). PLoS One 5:e8838.

Shipley MT, Ennis M, Puche AC (2004) Olfactory system. In: The rat nervous system (Paxinos G, ed), pp 923-964. San Diego and London: Elsevier Academic Press.

Shultz S, Dunbar RI (2007) The evolution of the social brain: anthropoid primates contrast with other vertebrates. Proc Biol Sci 274:2429-2436.

Simmons NB, Seymour KL, Habersetzer J, Gunnell GF (2008) Primitive early Eocene bat from Wyoming and the evolution of flight and echolocation. Nature 451:818-821.

Slomianka L, West MJ (1989) Comparative quantitative study of the hippocampal region of two closely related species of wild mice: interspecific and intraspecific variations in volumes of hippocampal components. J Comp Neurol 280:544-552.

Snyder JS, Radik R, Wojtowicz M, Cameron HA (2009) Anatomical gradients of adult neurogenesis and activity: Young neurons in the ventral dentate gyrus are activated by water maze training. Hippocampus 19:360-370.
Stark AK, Petersen AO, Gardi J, Gundersen HJG, Pakkenberg B (2007) Spatial distribution of human neocortical neurons and glial cells according to sex and age measured by the saucer method. Journal of Neuroscience Methods 164:19-26.
Suthers RA (I970) Vision, olfaction, taste. In: Biology of bats. (Wimsatt WA, ed), vol 2, pp 265-304. New York: Academic press.
Teeling EC, Scally M, Kao DJ, Romagnoli ML, Springer MS, Stanhope MJ (2000) Molecular evidence regarding the origin of echolocation and flight in bats. Nature 403:188-192.
Treves A, Tashiro A, Witter MP, Moser EI (2008) What is the mammalian dentate gyrus good for? Neuroscience 154:1155-1172.
Tuñón T, Insausti R, Ferrer I, Sobreviela T, Soriano E (1992) Parvalbumin and calbindin D-28K in the human entorhinal cortex. An immunohistochemical study. Brain Res 589:24-32.
Ulanovsky N, Moss CF (2007) Hippocampal cellular and network activity in freely moving echolocating bats. Nat Neurosci 10:224-233.
Uva L, Grüschke S, Biella G, De Curtis M, Witter MP (2004) Cytoarchitectonic characterization of the parahippocampal region of the guinea pig. J Comp Neurol 474:289-303.
van Praag H, Schinder AF, Christie BR, Toni N, Palmer TD, Gage FH (2002) Functional neurogenesis in the adult hippocampus. Nature 415:1030-1034.
Wilkinson GS, South JM (2002) Life history, ecology and longevity in bats. Aging Cell 1:124-131.
Wilson RC, Steward O (1978) Polysynaptic activation of the dentate gyrus of the hippocampal formation: an olfactory input via the lateral entorhinal cortex. Exp Brain Res 33:523-534.
Winter Y, Stich KP (2005) Foraging in a complex naturalistic environment: capacity of spatial working memory in flower bats. J Exp Biol 208:539-548.
Witter MP (2007) The perforant path: projections from the entorhinal cortex to the dentate gyrus. Prog Brain Res 163:43-61.
Witter MP, Moser EI (2006) Spatial representation and the architecture of the entorhinal cortex. Trends Neurosci 29:671-678.
Witter MP, Wouterlood FG, Naber PA, Van Haeften T (2000) Anatomical organization of the parahippocampal-hippocampal network. Ann N Y Acad Sci 911:1-24.
Wood ER, Dudchenko PA, Eichenbaum H (1999) The global record of memory in hippocampal neuronal activity. Nature 397:613-616.
Wouterlood FG, Hartig W, Bruckner G, Witter MP (1995) Parvalbumin-immunoreactive neurons in the entorhinal cortex of the rat: localization, morphology, connectivity and ultrastructure. J Neurocytol 24:135-153.
Wouterlood FG, van Denderen JC, van Haeften T, Witter MP (2000) Calretinin in the entorhinal cortex of the rat: distribution, morphology, ultrastructure of neurons, and co-localization with gamma-aminobutyric acid and parvalbumin. J Comp Neurol 425:177-192.
Wóznicka A, Malinowska M, Kosmal A (2006) Cytoarchitectonic organization of the entorhinal cortex of the canine brain. Brain Res Rev 52:346-367.
Xiong K, Luo D-W, Patrylo PR, Luo X-G, Struble RG, Clough RW, Yan X-X (2008) Doublecortin-expressing cells are present in layer II across the adult guinea pig cerebral cortex: Partial colocalization with mature interneuron markers. Exp Neurol 211:271-282.

ORAL PRESENTATIONS

23 Sep 2009 **Neurogenesis in fruit bats**

Meeting of National Centre of Competence in Research (NCCR) Neural Plasticity and Repair, adult neurogenesis group

23 May 2009 **Adult hippocampal neurogenesis in two species of African fruit bats** (poster)

PhD Retreat Valens, Neuroscience Centre Zurich (ZNZ)

18 May 2009 **The entorhinal cortex of the Megachiroptera**

Progress report, laboratory meeting

20 Dec 2008 **Morphological correlates of spatial navigation and memory in African fruit bats**

IBRO Advanced Behavioural Neuroscience School, Nairobi

17 Oct 2007 **Low hippocampal neurogenesis coupled to high cortical plasticity**

Progress report, laboratory meeting

4 Apr 2007 **Adult hippocampal neurogenesis in fruit bats**

Progress report, laboratory meeting

ABSTRACTS OF POSTER PRESENTATIONS

Gatome C. W., Slomianka L., Lipp H.-P., Amrein I. 6 Jul 2010. Neuron numbers, densities and sizes in medial entorhinal area layer II in the rat and mouse. Federation of European Neuroscience Societies (FENS) Forum.

Institute of Anatomy, University of Zurich, Zurich, Switzerland

Modelling entorhinal function and the consequences of neuronal losses which accompany neurodegenerative disorders requires detailed information on the quantitative cellular composition of the entorhinal cortex. Using stereological methods, we estimated the number, proportion, densities and size of layer II cells in the medial entorhinal area (MEA), and its constituent caudal entorhinal (CE) and medial entorhinal (ME) fields, in the rat and mouse. We estimated MEA layer II to contain ~58,000 neurons in the rat and ~24,000 neurons in the mouse. Field CE accounted for more than three-quarters of the total in both species. In the rat, MEA layer II is comprised of 38% ovoid stellate cells, 29% polygonal pyramidal cells and 17% pyramidal cells. The remainder is comprised of much smaller populations of e.g. horizontal bipolar, tripolar, oblique pyramidal and small round neurons. In the mouse MEA layer II is comprised of 51% ovoid stellate cells, 23% polygonal pyramidal cells and 15% pyramidal cells. Significant species differences in the proportions of ovoid and polygonal stellate cells suggest differences in physiological and functional properties, perhaps mirroring differences in functional phenotypes in this layer. The vast majority of MEA layer II cell contribute to the entorhino-hippocampal pathways. The degree of divergence from MEA layer II to the dentate granule cells was similar in the rat and mouse. The only dorsoventral difference we observed is a gradient in polygonal stellate cell size, which may relate to the dorsoventral increase in the size and spacing of individual neuronal firing fields. Supported by Rita Levi Montalcini Fellowship for African Women in Neuroscience, SNF and NCCR “Neural Plasticity and Repair”.

Gatome C. W.[1], **Amrein I.**[1], **Mwangi D.K.**[2], **Slomianka L.**[1], **Lipp H.-P.**[1] 19 Oct 2009. A comparative study of the entorhinal cortex of the Megachiroptera: Wahlberg's epauletted fruit bat and the straw-coloured fruit bat. Society for Neuroscience (SfN), Abstract no. 464.21.

[1] Institute of Anatomy, University of Zurich, Zurich, Switzerland

[2] Department of Veterinary Anatomy and Physiology, University of Nairobi, Nairobi, Kenya

This study compares the cyto- and chemoarchitectonic organisation of the entorhinal cortex of the Megachiroptera, Straw-coloured fruit bat (*Eidolon helvum*) and Wahlberg's epauletted fruit bat (*Epomophorus wahlbergi*). Using Nissl and Timm stains, parvalbumin and SMI-32 immunohistochemistry, we identified medial and lateral entorhinal subdivisions. The medial subdivision (MEA) is characterised by a poor differentiation between layers II and III, a distinct layer IV and broad and stratified layers V and VI. The lateral subdivision (LEA) is distinguished by cell clusters in layer II, a clear differentiation between layers II and III, a wide columnar layer III, and a broad sublayer Va. We identified five fields based on the laminar cytoarchitecture. MEA in the Straw-coloured fruit bat presented a layer II with a prominence of pyramidal neurons, whereas stellate cells were commonly observed in Wahlberg's epauletted fruit bat. Clustering and island formation in layer II of LEA was more typical of the Straw-coloured fruit bat. Timm-staining was most intense in sublayer Ia, and layers II and III of LEA. Parvalbumin-like staining varied along a medio-lateral gradient with highest immunoreactivity in layers II and III of LEA. SMI 32-like immunoreactivity was seen primarily in layer III of LEA but only in Wahlberg's epauletted fruit bat suggesting differences in local microcircuitry. Stereological cell-size measurements in layer II of MEA shows 3 types of neurons, classified as large, intermediate and small. The ratio between the 3 neuronal types favours an intermediate-sized neuron as the main neuronal type in the Straw-coloured fruit bat. In Wahlberg's epauletted fruit bat, the large and intermediate neurons are approximately of equal proportion. These Megachiroptera present unique models for the functional investigation of the entorhinal cortex and role of the layer II pyramidal cell input into the hippocampus.

Supported by Rita Levi Montalcini Fellowship for African Women in Neuroscience, SNF and NCCR "Neural Plasticity and Repair"

Gatome C. W. [1], **Amrein I.** [1], **Mwangi D.K.** [2], **Slomianka L.** [1], **Lipp H.-P.** [1] 11 Sep 2009. A comparative study of the entorhinal cortex of the Megachiroptera. Neuroscience Centre Zurich (ZNZ) Symposium, Abstract no. 100.

[1] Institute of Anatomy, University of Zurich, Zurich, Switzerland

[2] Department of Veterinary Anatomy and Physiology, University of Nairobi, Nairobi, Kenya

This study compares the cyto- and chemoarchitectonic organisation of the entorhinal cortex of the Megachiroptera, Straw-coloured fruit bat (*Eidolon helvum*) and Wahlberg's epauletted fruit bat (*Epomophorus wahlbergi*). Using Nissl and Timm stains, parvalbumin and SMI-32 immunohistochemistry, we identified medial and lateral entorhinal subdivisions. The medial subdivision (MEA) is characterised by a poor differentiation between layers II and III, a distinct layer IV and broad and stratified layers V and VI. The lateral subdivision (LEA) is distinguished by cell clusters in layer II, a clear differentiation between layers II and III, a wide columnar layer III, and a broad sublayer Va. We identified five fields based on the laminar cytoarchitecture. MEA in the Straw-coloured fruit bat presented a layer II with a prominence of pyramidal neurons, whereas stellate cells were commonly observed in Wahlberg's epauletted fruit bat. Clustering and island formation in layer II of LEA was more typical of the Straw-coloured fruit bat. Timm-staining was most intense in sublayer Ia, and layers II and III of LEA. Parvalbumin-like staining varied along a medio-lateral gradient with highest immunoreactivity in layers II and III of LEA. SMI 32-like immunoreactivity was seen primarily in layer III of LEA but only in Wahlberg's epauletted fruit bat suggesting differences in local microcircuitry. Stereological cell-size measurements in layer II of MEA shows 3 types of neurons, classified as large, intermediate and small. The ratio between the 3 neuronal types favours an intermediate-sized neuron as the main neuronal type in the Straw-coloured fruit bat. In Wahlberg's epauletted fruit bat, the large and intermediate neurons are approximately of equal proportion. These Megachiroptera present unique models for the functional investigation of the entorhinal cortex and role of the layer II pyramidal cell input into the hippocampus.

Supported by Rita Levi Montalcini Fellowship for African Women in Neuroscience, SNF and NCCR "Neural Plasticity and Repair"

Gatome C. W.[1], **Mwangi D. K.**[2], **Kiama S. G.**[2], **Amrein I.**[1], **Lipp H.-P.**[1] 12 Sep 2008. Adult hippocampal neurogenesis and mossy fibre distribution in two species of African frugivorous bats. Neuroscience Centre Zurich (ZNZ) Symposium, Abstract no. 111.

[1] Institute of Anatomy, University of Zurich, Zurich, Switzerland

[2] Department of Veterinary Anatomy and Physiology, University of Nairobi, Nairobi, Kenya

Several reports have provided correlational evidence that adult hippocampal neurogenesis is involved in spatial learning and memory, while others have contradicted it. Therefore, we have started to study adult neurogenesis in bats, which are unique in small mammals with respect to navigational abilities. Recent published data in the different species of Microchiroptera showed absent to relatively low levels of adult hippocampal neurogenesis and varying mossy fiber distribution. However, these findings were difficult to correlate with the habitat type and foraging strategy. Fruit bats have a comparatively well developed hippocampus, and it is hypothesized that an enhanced spatial memory is important to remember unpredictable food sources, and also to support migratory behaviour. In this study, we investigated two fruit bats, *Eidolon helvum* and *Epomophorus wahlbergi*, differing in the complexity of their foraging strategies and migratory behaviour, for adult neurogenesis by means of immunohistochemistry, and visualized their hippocampal mossy fiber distribution by means of Timm staining. Early comparative results on neurogenesis and mossy fiber size will be presented.

Supported by SNF, IBRO and NCCR "Neural Plasticity and Repair".

Gatome C. W.[1], **Mwangi D. K.**[2], **Kiama S. G.**[2], **Amrein I.**[1], **Lipp H.-P.**[1] 14 Jul 2008. Adult hippocampal neurogenesis and mossy fibre distribution in two African frugivorous bats. Federation of European Neuroscience Societies (FENS) Forum, Abstract no. 074.16: 122.

[1] Institute of Anatomy, University of Zurich, Zurich, Switzerland

[2] Department of Veterinary Anatomy and Physiology, University of Nairobi, Nairobi, Kenya

Several reports have provided correlational evidence that adult hippocampal neurogenesis is involved in spatial learning and memory, while others have contradicted it. Therefore, we have started to study adult neurogenesis in bats, which are unique in small mammals with respect to navigational abilities. Recent published data in the different species of Microchiroptera showed absent to relatively low levels of adult hippocampal neurogenesis and varying mossy fiber distribution. However, these findings were difficult to correlate with the habitat type and foraging strategy. Fruit bats have a comparatively well developed hippocampus, and it is hypothesized that an enhanced spatial memory is important to remember unpredictable food sources, and also to support migratory behaviour. In this study, we investigated two fruit bats, *Eidolon helvum* and *Epomophorus wahlbergi*, differing in the complexity of their foraging strategies and migratory behaviour, for adult neurogenesis by means of immunohistochemistry, and visualized their hippocampal mossy fiber distribution by means of Timm staining. Early comparative results on neurogenesis and mossy fiber size will be presented.

Supported by SNF, IBRO and NCCR “Neural Plasticity and Repair”.

Gatome C. W.[1], Mwangi D. K.[2], Kiama S. G.[2], Amrein I.[1], Lipp H.-P. [1] 14 Sep 2007. Comparative study of adult neurogenesis in two frugivorous bats. Neuroscience Centre Zurich (ZNZ) Symposium, Abstract no. 30.

[1] Institute of Anatomy, University of Zurich, Zurich, Switzerland

[2] Department of Veterinary Anatomy and Physiology, University of Nairobi, Nairobi, Kenya

It was commonly believed that neurons in the central nervous system of higher vertebrates were formed during embryonic development and that no new neurons were formed postnatally. Currently, there is substantial evidence that a number of new neurons are continuously produced in the adult vertebrate brain and this has been shown in rodents, birds and primates. The hippocampus is one of the brain regions with lifelong neurogenesis in mammals. Several reports have provided corelational evidence that adult hippocampal neurogenesis is involved in learning and memory. The ability of bats to memorise structures within their foraging area has long been recognised, and anecdotal evidence suggests that spatial memory is crucial for orientation in bats. Comparative analysis of the size of sensory nuclei and hippocampus of numerous bat species has shown that habitat type and foraging strategy are the main factors determining the size of these structures. There are two suborders within the Chiroptera, the Microchiroptera and fruit bats. Fruit bats have the better developed hippocampus and they benefit from enhanced spatial memory by remembering the location of unpredictable but stationary food sources. They use vision as the major telereceptive sense. Microchiroptera differ from fruit bats in having an exceptionally well-developed auditory system and making use of echolocation to detect obstacles and prey. Recent published data in the Microchiroptera reports an absent to relatively low level of adult hippocampal neurogenesis. Using immunohistochemical and stereological techniques, this study attempts to correlate the extent of neurogenesis in the hippocampus of two free-living species of fruit bats (*Epomophorus wahlbergi* and *Eidolon helvum*) with their biology and behaviour. A comparison with also be made between these fruit bats and the findings in the Microchiroptera.

Study supported by IBRO studentship to CWG

ACKNOWLEDGEMENTS

To IBRO and Rita Levi Montalcini who were open to the project and resolutely supported it and me

To Hans-Peter Lipp who generously gave the opportunity, advice and mentorship

To Irmgard Amrein, Deter Mwangi and Lutz Slomianka who tirelessly supervised and mentored my scientific progress

To Inger Drescher and Rosmarie Lang on whose technical assistance I greatly relied upon

To Ben Agwanda and Francis Muchemi, for invaluable assistance in the field

To Nada BenAbdallah, for her companionship during those long lab days

To Fabienne Hauser, for her understanding

To colleagues in the lab for the passion in science

To my family, a pillar of strength

To Muriu and Emma, for the ever ready encouragement

To God, for the grace and fortitude to survive it

CURRICULUM VITAE

CATHERINE WAIRIMU GATOME

Institute of Anatomy, University of Zurich, Winterthurerstrasse 190, 8057 Zurich
Telephone: +41 44 6355340; Mobile: +41 79 385 4428; E-mail: c.gatome@anatom.uzh.ch

Education

2007 - Present	**University of Zurich**, Switzerland
	Institute of Anatomy
	· International PhD program in Neuroscience (Life Science Graduate School, Zurich)
	· Thesis title: The morphological correlates of spatial navigation, orientation and memory in African fruit bats
	· Investigated the morphological characteristics of the entorhinal cortex of fruit bats, rat and mouse, and adult neurogenesis in the fruit bats. The techniques applied include immunohistochemistry, stereology, and neuronal tracing.
2002 - 2003	**Royal College of Veterinary Surgeons**, United Kingdom
	Statutory examination for membership
	· Diploma of membership
2001 - 2002	**University of London, Royal Veterinary College**, London
	· Master of Science in wild animal health
	· Dissertation title: The health status of free-living African white-backed vultures
	· Investigations included physical examination, clinical haematology and biochemistry, and faeces analysis. Supervisors: Dr Tony Sainsbury (Institute of Zoology, London); Dr Munir Virani and Mr. Simon Thomsett (Peregrine Fund, USA)
1991 - 1997	**University of Nairobi**, Kenya
	Bachelor in Veterinary Medicine

Appointments

2004 - 2007	**University of Nairobi**, Nairobi, Kenya Tutorial fellow, Department of Veterinary Anatomy and Physiology · Teaching and research position
2003 - 2004	**Sarat Veterinary Clinic**, Nairobi, Kenya Veterinary Surgeon · Treated small animals and exotic species and advised on health and welfare issues.
1998-2001	**Pharmacia and Upjohn**, Nairobi, Kenya Medical Representative · Increased awareness and use of a broad portfolio of pharmaceutical products by healthcare professionals.

Awards

2010	Neuroscience Centre Zurich (ZNZ) travel award to FENS 2010
2009	Neuroscience Centre Zurich (ZNZ) travel award to SfN 2009
2008 – 2010	Rita Levi Montalcini Fellowship for African Women in Neuroscience
2007	International Brain Research Organization (IBRO) Scholarship

Memberships

Swiss Society for Neuroscience; IBRO Women in World Neuroscience; Royal College of Veterinary Surgeons ; Kenya Veterinary Association

Personal Details

Date of Birth	14 May 1972
Nationality	Kenyan

References

Prof. Dr. Hans-Peter Lipp
Division of Neurobiology and Behaviour
Institute of Anatomy
University of Zurich
Winterthurerstrasse 190
8057 Zurich
Tel: +41 44 63 55330
Email: hplipp@anatom.uzh.ch

Prof. Dr. David Wolfer
Division of Functional Neuroanatomy
Institute of Anatomy
University of Zurich
Winterthurerstrasse 190
8057 Zurich
Tel: +41 44 63 55312
Email: dpwolfer@anatom.uzh.ch